FORCED VIBRATIONS DURING GRINDING AND THEIR EFFECT ON SURFACE QUALITY

Thesis submitted to the University of Birmingham
for the degree of M.Sc.

By

A. D. SINDWANI

August, 1970.

SYNOPSIS

Two types of vibration, i.e. forced and self-excited, are generated during the grinding process. The forced vibration is mainly introduced due to the wheel unbalance and the self-excited vibration due to the machining process itself. An attempt has been made to analyse the forced vibration in order to help with the formulation of a basis for the dynamic acceptance test of a grinding machine. A systematic analysis of the effects of the wheel unbalance on the dynamic system of the grinding machine, grinding forces, macro and micro geometrical workpiece parameters and wheel wear has been made by conducting a series of grinding tests. A new approach has been made to study the motion of the wheelspindle in its bearings. A theoretical expression relating the wheel unbalance and workpiece waviness has also been derived.

A Churchill plain hydraulic cylindrical grinding machine was adapted for the present investigation. Three wheels of grades K, M and O were employed. A suitable experimental set up was developed to measure the various parameters involved.

The two most important conclusions which emerged from the present investigation are as follows:

1. With increase in wheel unbalance an increase in the wheelhead and wheelspindle vibration are noticed. The relative motion between the wheel and the workpiece, the variation in the grinding forces and the workpiece waviness are also increased with the increase in the wheel unbalance.
2. The wheel unbalance does not affect the temperature in the bearings, the grinding ratio, the average grinding forces and longitudinal surface roughness parameters. Some improvement in bearing area, however, was observed with the increase of wheel unbalance.

ACKNOWLEDGEMENTS.

The investigation was carried out in the Mechanical Engineering Department of the University of Birmingham, during the period 1968 - 70. The author wishes to thank Professor S. A. Tobias for granting facilities for the work.

The author is grateful to Dr. H. Kaliszer for the valuable guidance and help he has given throughout the project.

Thanks are also due to Mr. D. J. Grieve, Mr. Nicholls, Mr. M. Singh and Mr. B. Manning for help during the various stages of the work.

Finally, the author extends his thanks to M.T.I.R.A. for providing the financial assistance which enabled him to carry out the work.

Paper presented at the 10th Int. M.T.D.R. Conference, Manchester, 1969.

LIST OF FIGURES

CHAPTER 1

INTRODUCTION

1.1 General

There has been a growing interest in the dynamic testing of machine tools. Such tests are employed from the prototype development stage to the operational stage of the machine tools. The basic purpose of the dynamic tests is to predict the behaviour of machine tools in the presence of cutting forces and vibration. Usually due to vibration generated during cutting a relative motion will take place between the tool and the workpiece. This motion will to a large extent affect the machining accuracy and surface roughness. To minimise the relative motion modern machine tools are rigidly built. Normally machine tools consist of many degrees of freedom for which the mathematical models are complicated. Therefore, it is a normal practice to simplify the dynamic model by considering two essential subsystems, i.e. the workpiece system and the tool system. Since, grinding is a widely used finishing process it is important that the relative motion between the two subsystems should be minimised. To achieve this object the knowledge of vibration during grinding and the resulting dynamic behaviour of the machine and workpiece surface quality is important.

1.2 Vibration During Grinding

The irregularities produced on the workpiece depend upon the nature of the prevailing vibration. The vibration present may be due to the inherrent structual characteristics of the machine or due to some exciting or disturbing forces. The vibration during grinding can therefore be classified into two different types,

i) Self Excited Vibration.

ii) Forced Vibration (This also includes the vibration from sources outside the machine).

Although selfexcited vibrations do not form a part of the present investigation, but some literature survey was done about this type of vibration. A brief review of these vibrations is reported in the beginning and their importance is discussed.

1.2.1 Self Excited Vibration

Self excited vibration during grinding is generated by the cutting action itself without the presence of any external periodic forces [1]. The appearance of self excited vibration is dependent on time. With a freshly dressed wheel no vibration is noticed at the beginning. It is only when there is a considerable time interval after dressing that these vibrations appear. According to Landberg [2] as a result of these vibrations a waviness usually developes on a soft wheel where wear is predominant and loading developes on a wheel which is too hard. The growth of vibration, wheel waviness and workpiece roughness with time as observed by Landberg are shown in figure 1. He also assumes that the number of waves formed on the wheel periphery can be found by dividing the frequency of self excited vibration by the wheel frequency. According to Singhal and Kaliszer [3] the time between the wheel dressings and appearance of self excited vibration depends upon, a) the rigidity of the G.W.M. system, b) the type of grinding wheel used, and c) cutting conditions. The rigidity of the machine structure does play an important part as far as the amplitude and frequency of self excited vibration is concerned. According to authors [1,4,5,6] the amplitude of self excited vibration decreases and frequency increases with the increase of the rigidity of the machine structure. Because of the small amplitude of

COMBINATION OF WAVINESS VIBRATIONS AND ROUGHNESS FOR THREE TYPES OF WHEEL

a. AMPLITUDE OF VIBRATION IN mv

b. ROUGHNESS IN MICROINCHES

c. WAVINESS IN MICRONS

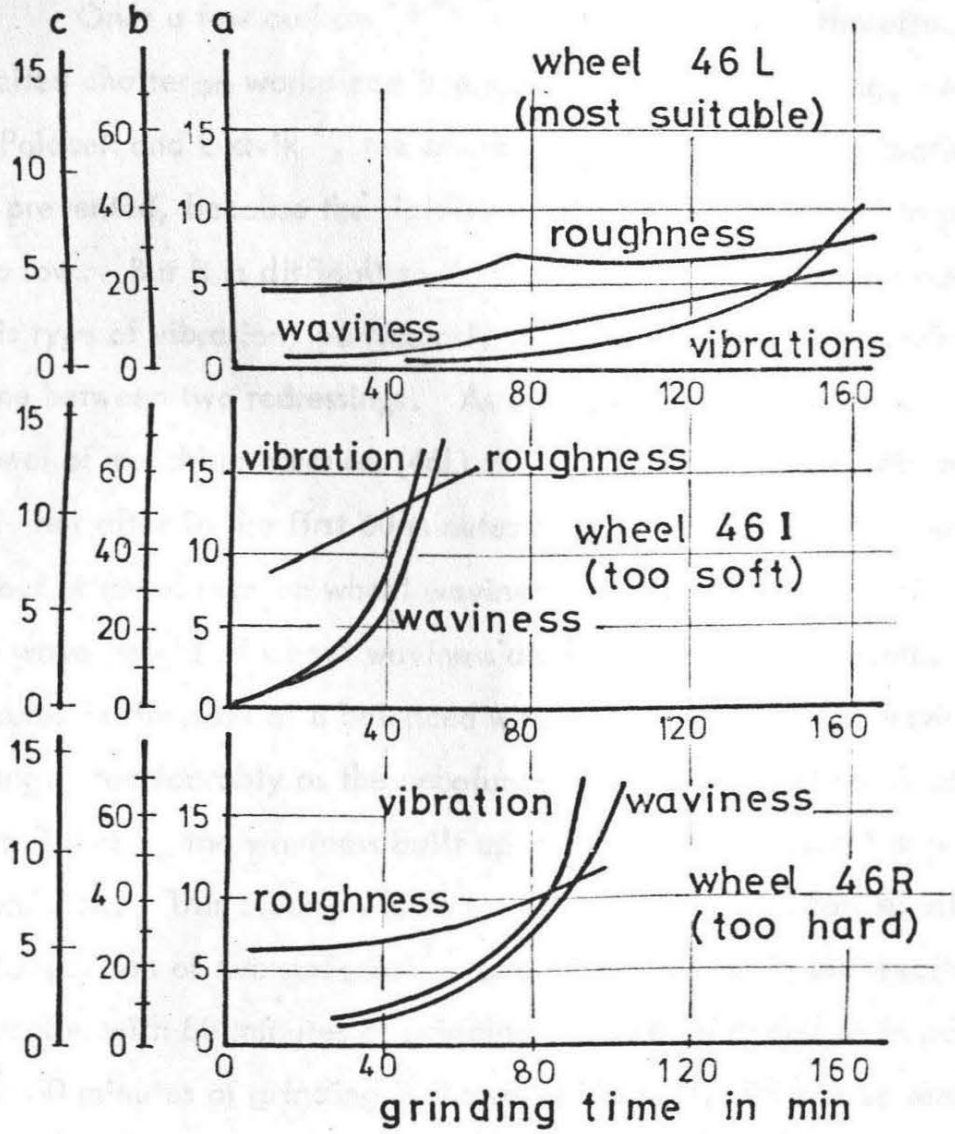

(Landberg[2])

FIG 1. VIBRATIONS AND SURFACE ROUGHNESS BUILT UP DUE TO SELF-EXICITED VIBRATIONS.

self excited vibration, only the workpiece vibrations are considered important and the wheelhead-wheelspindle system can be practically considered to be rigid. Therefore, some authors [1, 6, 7] have considered the rigidity of the machine structure as work-machine stiffness or work-wheel contact stiffness. They find that the frequency of the self excited vibration co-incides with the frequency of the assumed structure.

Only a few authors [2, 3, 7, 8] have dealt with the effect of self excited chatter on workpiece irregularities during grinding. According to Polacek and Ludvik [7], the occurence of self excited vibration cannot be prevented, because the rigidity which can be achieved in practice is too low. But it is difficult to find cases of poor workpiece quality due to this type of vibration, particularly if the grinding is not continued for a long time between two redressings. As can be seen from figure 1, that with a wheel of matching hardness (46L) the waviness and roughness materially does not alter in the first 60 minutes or so. Kaliszer [9] has studied the effect of unbalance on wheel waviness. As can be seen from figure 2(a) the wave height of wheel waviness does not change considerably in 60 minutes in the case of a balanced wheel. However, the wave height changes considerably as the unbalance increases. Further as can be seen from figure 2, the waviness built up is significant around the position of unbalance. This clearly points to the importan ce of forced vibration. A comparison of two surfaces [3], one obtained due to self excited vibration with 80 minutes of grinding and the other due to forced vibration with 30 minutes of grinding is shown in figure 3. As can be seen during self excited vibration, the amplitude of high frequency waviness may be ignored as compared to the amplitude of main waviness during forced vibration whose frequency corresponds to the rotational speed of the wheel.

FIG 2. VARIATION OF WHEEL SURFACE WAVES WITH TIME.

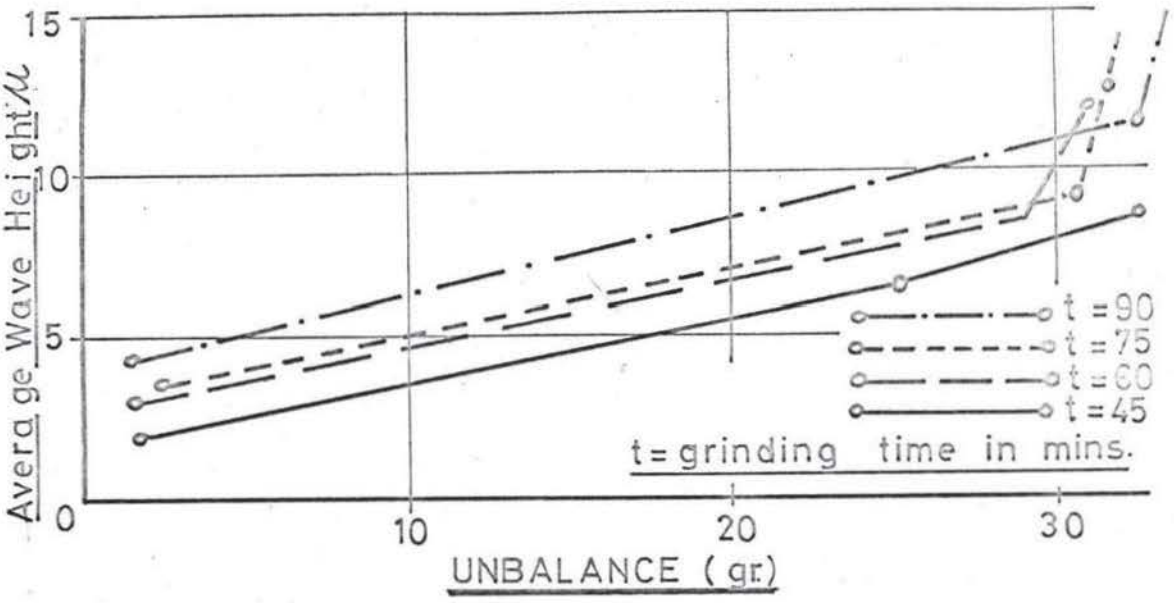

Fig 2a

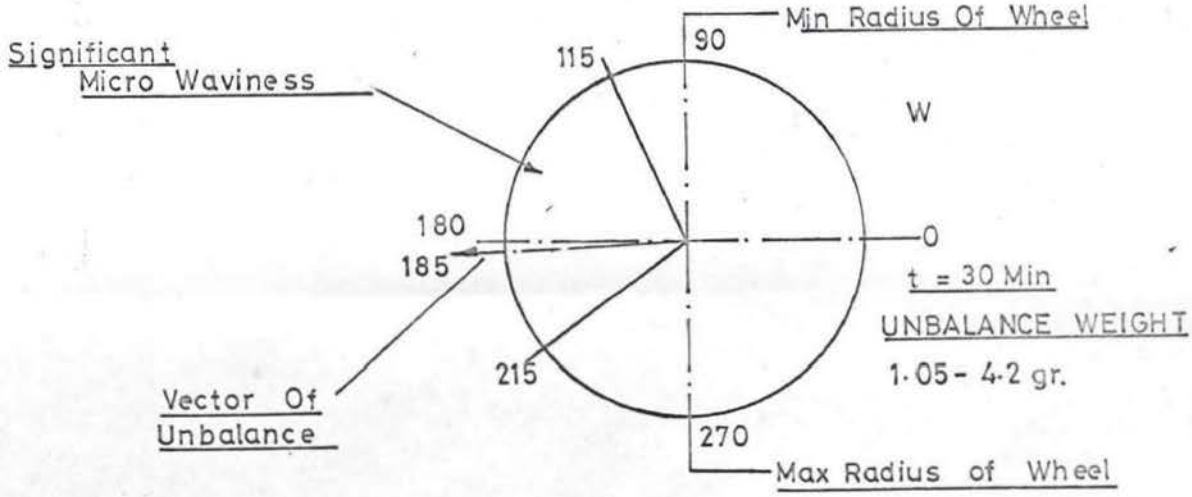

FIG 2b

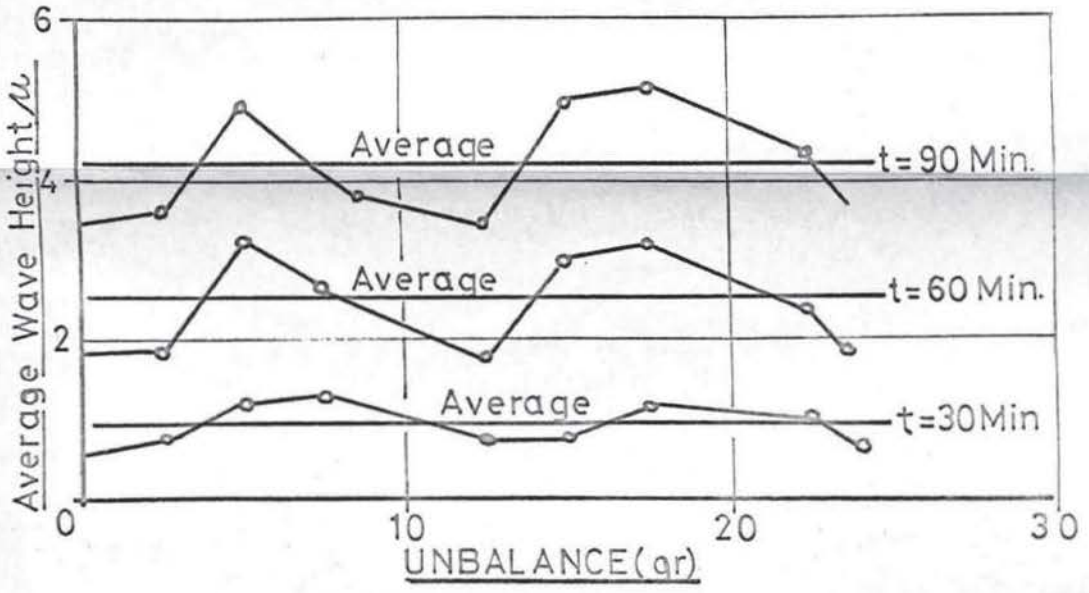

FIG 2C

(Kaliszer[9])

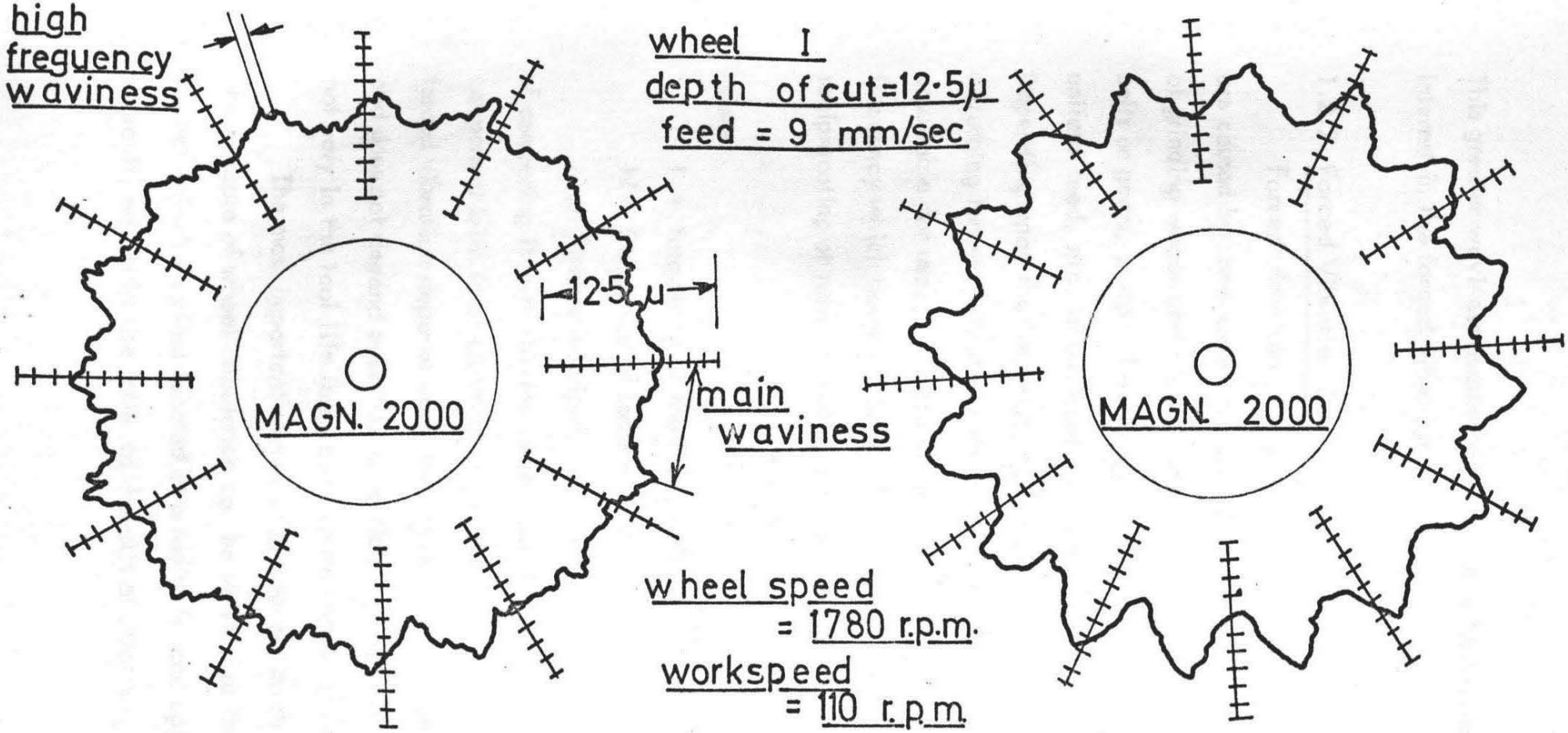

FIG. 3. WAVINESS ON THE WORKPIECE PERIPHERY DUE TO FORCED AND SELF EXCITED VIBRATIONS (SINGHAL[3] KALISZER)

This greater waviness associated with forced vibration has aroused more interest in the forced vibration.

1.2.2 Forced Vibration During Grinding

Forced vibration of the grinding machine tool structure or its parts are caused by some external factors or disturbing forces, like unbalance of grinding wheel and electric motor, faulty bearings, transmission by belts or gears, pumps, inertia forces from reciprocating masses, non-uniform feed, etc. or external forces transmitted via the foundation. Depending upon the location, direction, amplitude and frequency of these disturbing forces, vibrations are generated which can render the workpiece unsuitable for use. The presence of these factors can be identified by the frequency which normally co-incides with the frequency of some reciprocating or rotating parts, and is given by the relation,

$$f = n N$$

where

f = frequency of the forced vibration.

N= frequency of some rotating or reciprocating part.

n an integer multiple. Once f is known it is only a question of comparing it with the frequency of rotating or receiprocating component with in or external to the machine. The amplitude of the forced vibration depends upon the value of the initial disturbing force, and does not depend upon the conditions and time of grinding and does not vary in the tool life (between two dressings) of the grinding wheel [5].

The most important source of forced vibration is the wheel unbalance. The measure of wheel unbalance can be defined as the compensation (or correction) which when located at a radius 'r' and opposite to the centre of gravity will shift the latter to the axis of rotation. The presence of

unbalance shows either a lack of symmetry of structure or shape. Even if the wheel is balanced by gravitational methods the resultant unbalance may still be present, the value of which according to Kaliszer [10] is given

$$dr = df \pm dea \pm des \pm ds$$

where

dr = Resultant D.C.G. (Displacement of the centre of gravity)

df = D.C.G. due to rolling friction.

dea = D.C.G. due to the eccentricity of the arbor.

des = D. C. G. due to the eccentricity of the spindle.

ds = D.C.G. due to the unbalanced rotating masses of the spindle.

If all the factors favour the unbalance in one direction, the max m value of this unbalance is

$$dr = df + dea + des + ds$$

Further Kaliszer [10] also shows that non-uniform coolant absorption may take place and change the mass distribution. This is illustrated in figure 4. In addition to this not correctly designed workpiece carriers may also be responsible for forced vibration.

Although some authors have studied the dynamic behaviour of the machine due to forced vibration, but not enough literature is available on subjects delaing with the effect of forced vibration on workpiece surface.

Kaliszer [9] and Gelfeld [12] have concluded that in most practical cases the wheelhead and wheelspindle system should be considered as having two degrees of freedom. Later Singhal and Kaliszer [11] have considered the G.W.M. (Grinding Wheel - workpiece - machine system) as having three degrees of freedom. They have stressed the importance of the rigidity of the G.W.M. system while considering the

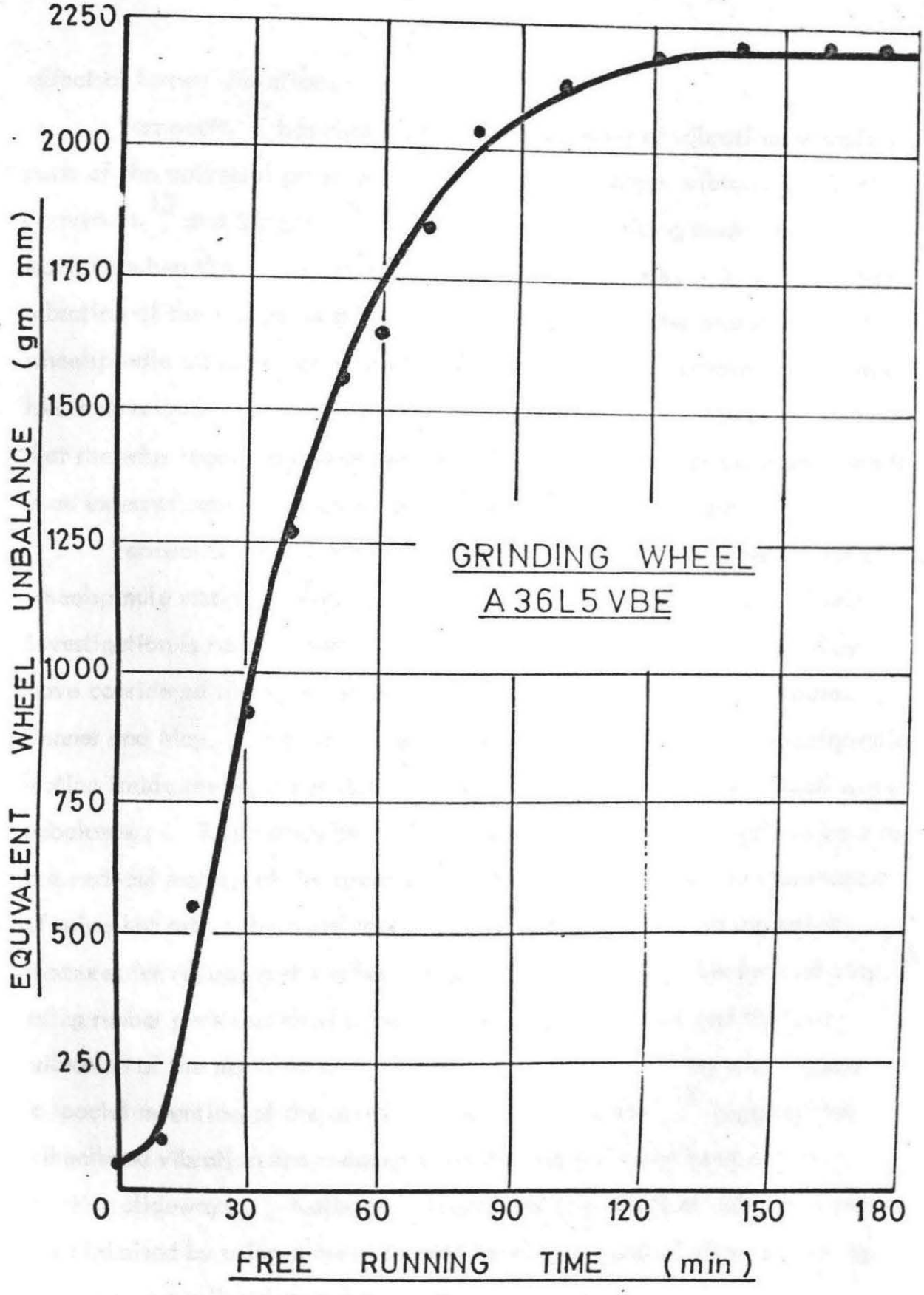

FIG 4. EQUIVALENT WHEEL UNBALANCE DUE TO COOLANT AS A FUNCTION OF FREE RUNNING TIME. (Kaliszer[10])

effect of forced vibration.

Farnworth [13] has studied the natural modes of vibration of various parts of the universal grinding machine due to forced vibration. Both Farnworth [13] and Singhal [14] have noticed the rocking mode of the machine when the whole machine rocks about its base. In studying the vibration of the system most of the authors find that the wheelhead and wheelspindle vibration amplitudes increase with the increase of centrifugal forces developed due to the unbalance. Gelfeld [12], however, stresses that the wheelhead and wheelspindle vibration behaviour changes when there is an external radial load applied in the grinding wheel plane.

Farnworth [13] and Singhal [14] have also studied the behaviour of the wheelspindle motion under the influence of forced vibration. Their investigation is not complete, however, in this respect because they have considered the wheelspindle motion at one plane of the spindle. Bennet and May [15] have investigated the behaviour of the wheelspindle motion inside the bearings due to both gravitational and centrifugal wheel unbalance. Their study in the bearings is, however, confined only to the vertical motion of the spindle. They have stressed the importance of using hot oil in the bearings. Some authors have also suggested measures for reducing the effect of forced vibration. Bennet and May [15] using rubber pads and steel shims in the foundation, noticed that the vibration of the machine was enormously reduced. They also suggest a special mounting of the grinding wheel. Gelfeld [12] suggests that wheelhead vibration are reduced by mounting the wheelhead on anti-friction slideways. Kaliszer [9] found that the effect of unbalance may be minimised by using a plain journal bearing instead of a roller bearing inside the wheelhead assembly.

Some authors have also studied the effect of dressing an unbalanced

wheel. Gelfeld [12] investigated the effect of dressing an unbalanced wheel by placing the diamond at three different positions on the machine, i.e. i) wheelhead, ii) machine table and, iii) longitudinal table. According to him the best results are obtained with diamond placed on the machine table. Bennet and May [15] suggest that small amounts of unbalance does not have any appreciable effect if the truing of the wheel is done properly at a slow speed. Singhal and Kaliszer [3] observe that when a wheel with an unbalance present is dressed, a sine wave develops on the wheel. The waviness on the wheel develops whether the unbalance is present before dressing or added after dressing. They have also shown that the amplitude of wheel waviness also depends upon the wheel-work contact stiffness. With the increase of wheel work contact stiffness the amplitude of waviness decreases.

Regarding the effect of forced vibration on workpiece waviness almost all the authors agree that the amplitude of waviness increases with the increase of unbalance. Singhal and Kaliszer [11] found that the amplitude of waviness produced on workpiece depends upon the following factors:

i) The rigidity of the Grinding wheel - Workpiece - Machine (G.W.M.) systems.

ii) Magnitude of the grinding wheel unbalance.

iii) Dressing and grinding conditions.

The number of waves formed on the workpiece periphery is proportional to the frequency of the forced vibration caused by the wheel unbalance. Authors Terantana and others [16] found that the number of waves on the workpiece periphery co-incided with the ratio of the frequency of the forced vibration to the frequency of the workpiece rotation, a fact outlined by Kaliszer [10] as well. From this they imply that this ratio

should not be a whole number. If this ratio is not a full number the successive cuts will have a smoothing effect on workpiece waviness. They also observed that the table traverse had a detrimental effect on workpiece surface. Inazaki and Yonetsu [17] have studied forced vibration in a surface grinding machine. According to them in surface grinding the elastic deformations of the workpiece can be neglected. They have also shown that besides the unbalance the workpiece waviness is also affected by the term grinding stiffness. Regarding the effect of unbalance on surface roughness, the general belief shared by [13,15,17] is that the surface roughness is not appreciably affected by the unbalance. However, [17] says that in the case of surface grinding the surface roughness increases with unbalance in a direction perpendicular to the direction of grinding. This would be expected because the roughness in perpendicular direction in surface grinding corresponds to waviness in cylindrical grinding.

It is, however, interesting to note that not all forced vibrations are detrimental. Colwell [18] reports that advantages are gained by introducing high frequency (ultrasonic) forced vibration into the grinding process. He found an improvement in surface finish due to these. This according to him may be due to two reasons:

i) Fewer and smaller built up edges.

ii) Continuous uniform redressing resulting from fragmentation of an individual abrasive grain.

1.2.3 Discussion

It is seen from the above review that although some authors [13,14] have studied the dynamic behaviour of the machine due to forced vibration, their work is not complete in the absence of investigation of the wheelspindle

motion. Also only the macro irregularities (waviness) have been generally considered and the micro surface analysis of the workpiece due to forced vibration has not been taken into account. Little effort has been made to relate the effects of forced vibration with different wheel grades, workpiece materials and tool life of the wheel (wheel wear). All these factors have been dealt with in the following investigation.

1.3 Scope of the Present Investigation

In the present investigation only the forced vibrations are considered. Grinding wheel is the most probable source of forced vibration in spite of the greatest care which may be taken in its manufacture. Depending upon the level of unbalance it influences the relative motion between the wheel and the workpiece and the quality of the ground surface. Because of the fine clearances involved between the mating surfaces in modern design the undulations of the surface due to unbalance can have detrimental effects. Sharp undulations with small spacing will cause the break in the oil film in the case of plain bearings. Undualtion with relatively large spacing due to a smooth shape would result in a gradual decrease in the oil film. This does not affect the carrying capacity, but increases the danger of breaking the oil film because of very high frequency undulations superimposed on the undualtions with large spacing. Therefore, in order to determine the running in conditions it is essential to establish a relationship between the profile spectrum of the workpiece and the dynamic behaviour of the machine due to forced vibration.

"The present investigation deals with the effect of forced vibration on workpiece quality during grinding. Wheel unbalance is considered as

source of unbalance and both macro and micro irregularities due to this are analysed."

CHAPTER 2

GRINDING MACHINE SYSTEM

2.1 Dynamic System of the Grinding Machine

In order to analyse the grinding machine vibration and surface quality due to wheel unbalance, it is necessary to represent the grinding machine system by equivalent springs and masses. A number of investigations [3, 12] have shown that for this purpose a simplified dynamic system can be introduced. In such a system the determining factors are the vibration of the wheelspindle, wheelhead and workpiece. In actual fact in the case of loosely coupled systems, any multimass system can be divided into separate partial single mass systems [12]. Thus an assumption has been made that the three mass vibrating system can be separated into two subsystems, i.e. wheelspindle-wheelhead system and the workpiece system subject to elastic coupling taking place during grinding [3,12]. To investigate the above assumption extensive rigidity measurements were carried out [11]. Both the subsystems comprising wheelhead and wheelspindle masses and the system comprising the headstock, tailstock and workpiece masses were excited at different frequencies and amplitude measurements carried out. From these tests frequencies of various modes were obtained (Table 1).

As can be seen from the Table the wheelhead-wheelspindle system has two different modes of vibration, (one corresponding to the resonance of each mass), and may therefore be represented by a two degree of freedom system, as shown diagrammatically in Figure 5 (above the workpiece).

Table 1 also shows that there are three modes of vibration in the workpiece system, ie. the resonance of the headstock, tailstock and the workpiece. Therefore, the workpiece holding system may be represented as having three degrees of freedom, as shown in Figure 5. In this system the

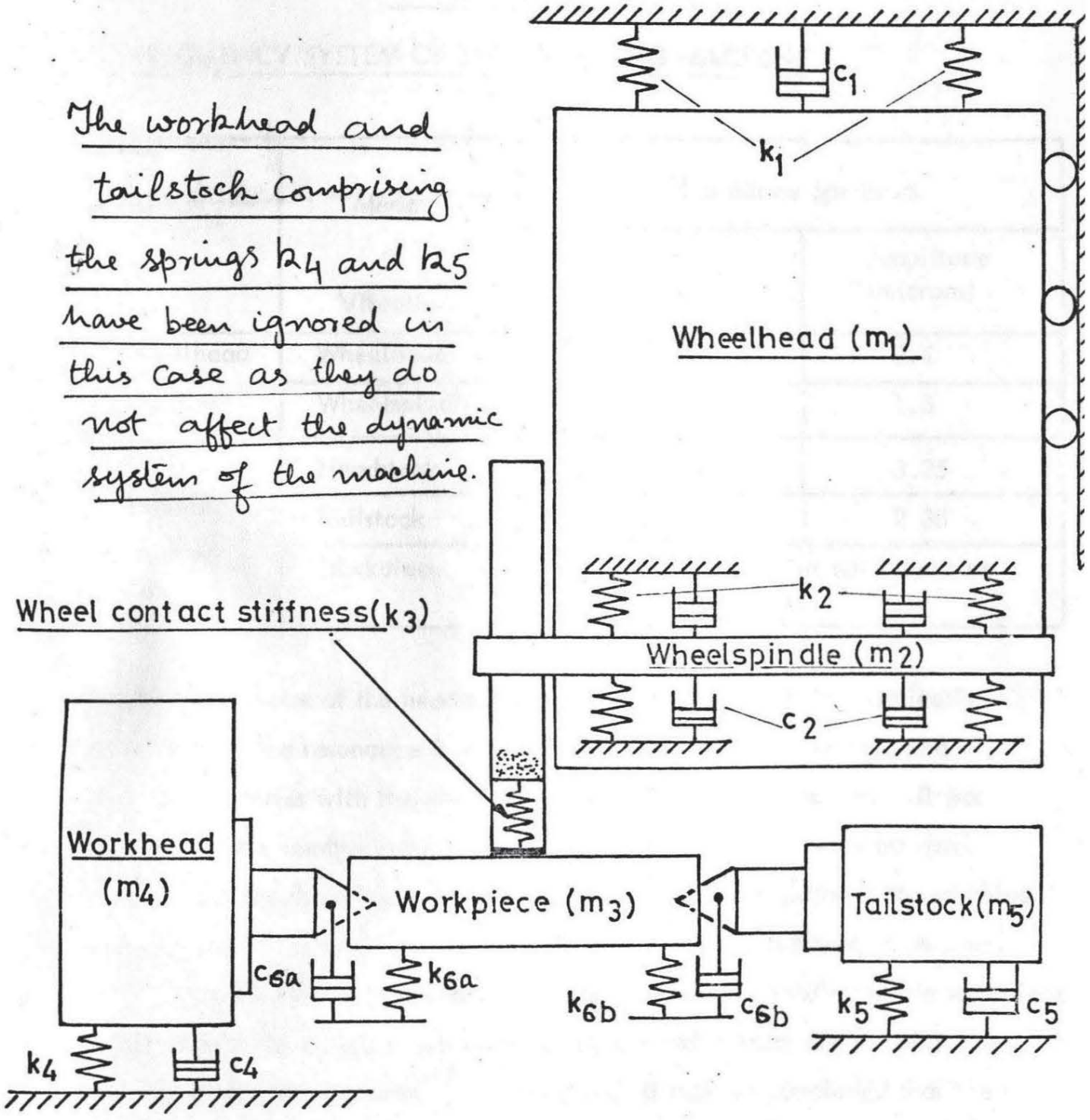

FIG 5. DYNAMICAL REPRESENTATION OF THE GRINDING WHEEL WORKPIECE MACHINE TOOL SYSTEM.

TABLE 1

FREQUENCY SYSTEM OF THE GRINDING MACHINE

SYSTEM	Modes of Vibration	Resonance Spectrum	
		Frequency c.p.s	Amplitude (microns)
Wheelhead System	Wheelhead	90	0.4
	Wheelspindle	190	1.3
Workpiece System	Headstock	240	3.25
	Tailstock	470	2.38
	Workpiece	Frequency varies with the mass of the workpiece	

natural frequencies of the headstock and the tailstock remain practically unchanged. The resonance frequency of the workpiece does not remain constant but varies with the change in the workpiece dimensions. It was thought that the centres supporting the workpiece form the weakest link. In order to study the effect of these dimensions on the rigidity of the machine centres a static test was carried out with workpieces of different diameters.

As follows from these tests there is virtually no bending of the workpiece irrespective of its diameter while considerable deflections are noted at the workpiece supporting points [12]. Therefore, it may be concluded that the workpiece held between centres acts as a mass supported on springs as shown in Figure 5. In order to verify the assumption that the workpiece held between the centres has a single degree of freedom and to study the vibrational modes of the other parts of the workpiece holding system, (such as headstock, tailstock and the machine table), dynamic tests were carried out using workpiece

of different masses. The calculated value of natural frequency from static tests and the one obtained from the dynamic tests for different masses of the workpieces, were found to be close to each other [11]. Thus the workpiece holding system can be considered as a single mass spring system; the headstock, tailstock and the machine table being assumed to be rigid in comparison to the centres supporting the workpiece. During grinding, when the wheel spindle and workpiece are connected together, following Peklenik's[19] suggestion, the grinding wheel is tentatively assumed to be a single spring in compression. The definition of the stiffness of such a spring is suitably modified to account for the essential difference between the static and dynamic conditions. Under static conditions, the stiffness of the spring is defined as the force required per unit elastic deformation. Under dynamic conditions, the force required for the crushing of the grain support per unit depth will be taken as the stiffness of this spring. Hence it is possible to represent the whole grinding wheel-workpiece-grinding machine system having three degrees of freedom as shown in Figure 5, where the only variables for the same grinding wheel are the mass of the workpiece and the wheel unbalance. During dressing the workpiece system is not coupled. Since the area of contact between the wheel and diamond wheel is negligible, the effective stiffness of the grinding wheel will be very small in this case. Hence during dressing only a two degree of freedom system is considered.

The analysis of the relative motion between the wheel and the workpiece requires the knowledge of the vibration in the horizontal (radial) direction. Therefore, in analysing the vibration of the [redacted] radial motion of the wheel-head, workpiece and wheelspindle system has been considered. The importance of the radial motion also follows from the fact that the wheelhead carrying the wheelspindle has a much smaller rigidity in the radial direction than in the vertical direction. This has been shown in previous investigations [9] where

the magnitude of the radial vibration was found to be 7-10 times larger than the vertical vibration amplitude. The radial motion of the wheelhead and workpiece was investigated by Singhal [14] and it was suggested that for the complete investigation of the system it would be necessary to measure the spindle vibration. Therefore, an attempt has been made here to analyse the spindle behaviour in the radial direction.

2.2 Analysis of the Wheelspindle Motion

Very little is known about an effective method of analysing the radial motion of the wheelspindle inside the wheelhead. Bennet and May [15], using capacitance probes, have measured only the vertical motion of the wheelspindle. The method previously used [11] in the analysis of the radial motion of the wheel-end had the capacitance probe fixed to the wheelguard. Besides being ineffecti in analysing the motion inside the wheelhead, this had some other disadvantages also.

i) The spindle end at the wheelguard position may be slightly bent from the true axis and so may give erroneous results.

ii) The wheelguard being itself under the influence of vibration does not provide a rigid mounting and may, therefore, result in disturbing the probe setting.

A new method of measuring the radial wheelspindle motion inside the wheelhead bearings has been adapted by using miniature proximity transducers of inductive type, Figure 6. These transducers, which are fitted in pairs in each bearing, form a differential connection and have a sensitivity of up to 0.1 micron.

The nominal clearance between the bearing and spindle diameters is 38.0 microns. On actual measurement this was found to be 45 microns and 40 microns respectively in the front bearing (wheel end) and rear bearing

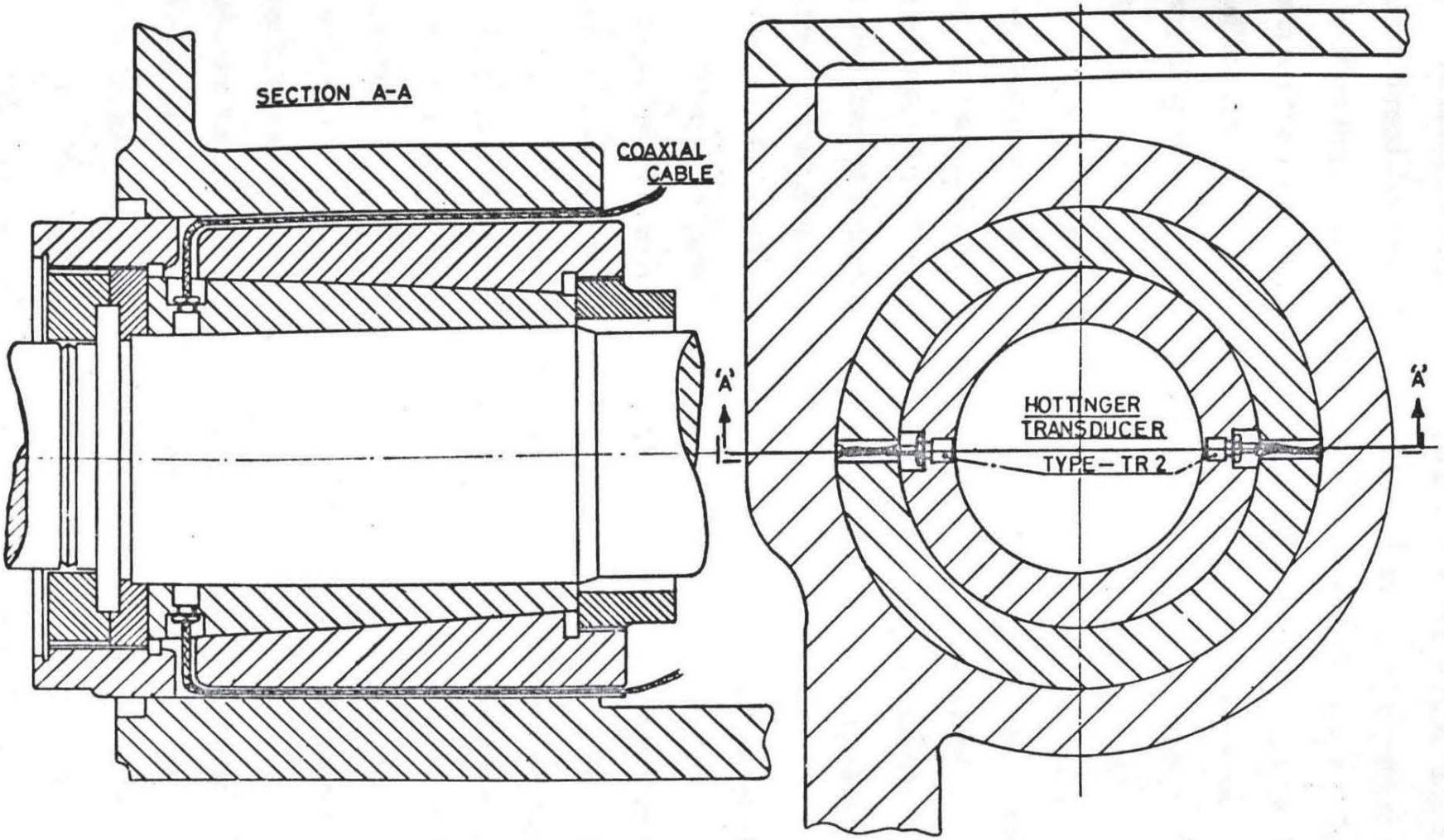

Fig. 6 LOCATION OF PROXIMITY INDUCTIVE DISPLACEMENT TRANSDUCERS IN THE SPINDLE BEARINGS.

(pulley end). To calibrate such a small clearance a direct loading and a differential screw thread device were used. In the direct loading method weights were applied through a number of pulleys as shown in Figure 7. To avoid any hysteresis the shaft was pulled forward and backwards. The general view of the calibration set-up is shown in Figure 8. The positions of the spindle corresponding to various loads is shown in Figure 9. The method of direct loading suffers, however, from the following disadvantages. The radial displacement of the spindle under any given load is not uniform, as indicated by various probes positioned along the length of the spindle, Figure 9. This is because the load could not be applied through the exact centre of gravity of the spindle. Also, the direct loading method does not achieve the small enough displacement increments necessary for obtaining a correct displacement pattern of the spindle.

The principle of the differential screw thread displacement device is shown diagrammatically in Figure 10. As can be seen from the diagram the displacement of the spindle can be achieved by means of a displacement screw 'S'. The thread connecting the block 'K' with the displacement screw 'S' has a pitch of 0.0625 ". The end of the screw connecting the ring 'R' has a pitch of 0.0500". As a result during one revolution of the screw 'S' the radial displacement of the spindle is equal to 0.0625" - 0.0500" = 0.0125" (0.30 mm). By applying a suitable arm (r = 200 mm) at the end of the screw, a displacement of the order of 0.0001" (2.5 μ) can be easily achieved. The displacement of the spindle has been recorded in three positions by applying inductive transducers of the Mitronic and Parnum types, Figure 11. The calibration of the spindle has been achieved in the following way. The ring 'R' mounted rigidly was considered to be an integral part of the spindle. Ten readings of the spindle were taken at equal intervals of 1.5×10^{-4} inches (3.75 μ) between the extreme radial positions in the bearings. The corresponding readings of the Hottinger bridges plotted against the spindle displacements are shown in Figure 12. The

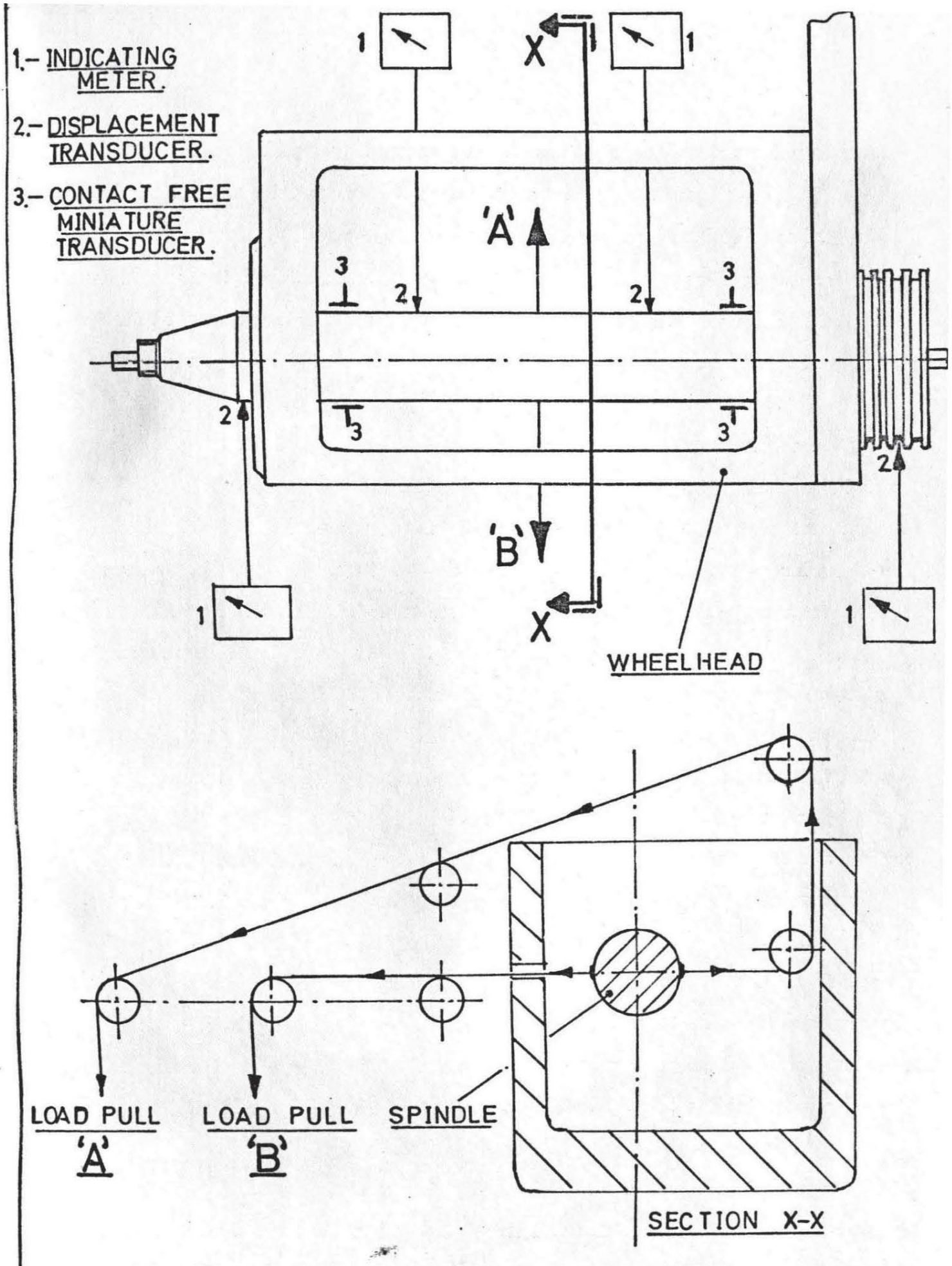

FIG. 7. DIRECT LOADING METHOD FOR THE WHEELSPINDLE DISPLACEMEN

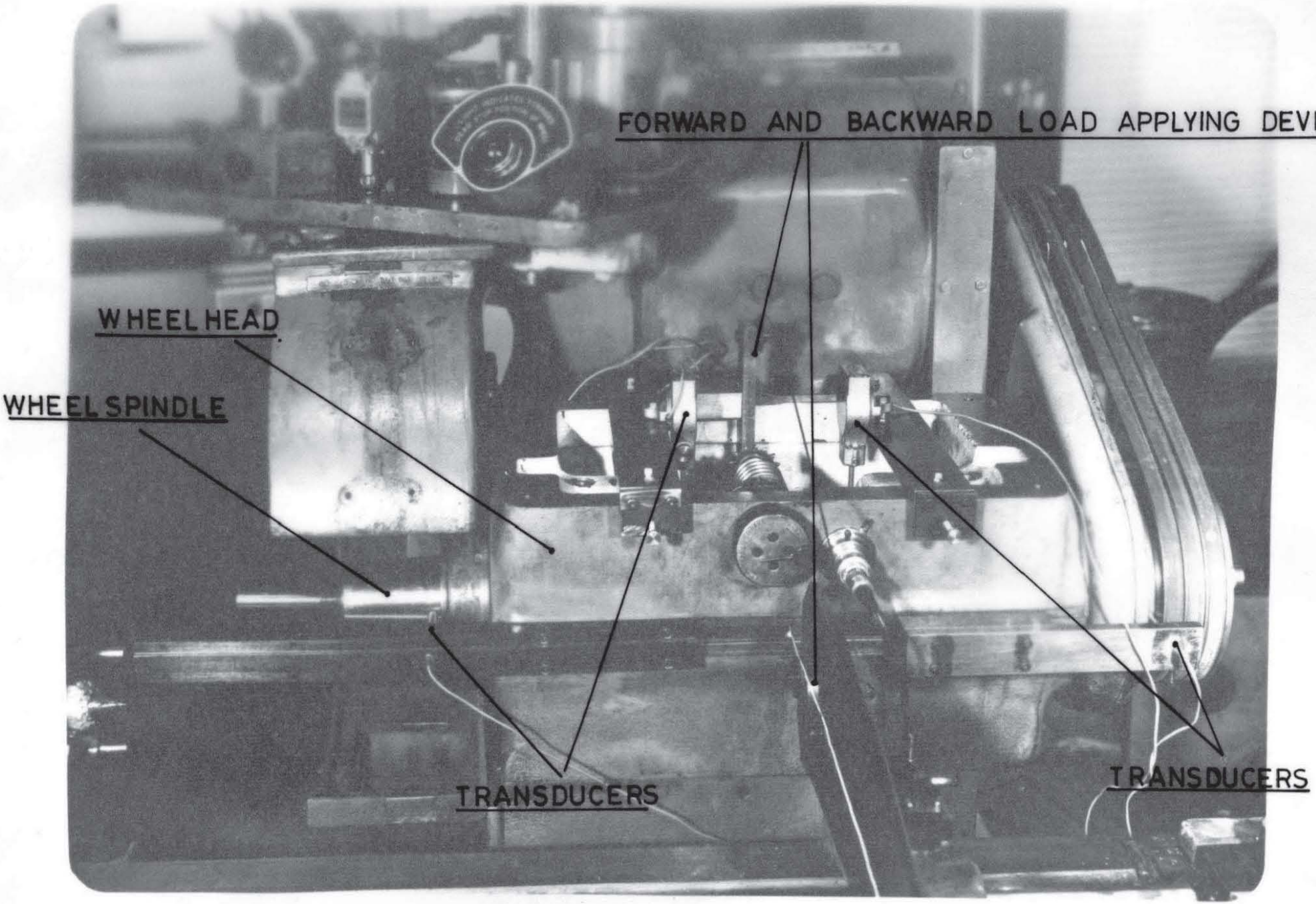

FIG. 8. GENERAL VIEW OF THE CALIBRATION SET UP FOR WHEELSPINDLE MOTION.

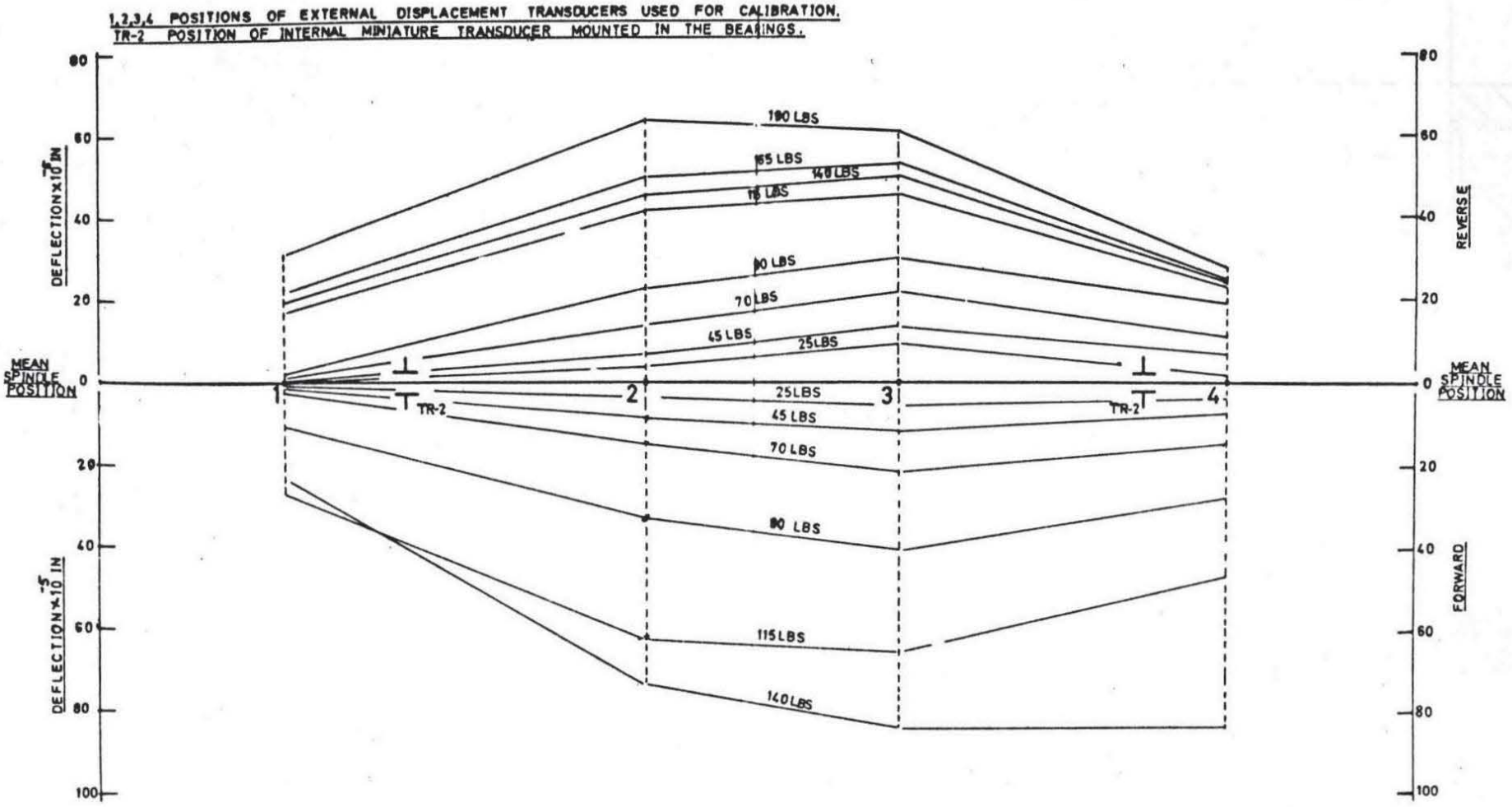

FIG 9 DISPLACEMENT OF THE WHEELSPINDLE AS A FUNCTION OF DIRECT LOAD

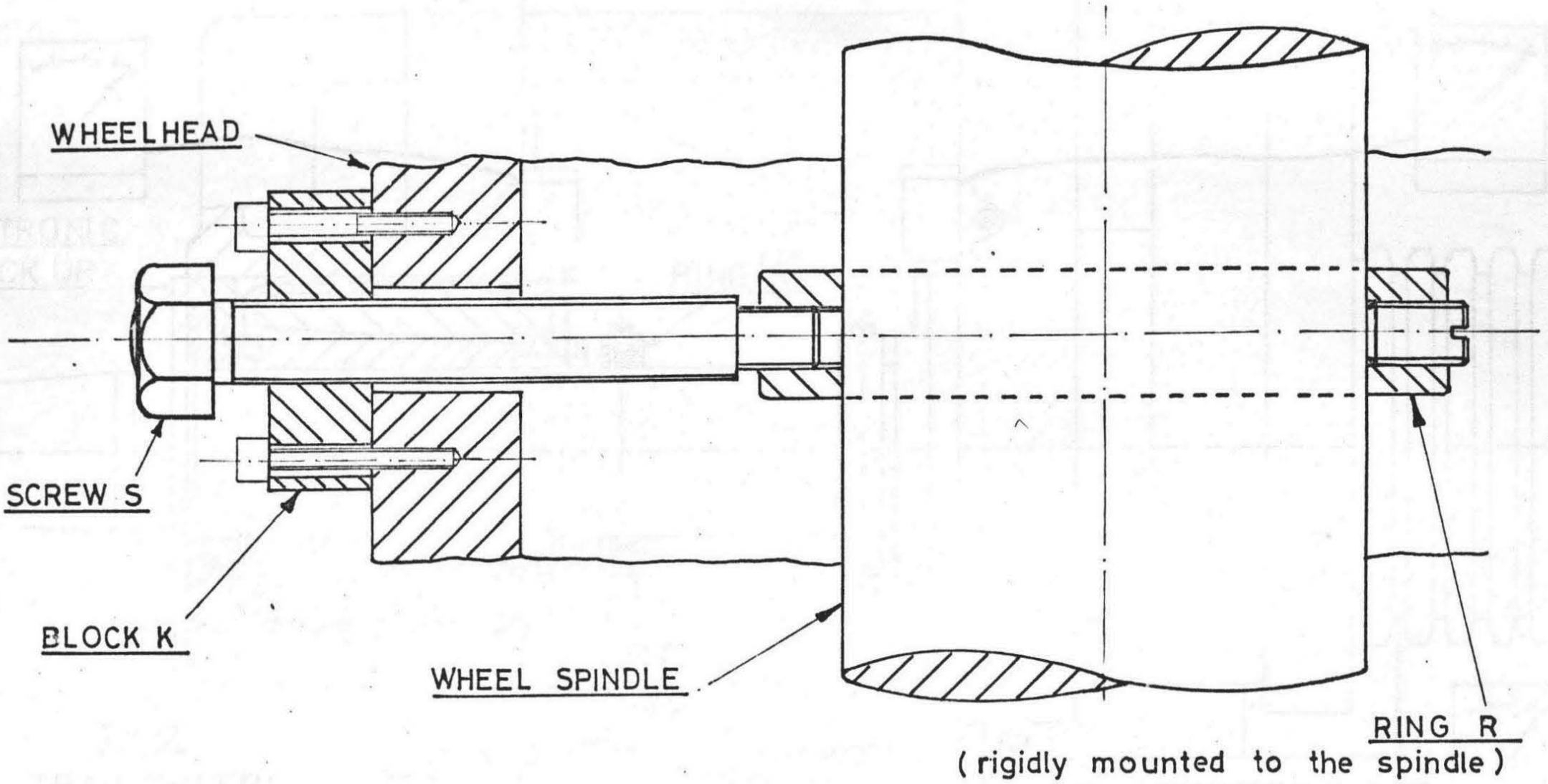

FIG 10. PRINCIPLE OF DIFFERENTIAL SCREW THREAD DEVICE FOR CALIBRATING THE SPINDLE DISPLACEMENT.

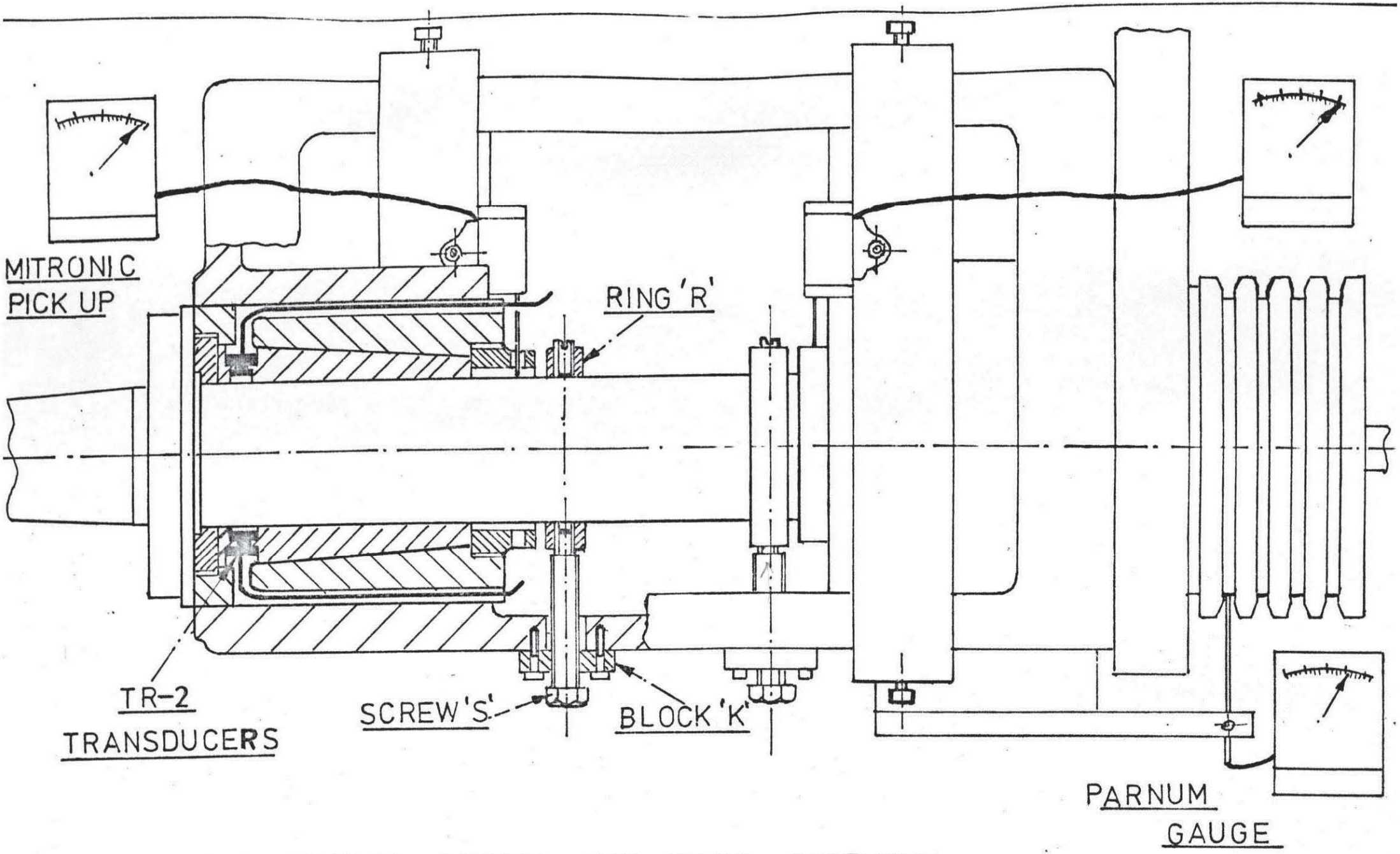

FIG. 11. GENERAL VIEW OF THE SCREW THREAD CALIBRATION DEVICE

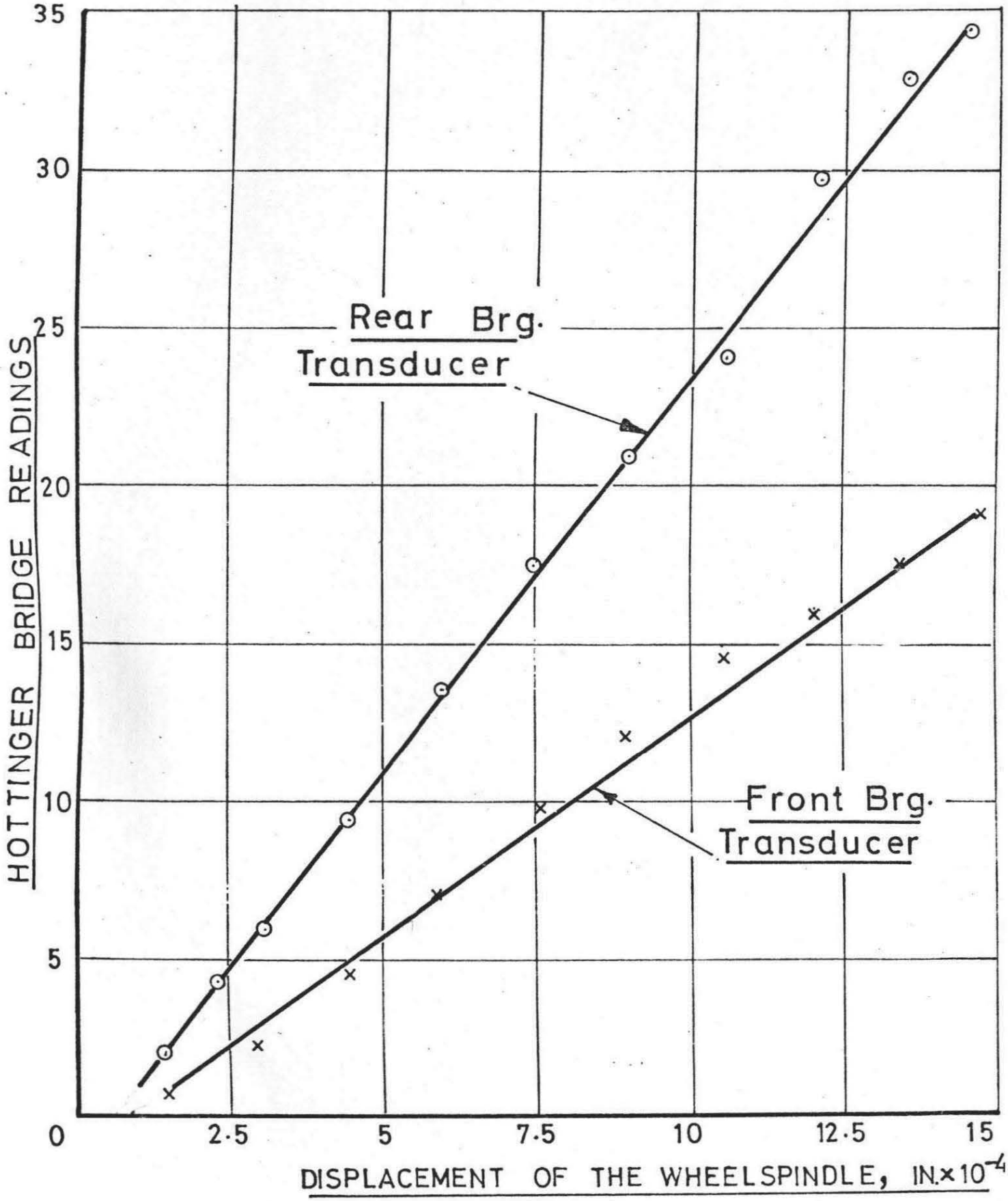

FIG 12. CALIBRATION OF THE WHEELSPINDLE BEARING CLEARANCE.

results show a linear relationship for both transducers with the rear one being more sensitive than the front one. This is due to the different initial airgap in the two bearings.

The two parameters which determine the behaviour of the spindle are the bearing clearance and the bearing temperature. The rigidity of the bearing assembly may differ from the rigidity determined in static conditions. Usually such a change in rigidity may be explained as follows [11]. The quantity of heat transferred from the bearings to the wheelhead body is larger than the quantity transferred through the spindle body. This is caused by the difference in heat conducting properties of the metals, both influences being in the same direction. As a result the diameter of the spindle journal expands more than that of the bearing bronze. This causes an increase in the contact area between the two, thereby reducing the specific pressure and raising the rigidity. In addition, the reduced clearance between the working surfaces causes the oil film to become thinner. As is well known from the hydrodynamic theory of film lubrication, the thinner the oil film in the narrowest part of the oil wedge the larger the specific pressure that can be borne by the bearing. Therefore, to consider the actual temperatures inside the bearings, thermocouples of copper-constantan type have been fitted in both the bearings, as shown in Figure 13.

2.3 Dynamic Behaviour of the Machine

Dynamic tests are employed for investigating the dynamic behaviour of the machine. These tests have been classified into three categories.

(a) Excitation Tests, whereby the application of harmonic exciting force, the frequency response of the various masses of the machine tool is obtained. Each natural frequency obtained in this way gives the modes or vibrating shapes of the machine structure. A clear picture of the motion of the structure becomes available and design changes

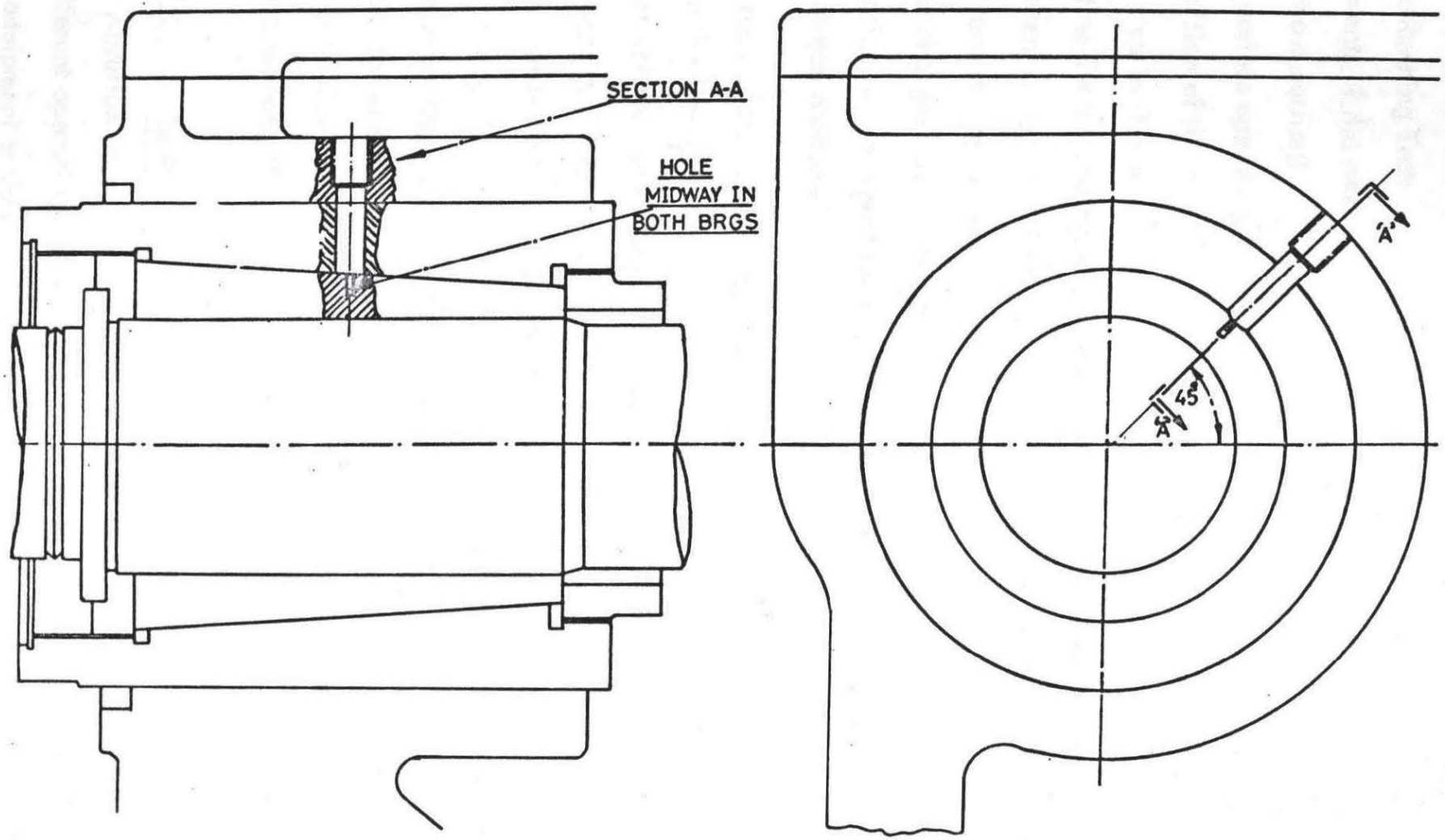

Fig.13 LOCATION OF THERMOCOUPLES INSIDE THE WHEELHEAD BEARINGS.

can be made to take care of the weak spots of the machine tool.

(b) Free Running Tests, in which the vibration measurement of the various elements of the machine tool is made when the machine is running free (without cutting). The response so obtained enables a comparison of the various operating frequencies to be made with the natural frequency condition of the machine tool. A suitable operating speed can be selected in this way.

(c) Cutting Tests, during which the vibration measurements are made under different cutting conditions. A comparison is made with the previous two tests as any variation might result due to wheel work contact or other changes due to the cutting process. The importance of these vibration set up is subsequently indicated by the surface quality of the workpiece produced.

The tests under (a) were conducted by Singhal [14]. They have been mentioned in the first part of this Chapter under "Dynamic System of the Machine", where the natural frequency and amplitude of the various masses are given. The cutting tests under (c) are described in Chapter 5 on "Grinding Results". In the present experiments some free running tests were conducted with a constant centrifugal force at different operating speeds of the machine. To maintain the centrifugal force constant various unbalance weights were used. Since it was not possible to measure vibration correctly due to the irregular surface structure of the wheel, it was replaced by an aluminium wheel of the same mass and moment of inertia for these experiments.

2.3.1 Rocking Mode of the Machine

The vibration characteristics of the wheelhead, workpiece and wheel-guard at different operating speed of the machine are shown in Figure 14. The diagram of equipment is shown in Figure 15. As can be seen from Figure 14,

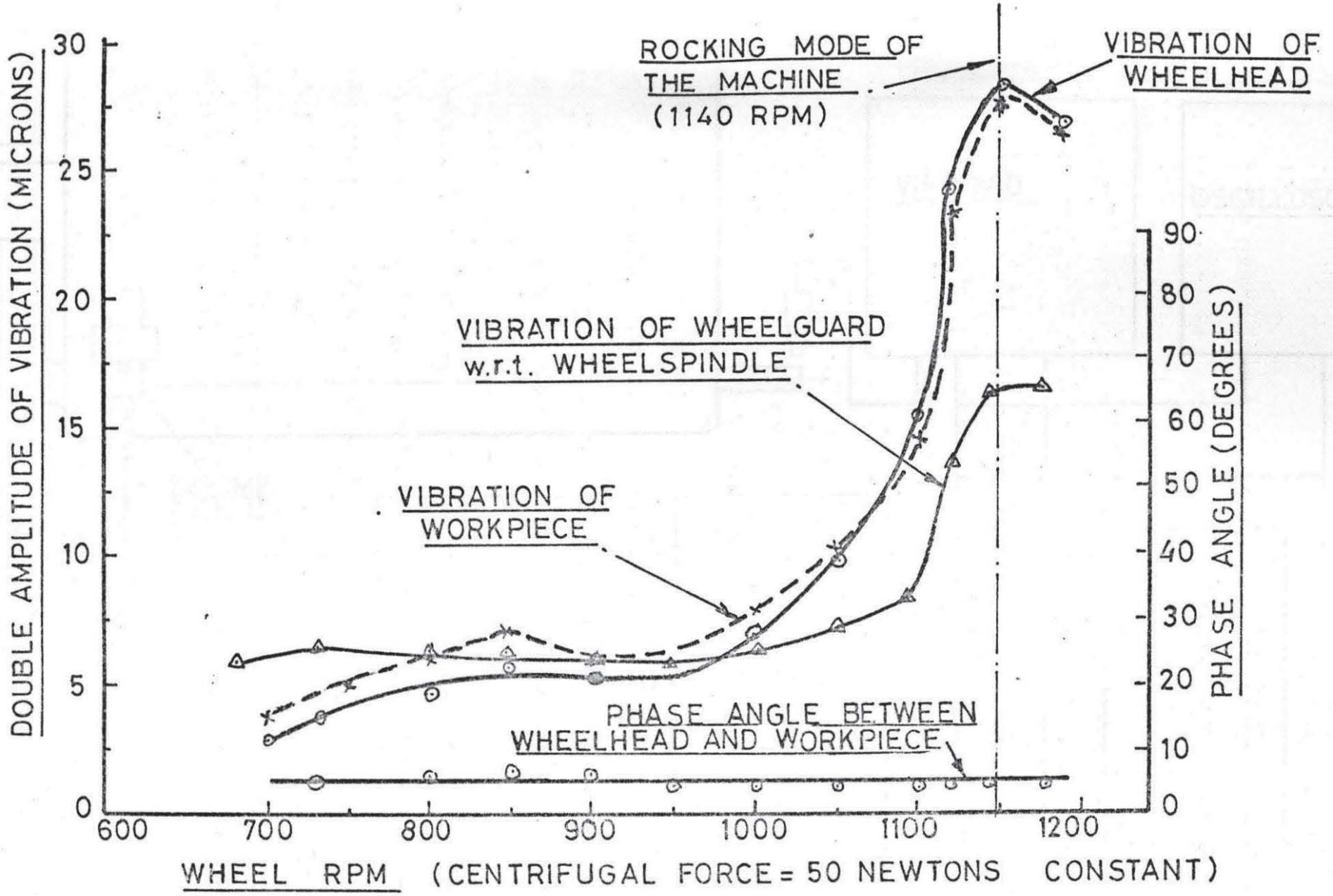

FIG 14. VIBRATION BEHAVIOUR OF THE MACHINE UNDER FREE RUNNING CONDITION.

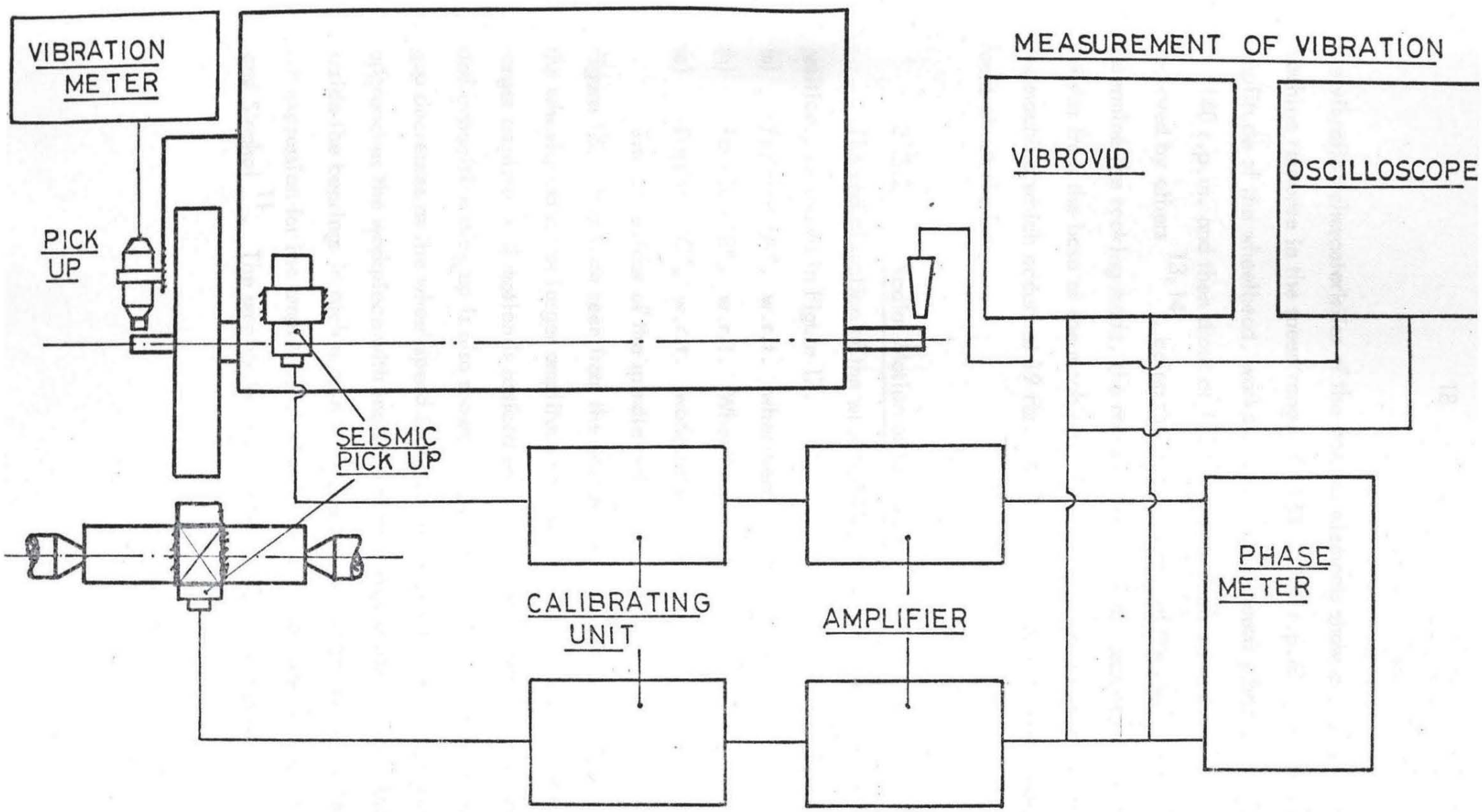

(SEE FIG 17 ALSO)

FIG 15. EQUIPMENT FOR ANALYSING THE VIBRATION BEHAVIOUR OF THE MACHINE.

the vibration characteristics of the various elements show a change in the machine response in the speed range of 1120 - 1160 r.p.m. The maximum amplitude of the wheelhead, workpiece and wheelguard vibration is attained at 1140 r.p.m. and then drops at 1160 r.p.m. Such a trend has also been observed by others [13,14], being the rocking mode of the machine. To determine the rocking mode, the radial vibration was measured at different heights from the base of the machine. Figure 16 shows the rocking mode of the machine which occurs at 19 Hz. At this frequency the whole machine rocks about the base.

2.3.2 Radial Motion of the Spindle

The radial motion of the wheelspindle has been considered at three positions, as shown in Figure 17.

(a) Position "A", w.r.t. wheelhead in the rear bearing.

(b) Position "B", w.r.t. Wheelhead in the front bearing.

(c) Position "C", w.r.t. workpiece.

The behaviour of the spindle motion at these three positions is shown in Figure 18. It can be seen from the graphs that at lower speeds (below 1050 r.p.m. the wheelspindle has larger amplitude of motion at "A" and at higher speeds the larger amplitude of motion is noticed at "C". The air gap between the wheel and capacitive pick up is also shown in Figure 18. As can be seen, the air gap decreases as the wheel speed increases which means that the wheelspindle approaches the workpiece with increase of the wheelspeed. The spindle position inside the bearings in such a case would be similar to the one suggested by Doi [20]. An expression for the amplitude of wheel vibration has been derived by Kaliszer and Singhal [11]. The amplitude 'A_2' of wheel vibration is given by

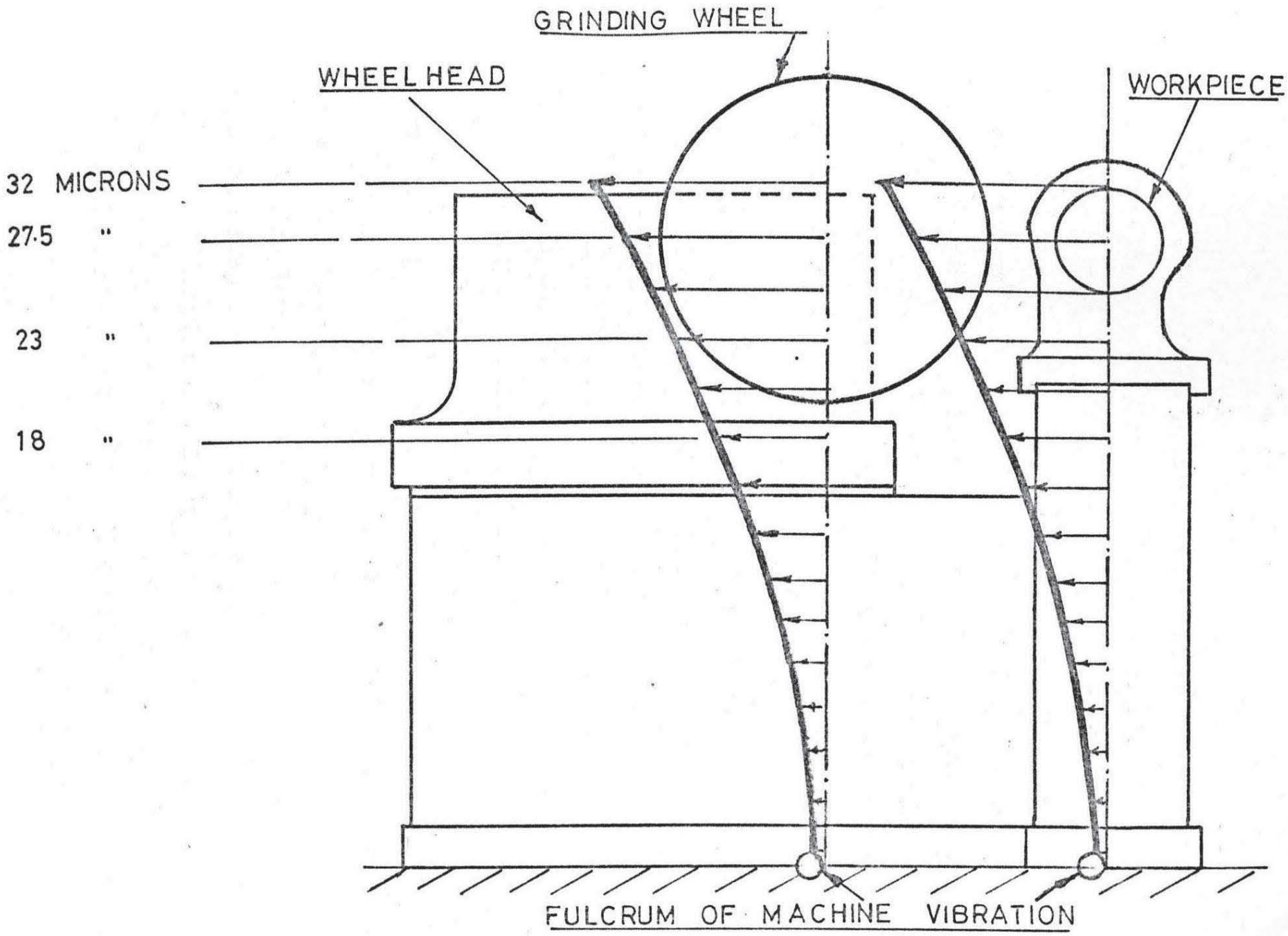

FIG 16. VIBRATION OF THE MACHINE AT THE ROCKING MODE.

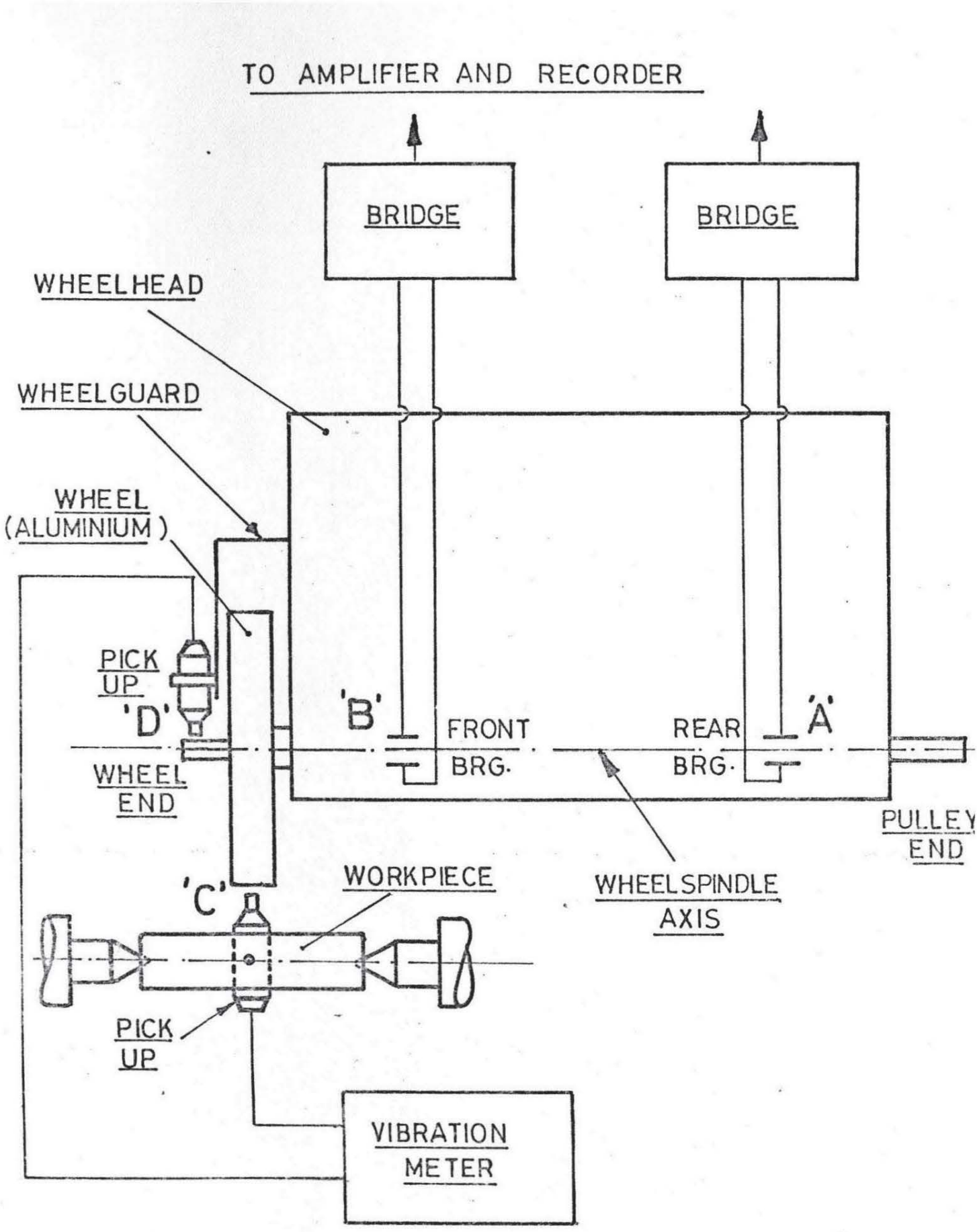

FIG 17. EQUIPMENT FOR ANALYSING THE RADIAL MOTION OF THE WHEELSPINDLE.

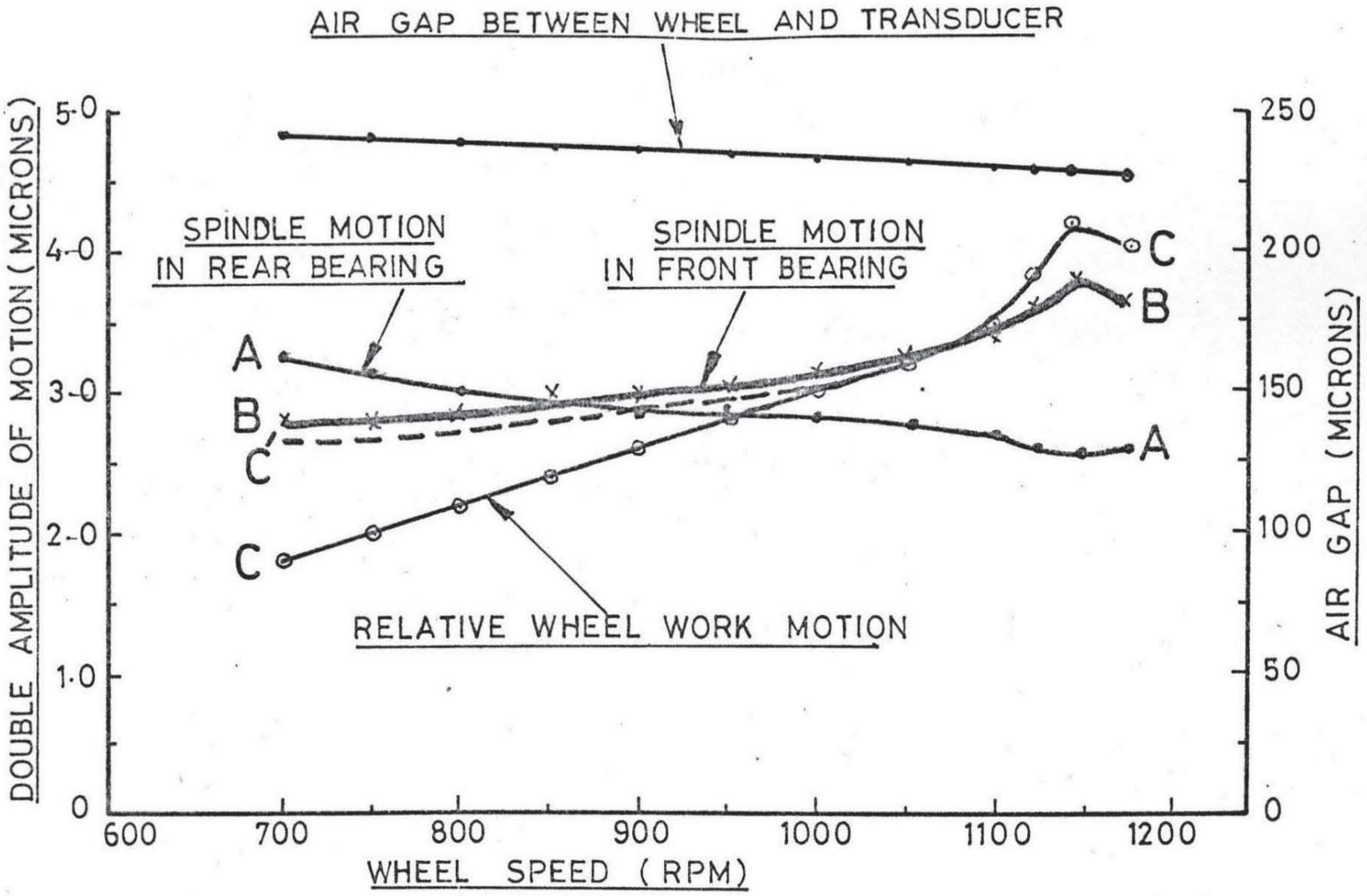

FIG 18. BEHAVIOUR OF THE SPINDLE MOTION AT DIFFERENT WHEEL SPEEDS.

$$A_2 = \frac{\frac{w}{g} \cdot \omega^2 \cdot r}{k_2 (1 - \omega^2 \frac{m_2}{k_2})} = \frac{F}{k_2 (1 - \frac{\omega^2 \cdot m_2}{k_2})}$$

where

$F = \frac{w}{g} \cdot \omega^2 \cdot r$ = Centrifugal force due to wheel unbalance w.

k_2 = Rigidity of the wheelspindle bearing.

m_2 = Mass of the wheelspindle assembly.

ω = Frequency of wheel rotation.

The damping term in this expression has not been considered by the authors. The centrifugal force 'F' was kept constant in these experiments. Mass m_2 of the wheelspindle assembly is also constant. The rigidity k_2 amy change with the rise of temperature [11], but since the vibration in these tests was measured after the machine was warmed up, this value of k_2 is assumed to be constant. Because F, k_2 and m_2 are constant, therefore, assume $F/k_2 = D$ and $\frac{m_2}{k_2} = \frac{1}{\rho^2}$, where ρ is the natural frequency of the spindle. Since the test frequency (20 cps) is much lower than the natural frequency (190 cps), therefore ρ can be considered practically constant. The expression for A_2 therefore becomes

$$A_2 = \frac{D}{(1 - \frac{\omega^2}{\rho^2})}$$

where D and ρ are constant.

Now as ω increases, the value of $1 - K\omega^2$ decreases and, therefore, A_2 increases. This explains why the amplitude of motion at C increases with the increase of ω. Now considering the spindle position in Figure 19, it can be seen that the motion in the front bearing at 'B' will also increase with the increase of wheel speed. The motion in this case will, however, be less than the motion at C. This follows in accordance with the graphs in Figure 19. The decrease of spindle motion in the rear bearing

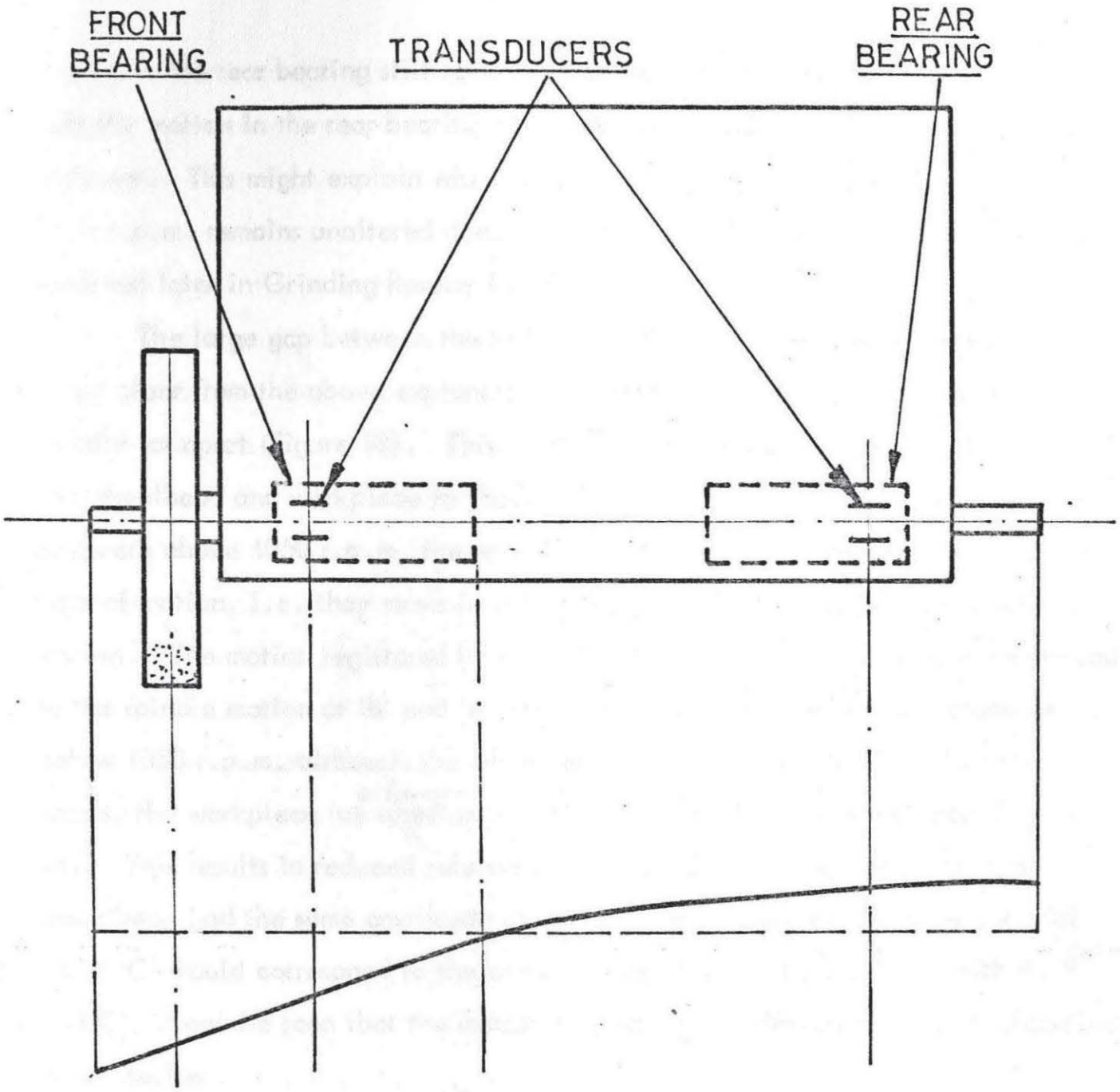

FIG 19. WHEEL SPINDLE POSITION INSIDE THE BEARINGS.

motion in the rear bearing still remains unexplained. However, it is clear that the motion in the rear bearing at speeds above 1100 r.p.m. almost becomes constant. This might explain why the spindle motion in the rear bearing at 1175 r.p.m. remains unaltered due to increase of unbalance as has been observed later in Grinding Results (Chapter 5).

The large gap between the motions at 'B' and 'C' at slower speeds is not clear from the above explanation, although the two positions are not axially far apart (Figure 18). This is explained by considering the motion of the wheelhead and workpiece in Figure 14. As can be seen from this Figure, at speeds above 1050 r.p.m. the wheelhead and workpiece experience the same type of motion, i.e. they move in the same phase and with similar amplitude of motion. The motion registered by the pickup at 'C' in this case would correspond to the spindle motion at 'B' and 'A' inside the bearings. However, at speeds below 1050 r.p.m. although the wheelhead and workpiece move in the same phase, the workpiece has a larger amplitude of motion than the wheelhead (Figure 14). This results in reduced relative motion at 'C'. If the workpiece and wheelhead had the same amplitude of motion, the motion registered by the pick up at 'C' would correspond to the dotted curve at C' in Figure 18. With A, B and C', it can be seen that the motion follows in accordance with the explanation given earlier.

2.3.3 Motion of the Wheelguard

The radial motion of the wheelspindle was also investigated at wheel-guard position "D". This has already been shown in Figure 14. On comparing this motion at D (Figure 14) with the relative wheel work motion at 'C' (Figure 18), it can be seen that the amplitude behaviour of the two motions is very different. The amplitude of the wheelguard motion at "D" is much larger than the relative wheel-workpiece motion at "C" although the axial distance between the two positions is not large. This difference is particularly noticeable in the

higher speed range of 1120 to 1175 r.p.m. On investigating the phase difference between the wheelhead and the workpiece, it was found that both of them moved in the same phase (Figure 14). Since the wheelguard is mounted on the wheelhead, it follows that this larger motion at the wheelend is caused by some special phenomenon. Following a suggestion by Bennet and May [15] it was thought that this may be due to the wheelwhirling displacement as shown in Figure 20. This assumption, however, did not apply as has been shown by the motion of the spindle measured along its axis after removing the wheelguard. This suggests that the wheelguard itself accounts for this large difference. On replacing the wheelguard the vibration of the relevant masses, workpiece, wheelhead and wheelguard were measured again without applying any forced vibration (balanced wheel). The new vibration pattern is shown in Figure 21. As can be seen the vibration of the workpiece and wheelhead are almost negligible whereas the vibration at the wheelguard remains very large and almost unchanged (compare Figure 14). This clearly indicates a low rigidity of the wheelguard due to insufficient mounting. The effect of this low rigidity is most pronounced at the rocking frequency of the machine (19 Hz).

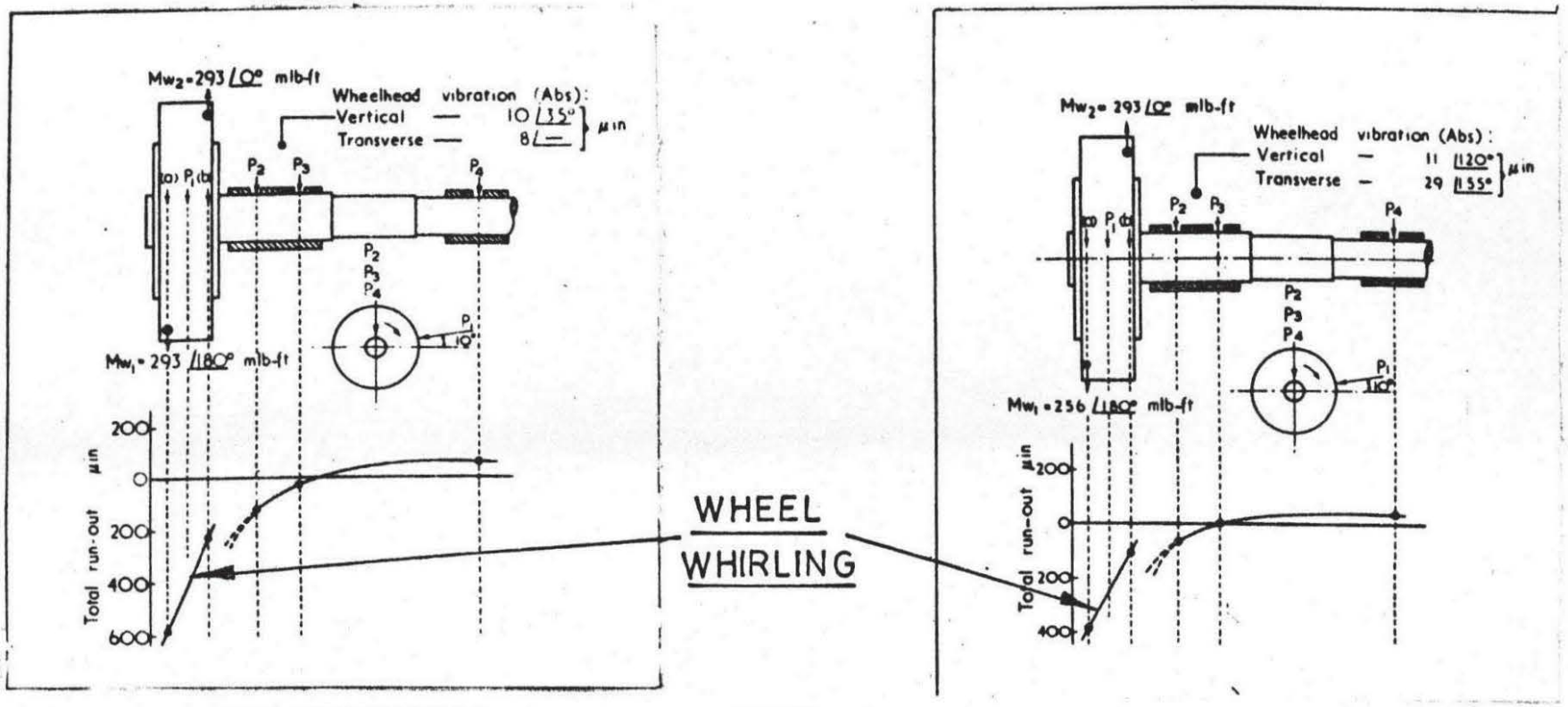

WHEEL AND SPINDLE WHIRLING DISPLACEMENTS WITH WHEEL STATICALLY BALANCED BUT DYNAMICALLY UNBALANCED.

WHEEL AND SPINDLE WHIRLING DISPLACEMENT WITH STATIC AND DYNAMIC UNBALANCE.

15

(BENNET AND MAY)

FIG 20. WHIRLING DISPLACEMENT OF THE WHEEL.

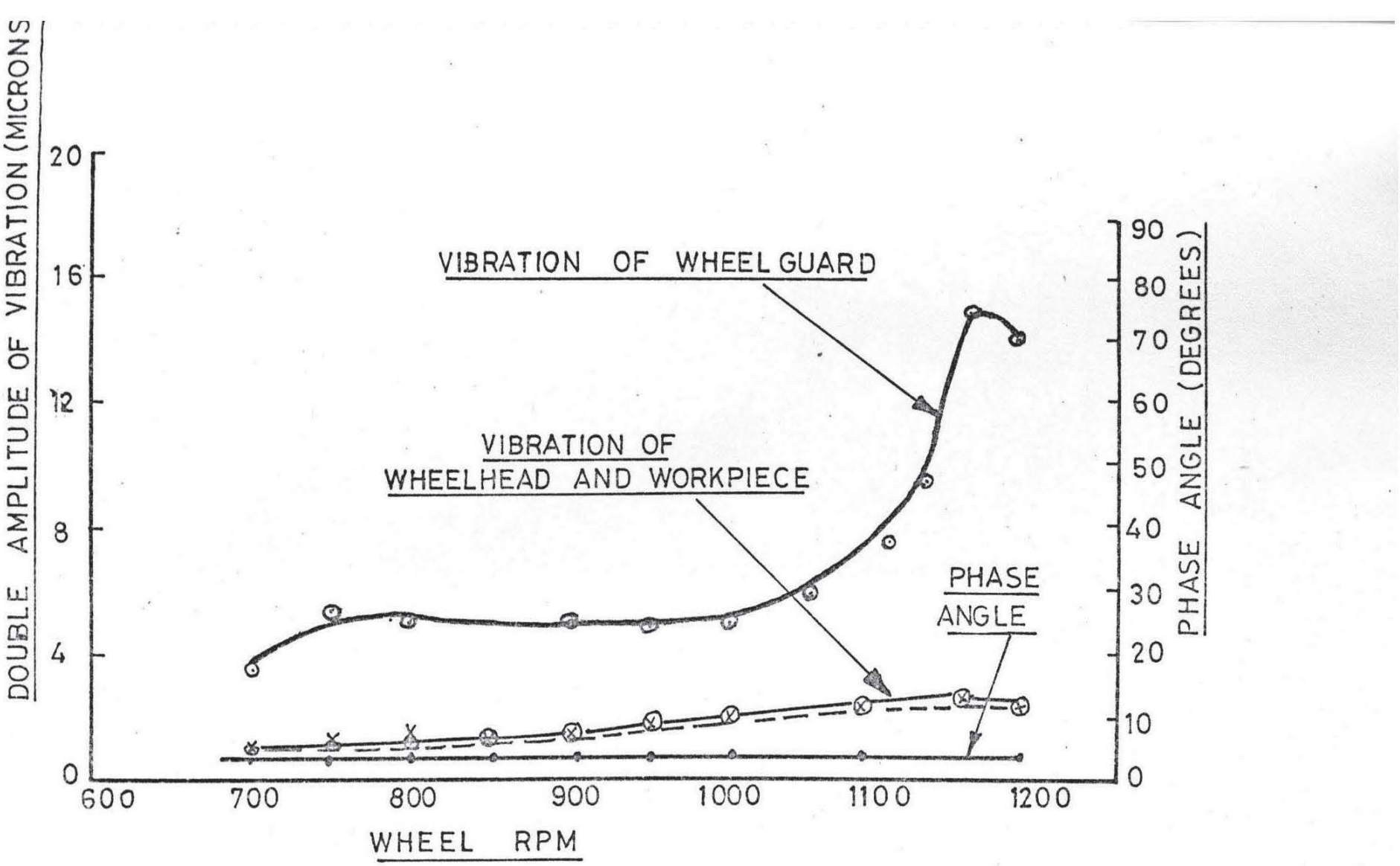

FIG 21. FREE RUNNING BEHAVIOUR OF THE MACHINE WITH A BALACED WHEEL.

CHAPTER 3

WHEEL UNBALANCE AND WORKPIECE SURFACE QUALITY

Both micro and macro irregularities may be generated as a result of vibration during grinding. The surface irregularities considered in the present investigation are shown in Figure 22. The irregularities along the axis of the workpiece are composed of two components, i.e. longitudinal waviness (Figure 22a) and surface roughness (Figure 22b). The two components superimposed on each other are shown in Figure 22c. Besides these two types there is also a waviness generated on the workpiece periphery as shown in Figure 22d.

3.1 Workpiece Waviness Due to the Wheel Unbalance

As a result of vibration generated during grinding, certain waviness usually appears on the workpiece and grinding wheel circumferences [14]. A typical case of vibration may develop when the grinding machine is under the influence of periodic external forces as for example centrifugal forces due to wheel unbalance. Such forces will induce a relative vibratory motion between the wheel and the workpiece. The amplitude of this vibratory motion depends upon the rigidity of the grinding machine and is largely affected by the wheel and workpiece parameters.

The number of waves formed on the workpiece periphery can be derived by dividing the rotational speed of the wheel by that of the workpiece irrespective of the cause of vibration [10].

$$i = \frac{n_g}{n_w} = \frac{30\,\omega}{n_w} \approx 10\,\frac{\omega}{n_w} \qquad (1)$$

A typical polargraph taken by means of a Talyrond is shown in Figure 23. From equation (1) the wavelength of the waviness can be derived

LONGITUDINAL WAVINESS

FIG 22 a

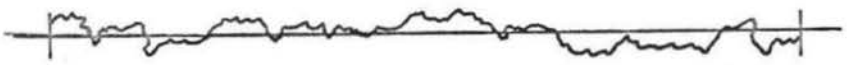

ROUGHNESS

FIG 22b

ROUGHNESS IMPOSED UPON LONGITUDINAL WAVINESS

FIG 22 c

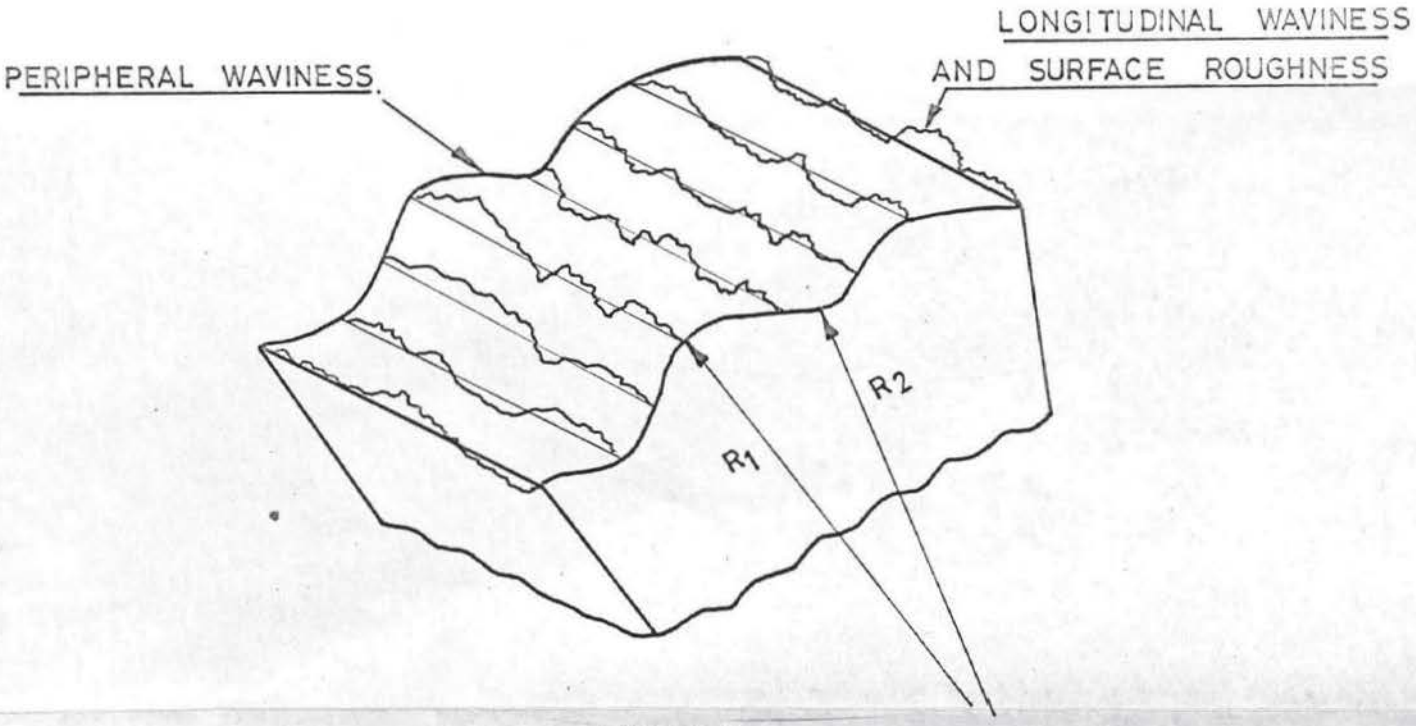

FIG 22d

FIG 22. MICRO AND MACRO IRREGULARITIES ON A CYLINDERICAL SURFACE.

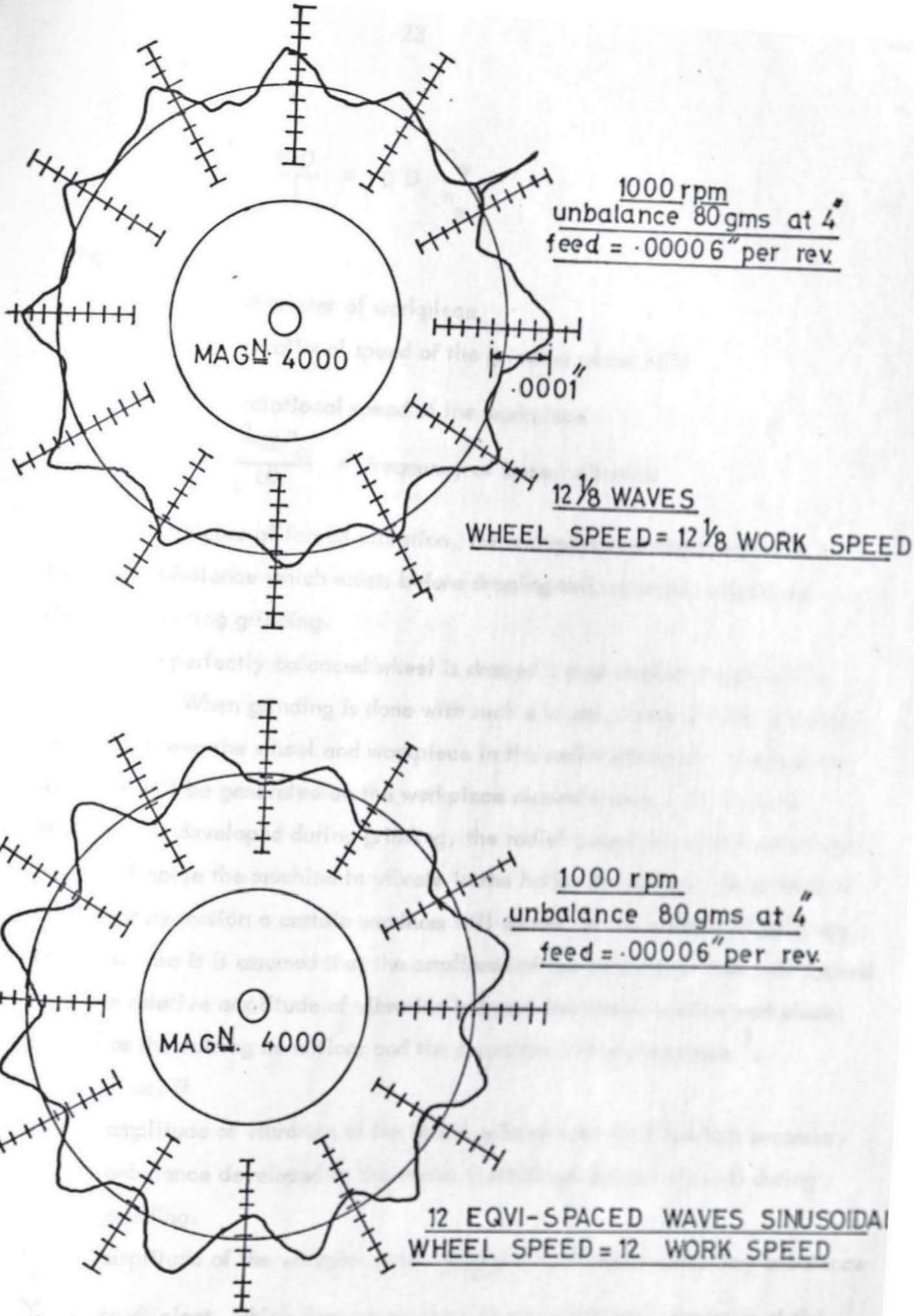

FIG. 23 WAVINESS OF THE WORKPIECE PERIPHERY DUE TO FORCED VIBRATION

$$\lambda = \frac{\pi D}{i} = \pi D \frac{n_w}{n_g} \qquad (2)$$

where

D = diameter of workpiece

n_g = rotational speed of the grinding wheel RPM

n_w = rotational speed of the workpiece

$\omega = \frac{2.\pi.n_g}{60}$ = frequency of forced vibration

In the case of forced vibration, the workpiece waviness may be due to initial unbalance which exists before dressing and secondary unbalance developed during grinding.

If a perfectly balanced wheel is dressed a true circular shape will be generated. When grinding is done with such a wheel, there will be no relative motion between the wheel and workpiece in the radial direction. Hence, no waviness will be generated on the workpiece circumference. If, however, unbalance is developed during grinding, the radial component of the centrifugal force will cause the machine to vibrate in the horizontal plane. As a result of this vibratory motion a certain waviness will appear on the workpiece periphery. In such a case it is assumed that the amplitude of the formed waviness will depend upon the relative amplitude of vibration between the wheel and the workpiece, as well as the cutting conditions and the properties of the workpiece [3].

Thus, if

a_1 = amplitude of vibration of the wheel spindle mass (m_2) due to a secondary unbalance developed in the wheel (centrifugal force $F \sin \omega t$) during grinding.

a_2 = amplitude of the workpiece mass (m_3) due to the same secondary unbalance

γ = coefficient, which depends on the cutting conditions, properties of the

workpiece grinding wheel, etc.

Then,

$$A_{wa} = \gamma\ (a_1 - a_2) \qquad (3)$$

where

A_{wa} = amplitude of workpiece waviness due to wheel unbalance developed during grinding.

When an unbalanced wheel is dressed, the wheel develops an oval shape. During grinding, if the workpiece is in the same position with respect to the wheel as the diamond, the oval shape and the vibration of the wheel being in opposite phase tend to nulify the effects of each other. However, owing to different dynamic conditions during dressing and grinding the two are not equal. As a result, the effect of unbalance still remains and consequently, waviness is generated on the workpiece periphery [14].

Referring to Figure 24, 0 represents the geometric axis of the bearing and G the centre of gravity of the wheel (the wheelhead and the workpiece are assumed to have no movement in the radial direction).

In Figure 24a and Figure 24b, the centre of gravity of the wheel G is at a distance a from 0. In the figure, "a" represents an amplitude of vibration of the wheel assembly developed during dressing due to the presence of a centrifugal force F $\sin\omega t$. The distance between the dressing diamond and the centre of the bearing is R_1. As follows from the figure,

$$0A = 0B = R_1 \quad \text{and} \quad 0G = a$$

The radial distance between the C.G. of the wheel and the cutting point is minimum at GA. As can be seen from Figure 24a,

$$GA = A0 - 0G = R_1 - a$$

and maximum at BG. According to Figure 24b,

$$GB = 0B + 0G = R_1 + a$$

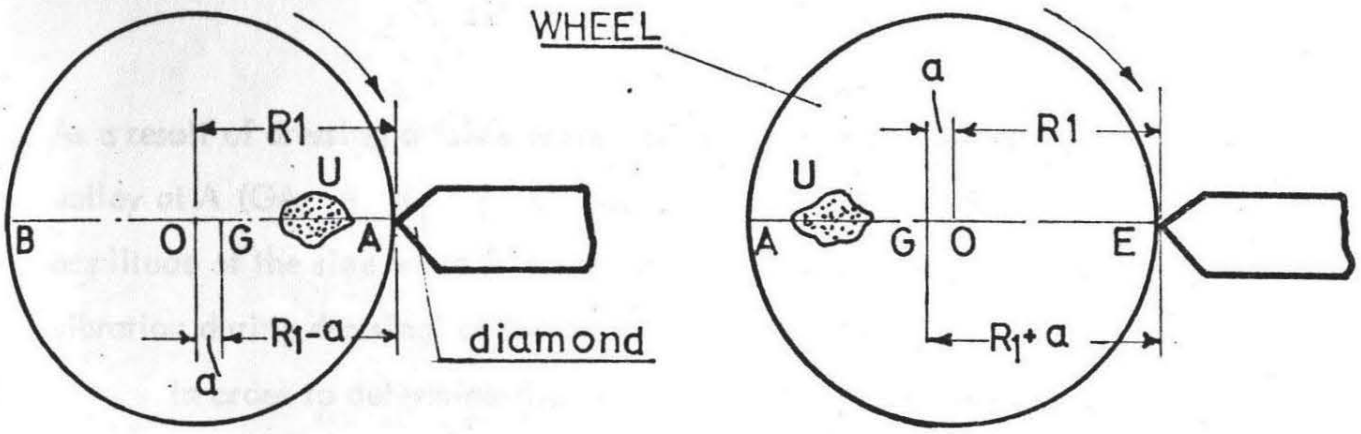

Fig 24a

Fig 24b

DRESSING OPERATION (unbalance U shown in two extreme positions)

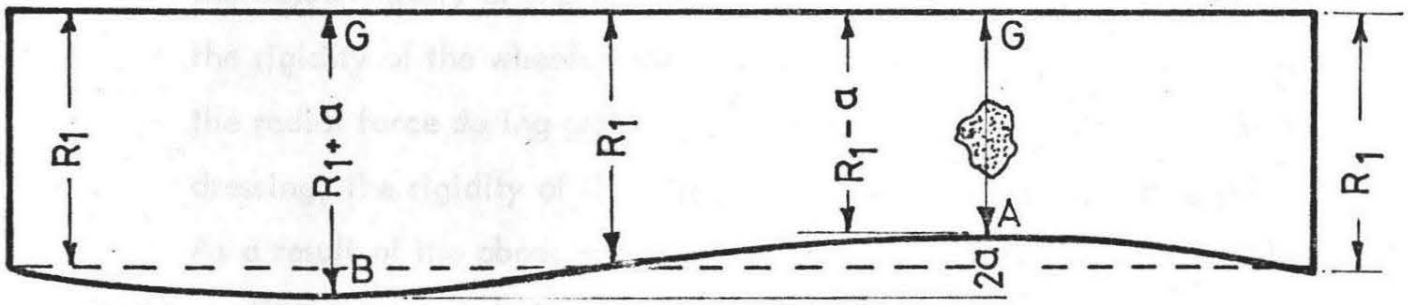

WHEEL PROFILE AFTER DRESSING

(in static conditions G and O coincide)

Fig 24c

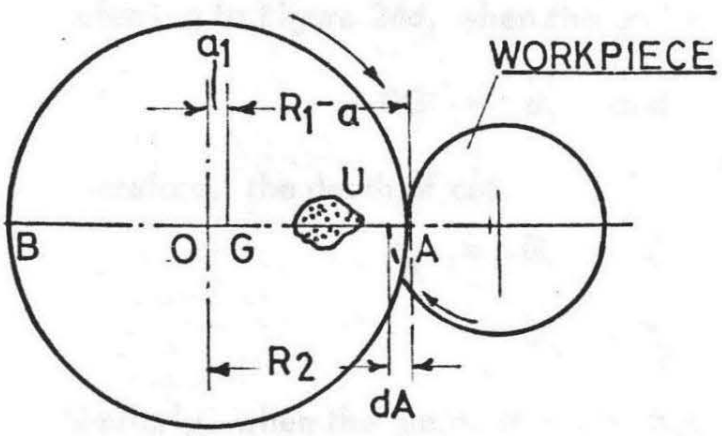

Fig 24d

GRINDING OPERATION

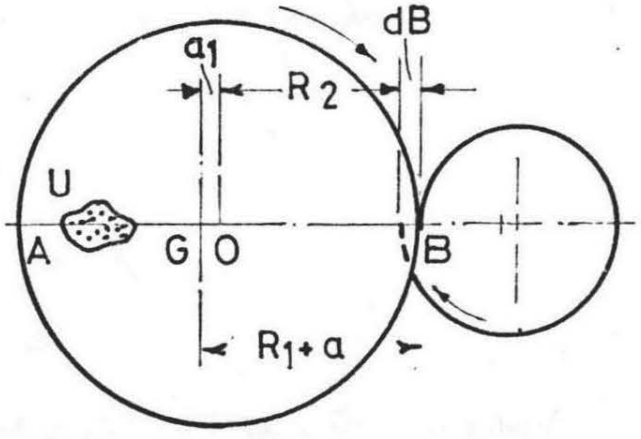

Fig 24e

(unbalance U shown in two extreme positions)

FIG 24. EFFECT OF DRESSING A GRINDING WHEEL HAVING AN INITIAL UNBALANCE.

As a result of dressing a "sine wave" appears on the wheel periphery with the valley at A ($GA = R_1 - a$) and peak at B ($GB = R_1 + a$). The amplitude of the sine wave is equal to 2a (or twice the amplitude of wheel vibration during dressing) as shown in Figure 24c.

In order to determine the amplitude of vibration during grinding the following changes in the dynamic conditions of the system should be considered:

1) Additional coupling between the wheelspindle and the workpiece which introduces additional springs, masses, etc., into the existing system.
2) Increased rigidity of the wheelspindle. As follows from previous tests [14] the rigidity of the wheelspindle increases as the load increases. Since the radial force during grinding is considerably larger than that during dressing, the rigidity of the wheelspindle will be higher during grinding.

As a result of the above-mentioned factors, the amplitude of the wheel vibration will be reduced during grinding.

Hence,

$a_1 < a$ if

R_2 = the distance of the workpiece periphery from 0 during grinding, then nominal depth of cut $= R_1 - R_2$.

Referring to Figure 24d, when the grains at A are engaged in cutting,

$$0G = a_1 \quad \text{and} \quad GA = R_1 - a$$

Therefore, the depth of cut

$$d_A = (R_1 - a) + a_1 - R_2$$
$$= (R_1 - R_2) - (a - a_1)$$

Similarly, when the grains at B are engaged in cutting (Figure 24e), the depth of cut

$$d_B = (R_1 + a) - a_1 - R_2$$
$$= (R_1 - R_2) + (a - a_1)$$

Hence

$$d_B - d_A = 2(a - a_1)$$

(Since $a > a_1$, the depth of cut at B is higher than that at A. Hence, the wheel wear at B will be greater than at A. This will reduce the amplitude of the "sine wave" dressed on the wheel).

Thus, the depth of cut will vary sinusoidally between a minimum value at A and a maximum value at B, in every revolution of the grinding wheel. The cutting force will fluctuate accordingly and so forced vibration will be generated in the system, having the same frequency as the rotational speed of the grinding wheel.

The amplitude of workpiece waviness generated in this case cannot be directly calculated from Figure 24 because the workpiece was assumed to have no movement in the radial direction. Therefore, the amplitude of the waviness is found indirectly as shown in Table 2.

TABLE 2

Determination of amplitude of workpiece waviness (forced vibration)

	Condition of wheel unbalance	
	Unbalance developed during grinding	Unbalance present before dressing
The variation in the depth of cut (no radial movement of the workpiece).	$2a_1$	$2(a - a_1)$
Variation in the cutting force	dF	$dF' = \frac{a-a_1}{a_1}\ dF$
Amplitude of workpiece waviness	$\gamma\ (a_1 - a_2)$	$\frac{a-a_1}{a_1} \cdot \gamma \cdot (a_1 - a_2)$

In Table 2, dF represents the variation in the cutting force due to wheel unbalance developed during grinding. The remaining entries in the second column were discussed previously. The variation in the cutting force and the amplitude of workpiece waviness in the last column are calculated on the assumption that the cutting force and the amplitude of workpiece waviness are proportional to the variation in the depth of cut.

From the table, the amplitude of workpiece due to the wheel unbalance present before dressing can be expressed as:

$$A_{wb} = \frac{a - a_1}{a_1} \cdot \Upsilon \cdot (a_1 - a_2) \qquad (4)$$

where

A_{wb} = amplitude of workpiece waviness due to wheel unbalance present before dressing.

The amplitude of workpiece waviness as a function of wheel unbalance (added before and after dressing), wheel grade, and different workpiece materials, is given in Chapter 5.

3.2 Analysis of the Surface Roughness

Surface roughness may be characterised by many parameters, as outlined by Sharman [21] and Reason [22]. In the present investigation the following parameters have been considered,

i) CLA (British Standards)

ii) Maximum peak to valley height

iii) Bearing area.

It is convenient to measure surface parameters using stylus instruments. They provide the best way of finding the numerical value of the various parameters [21]. By using a digital voltmeter, the amplified signal from the stylus can be recorded on a punched tape. With the help of a suitable programme,

the digital computer can very rapidly and accurately determine the various parameters from the punched tape.

3.2.1 Application of Stylus Instruments

Modern equipment like the Talysurf III and IV is most commonly employed for the purpose of measuring surface roughness. Parameters such as the CLA is evaluated by an electrical integrating device incorporated in these instruments. Other parameters like bearing area and maximum peak to valley height are also calculated by some analogue devices incorporated in the multiparameter surface meters. A record of the profile of the surface can be obtained by a profile recorder. The use of these instruments for measuring surface roughness is limited because they could only calculate a few parameters with accuracy. This difficulty has been overcome with the introduction of recent analogue to digital converting devices which enable the stylus signal to be recorded in a digital form. By using a digital computer, virtually any surface parameter can be calculated from this digital record provided some real mathematical expression is available. The stored information on punched tape is also useful for future reference. A very large number of ordinates may be considered depending upon the computer capacity.

3.2.2 Analogue to Digital Conversion

The equipment used for analogue to digital conversion is shown in photograph Figure 25 and a general arrangement of the whole set-up is shown in Figure 26. The first step is to select a suitable ordinate spacing.

Ordinate spacing or sampling rate depends upon the traverse speed of the Talysurf stylus and the digitising rate of the A.D. converter. For the equipment used different values of the above two factors are tabulated in the Following Table, No. 3.

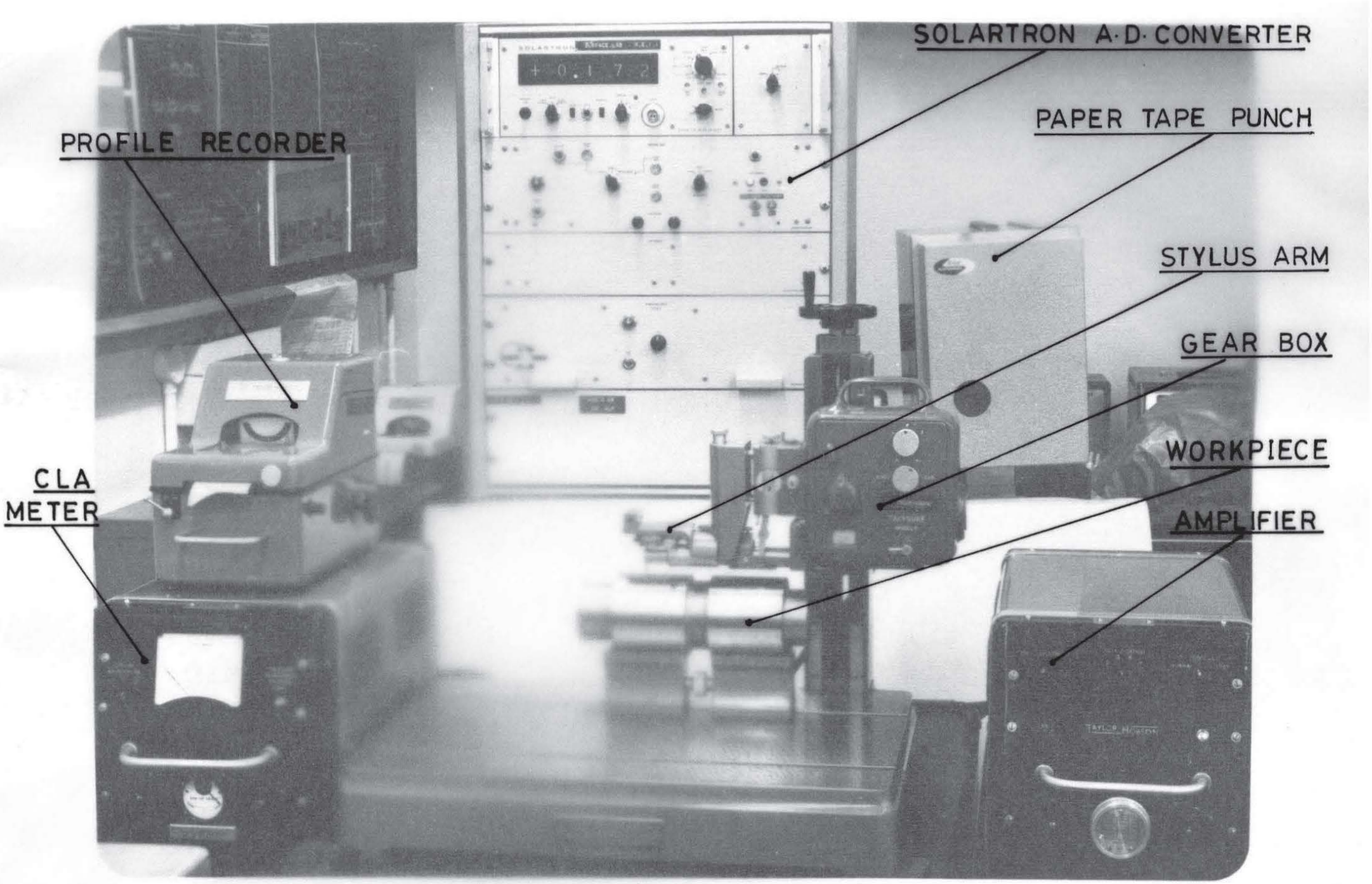

FIG. 25. PHOTOGRAPH OF THE SURFACE ROUGHNESS MEASURING EQUIPMENT.

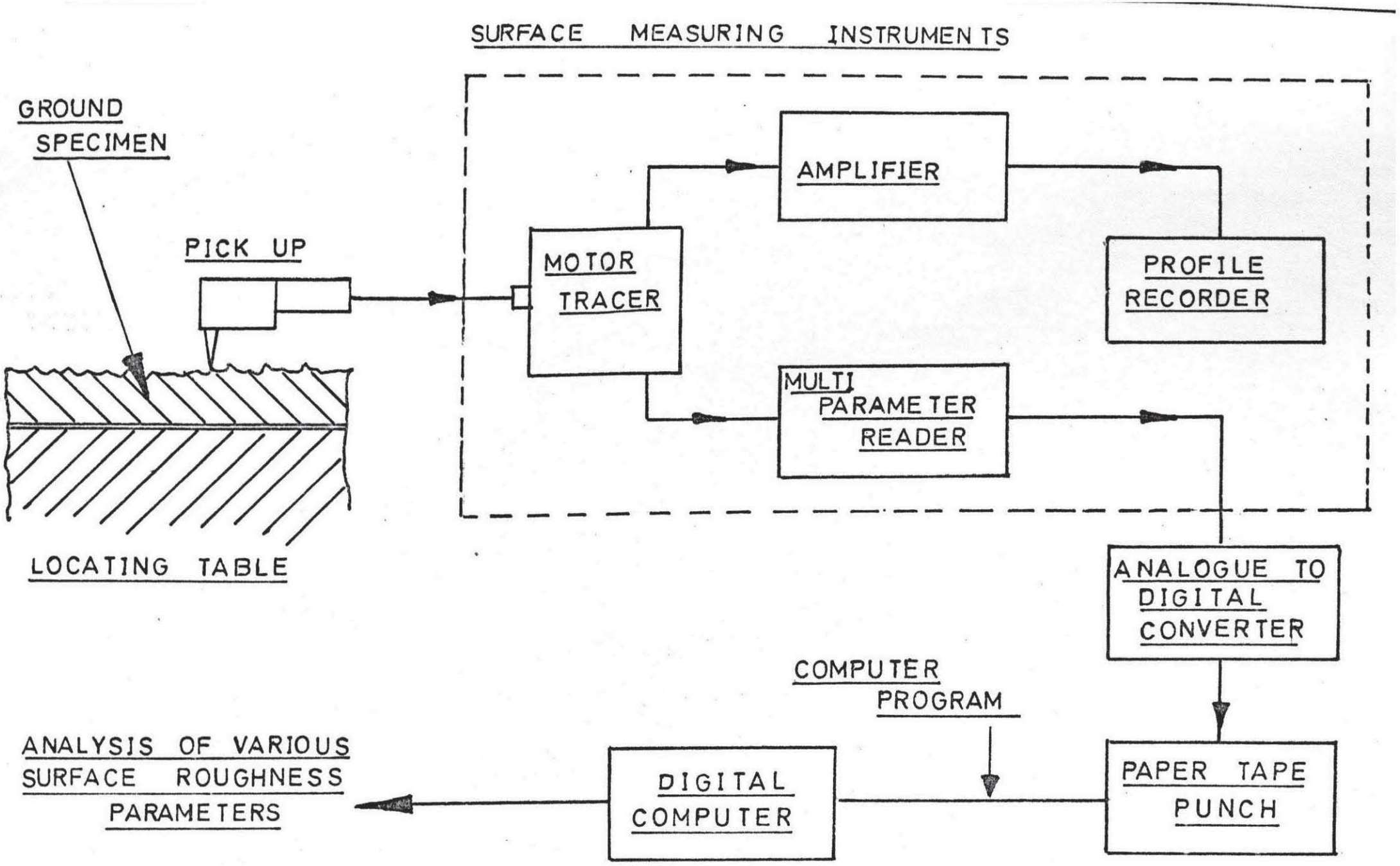

FIG 26. EQUIMENT FOR MEASURING SURFACE ROUGHNESS

TABLE 3

Digitising Rate ordinates/sec.		4	10	12
Stylus Speed mm/sec.	Gearbox Horizontal Magnification Setting	Ordinate Spacing (mm)		
1.0	Av. (X5)	.250	.100	.0833
.25	X20	.0625	.025	.0208
.05	X100	.0125	.005	.0042

The minimum ordinate spacing for which the stylus can be used is 5 microns and so this was adapted. With a X100 horizontal gearbox magnification this would require a digitising rate of 10 ordinates/sec from Table 3. The A.D.C. converter is capable of producing 4, 10, 20 conversions per second, which is sufficient to provide the required ordinate spacing.

The ordinates were recorded to three significant figures, these being numerically accurate to 1 part in 500 which was thought to be at least equal to the accuracy limit of the Talysurf equipment. Each recorded ordinate contained 4 or 5 characters, which consisted of 3 characters representing the above three figures plus one or two terminating characters for carriage return or line feed. Three recording mediums, i.e., magnetic tape, punch paper tape and cards were available for recording these ordinates. Grieve [23] has considered the choice of a recording medium on merits of recording characters per second, comparative density of records and cost installation. In the case of punched cards the recording rate and the record density is not considered enough. Punched paper tape has been considered the most suitable because

it had the required recording speed and record density and is cheaper than magnetic tape. Following these suggestions paper tape was used as the medium of recording.

To obtain consistent results in the case of a single profile it was essential to keep the sample size constant. Based on experimental work, a sample size of 1200 ordinates representing about 6.3 mm of sample length was used throughout. With the digitising rate of 10 ordinates/sec this required a time of 2 minutes. In the experiments the digitising was carried out for $2\frac{1}{2}$ minutes. Next, the equipment was set to give an ordinate spacing of .005 mm. The Talysurf stylus traverse was set parallel to the sample surface. The stylus amplification was increased in steps to 4 (10000 magnification),setting the traverse parallel to the sample every time. At this magnification (10000), 25.4 mm of Talysurf scale corresponded to 396 digits of the digitiser. Therefore, one digit of digitiser represented

$$= \frac{25.4}{396 \times 10000} = .0000063 \text{ mm}$$

After digitising, control variables were put at the beginning of each data tape specifying the title of data and certain fixed parameters (Appendix I). At the end of each data certain characters were put to denote end of data, to start computation on the next tape and end of tape. This is also given in Appendix I. Control variables were printed out as soon as they were read by the computer to facilitate accuracy checks.

3.2.3 Computer Programme

A computer programme described in the Appendix was used to evaluate the parameters mentioned earlier. The programme along with the digital data on paper tape, was fed to the K.D.F.9 English Electric computer. The principle languages which could be used for this computer were 'K' Autocode and Egdon III,

a version of Fortran IV. 'K' Autocode is the usual programming language for paper tape and is ideal for a programme of small size, as used in this investigation, so the 'K' Autocode Non Egdon programming language was used.

The calculation of parameters was carried out by fitting a least square centre line to the recorded data and finding the new ordinates w.r.t this line (Appendix II). For calculating peak heights, the ordinates w.r.t. least square line were smoothed by fitting a fourth order polynomial to seven adjacent points (Appendix III). The formulae for calculation of CLA using least square ordinates and other peak to valley height parameters are given in Appendix IV. The bearing area was evaluated by numerical integration. The arrays containing ordinates (B) w.r.t. least square line were interrogated at different height levels "h" from the centre line (least square line). If the ordinate in the array was above the level "h" it was added to the cumulative totals (bearing area). Starting from 3.4 CLA height above the centre line the level was decreased in steps of 0.2 times the CLA value each time and bearing area was evaluated at 36 levels i.e. from 3.4 CLA height level above to 3.6 CLA height level below the centre line. Finally some ordinate values were printed to have an idea of their comparative values. The computer programme is described in Appendix V and the printer output is shown in Appendix VI.

CHAPTER 4

EXPERIMENTAL WORK

This investigation was carried out on a Churchill 10" x 20" hydraulic plain cylindrical grinding machine. The kinematics of the machine were not altered during dressing and grinding. The only variable parameters were the wheel unbalance, grinding wheel grade and the workpiece material.

4.1. Grinding Parameters

(a) Dressing Conditions (Constant)

Peripheral Wheel Speed = 31 meters per second

Dressing lead = 0.15 mm per rev. of wheel

Radial infeed:

1st stroke	-	variable
2nd stroke	-	.0185 mm per double traverse
3rd and 4th stroke	-	same as second
5th stroke	-	.01 mm in one traverse and return with spark out

(b) Grinding Conditions (Constant)

Wheel Speed	=	31 meters per second
Work Speed	=	25 meters per minute
Radial Infeed	=	2.5 μ per single traverse
Table Traverse	=	0.65 meters per minute

(c) Grinding Coolant

Simcool S-4 (Charles Churchill Co., Coventry Road, Birmingham).

(d) Work Material

i) Soft material: EN - 8 steel with following composition

Carbon = 0.45

Mn 0.8

Si 0.35

Hardness V.P.N. = 213

ii) Hard Material: EN - 32B Case hardened steel

Depth of case = 3 mm

Hardness V.P.N. = 800 to 850

(e) Dimensions of the Workpiece

See Figure 27

(f) Dimensions of the Grinding Wheel

500 mm x 50 mm x 200 mm

(g) Grades of Wheels Used

WA 46 KV

WA 46 MV

WA 46 OV

Universal Grinding Wheel Co., Stafford, England.

(h) Grinding Time

It was important to fix the grinding time so as to avoid any significant influence of self excited vibration on surface texture. Based on previous experience, a grinding time of 45 minutes was adopted for each test.

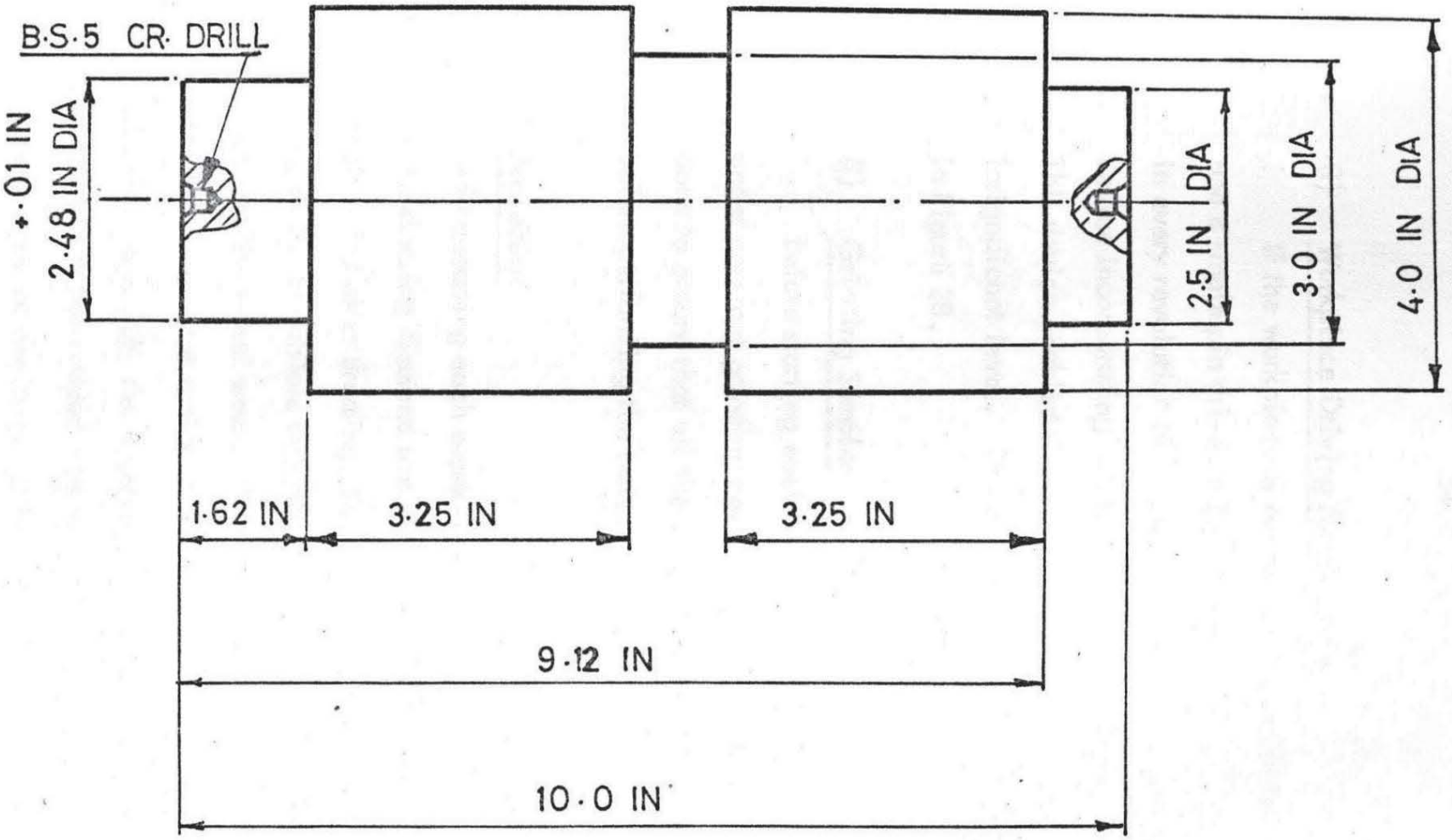

SCALE:
HALF FULL SIZE·

FIG 27· DIGRAM OF THE WORKPIECE·

(i) Workpiece Driving Arrangement

If the workpiece is driven in a conventional way using a carrier and a single pin drive, a force fluctuation occurs on the strain gauges in every revolution of the workpiece. To overcome this a special device incorporating two drive pins and flexible drive links was used. This device enabled the force fluctuations to be reduced to a practically insignificant level. The two devices with their force diagrams are shown in Figure 28.

(j) Grinding Samples

Before starting each experiment, all the workpieces were ground under constant grinding conditions using a balanced wheel. This was done to ensure that all the samples had similar surface characteristics before performing the tests.

4.2 Procedure

Before starting each experiment the machine was warmed up for half an hour. The dressing diamond was fixed to the tailstock. For experiments with unbalance added after dressing, the wheel was balanced first and then dressed according to the conditions described earlier. A step was made on the wheel for measuring the wheel wear. Plasticine was used as the source of unbalance and added at a constant radius at the wheel. For experiment with unbalance present before dressing, the wheel was balanced first. The required amount of unbalance was then added and the dressing operation performed. To maintain the sharpness of the diamond tip, the diamond tip was rotated by 1/7th of a turn every time before performing the dressing operation. The producedure ensured the uniformity of the wheel surface.

Before starting grinding, the diameters of the workpiece samples and wheel wear were recorded. During the experiment the following observations

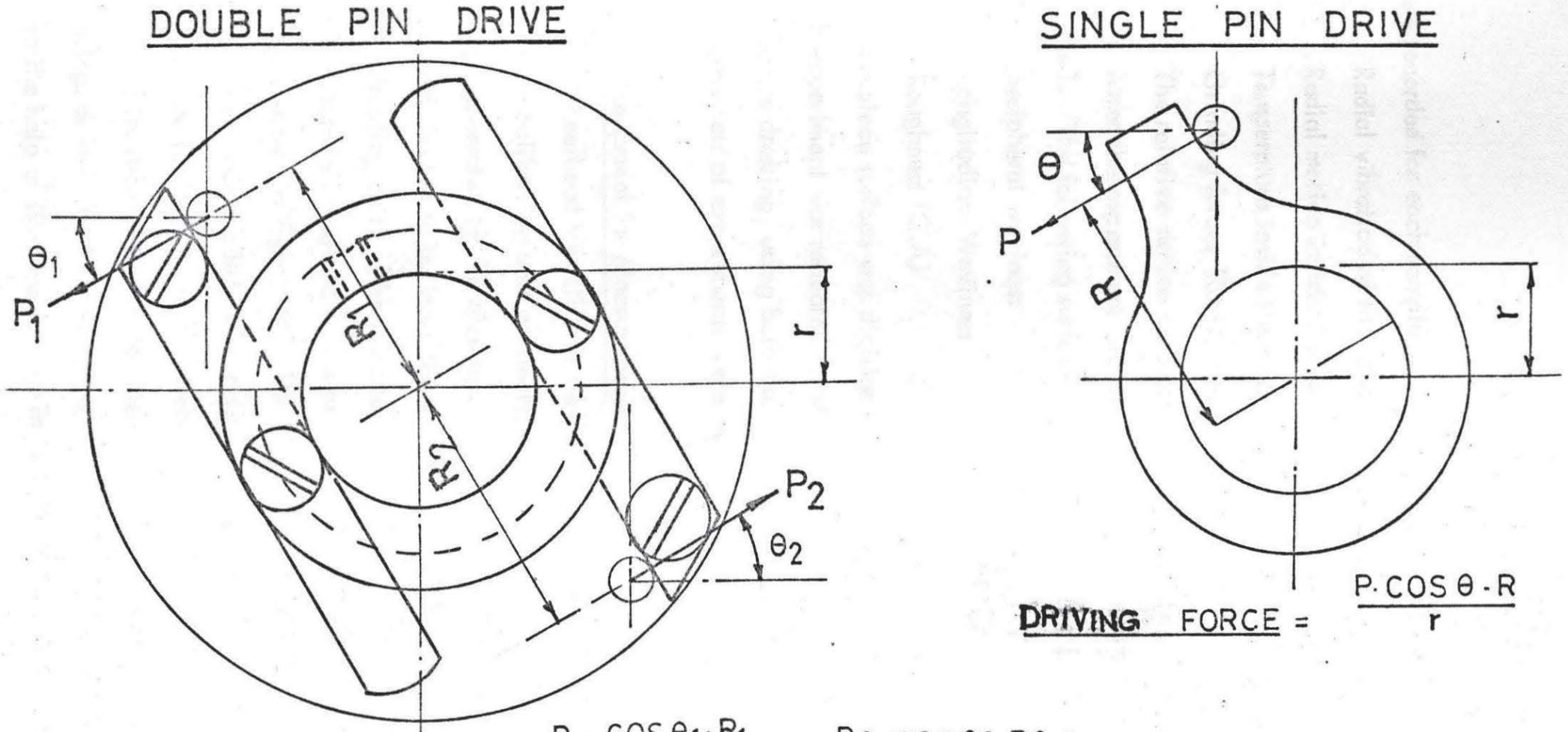

FIG 28. WORKPIECE DRIVING ARRANGEMENT.

were recorded for each sample.

(a) Radial vibration of the wheelhead.

(b) Radial motion inside the spindle bearings.

(c) Temperature inside the bearings.

(d) Grinding forces (Radial and Tangential).

(e) The relative motion between the wheel and the workpiece.

After the experiment the wheelwear and workpiece diameters were recorded. The following surface parameters were measured for each sample:

i) peripheral waviness

ii) Longitudinal Waviness

iii) Roughness (CLA)

The workpiece surface was digitised for computing surface roughness parameters. Each experiment was repeated for different ammounts of unbalance added after and before dressing, using both the soft and hardened workpiece material. All the above sets of experiments were repeated for three different wheels.

4.3 Equipment for Measurement

Wheelhead Vibration is measured with a seismic (electrodynamic) pick up. The calibrating unit connected in the circuit gives the amplitude value of the voltage generated by the pick up. A Schenck vectormeter type of wattmeter (Vibrovid) is used to indicate the vibration by utilising the output voltage from the calibrating unit. The necessary phase current for the vibrovid is provided by the photocell mounted on the rotating end of the wheelspindle. The whole set up is shown in Figure 29. The Vibrovid can be calibrated for the amplitude of vibration with the help of the calibrating unit and the oscilloscope. Vibrovid is also used for balancing the wheel.

Vibration of the Wheelspindle w.r.t. wheelhead is measured inside the bearings as well as at the wheelend. The motion inside the bearings is measured with the help of TR-2 transducers already described in Chapter 2. The signal

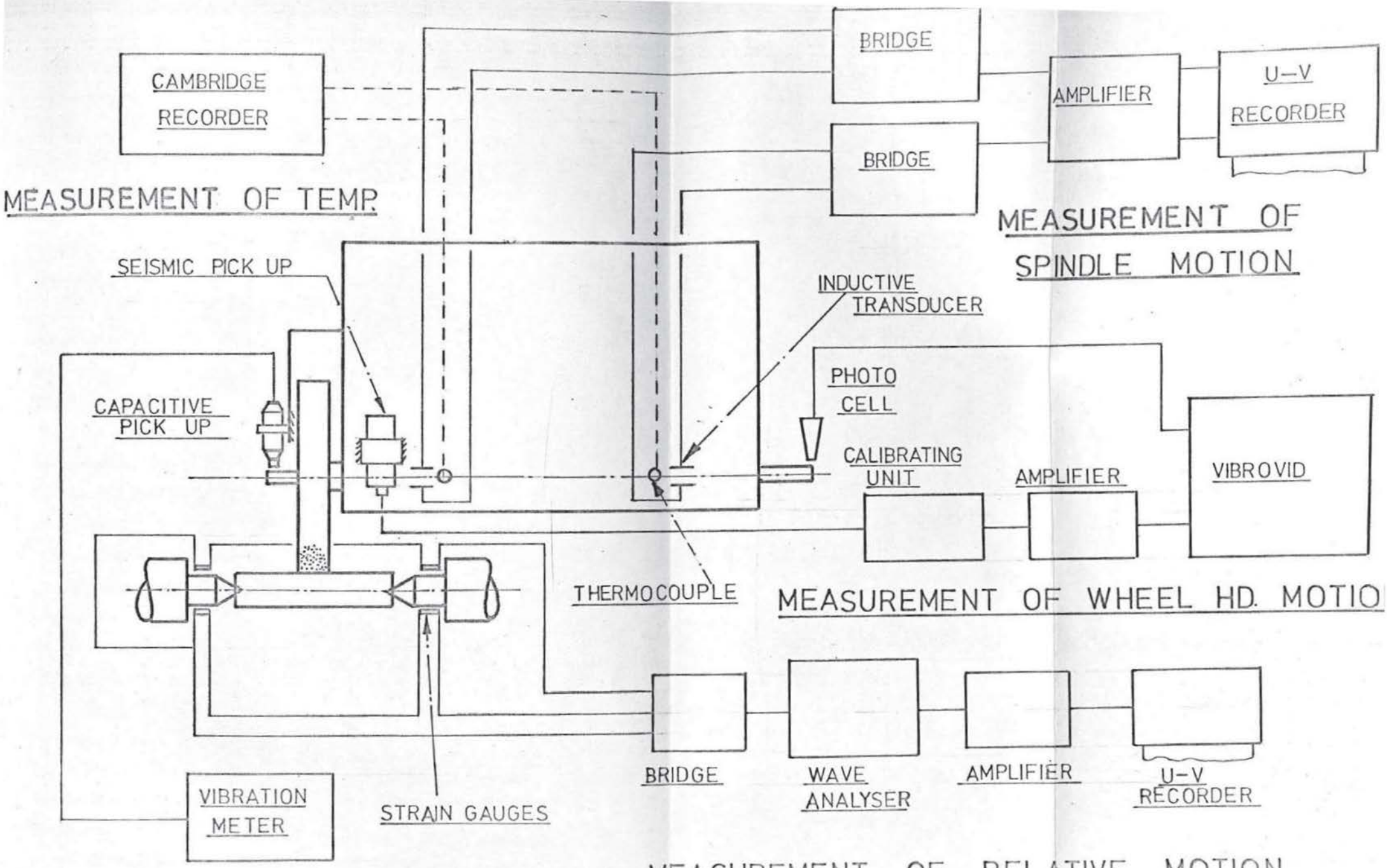

FIG 29. EQUIPMENT FOR ANALYSING THE DYNAMIC SYSTEM OF THE GRINDING M/C.

from the bridge is amplified by an amplifier and recorded on a U-V recorder. The equipment for this is shown in Figure 29 and a trace of wheelspindle motion is shown in Figure 30.

To measure the relative motion of the workpiece w.r.t wheel during grinding, the signal from the strain gauges fixed on the workpiece centres were fed to the wave analyser, which was previously calibrated for displacement. The wave analyser could be precisly tuned to the frequency of the forced vibration of the grinding wheel. The equipment is shown in Figure 29.

The Temperature inside the bearings during grinding is measured by the copper-Constantan thermocouples as described earlier. The thermocouples are connected to a cambridge temperature recorder which has a range of 0 to 100°C (Figure 29).

Grinding forces are measured with the help of strain gauges fixed to the workpiece holding centres. Each centre carries four strain gauges, two for measuring the radial forces and two for the tangential forces. The strain gauges are connected to form a half bridge inside the Hottinger bridges. Low pass filters are used to reduce the noise. The signal from the filters is amplified by an amplifier and recorded on a U-V recorder. The set up is shown in Figure 31. The calibration of strain gauges is performed with a device capable of exerting horizontal and vertical pull on the workpiece through a set of pulleys, as shown in Figure 8.

Peripheral waviness of the workpiece was measured by a Taylor Hobson Talyrond. A 5" arm and a magnification of 5000 was used throughout. The instrument consists of an inductive pick up arm which traces the periphery of the workpiece component at various magnifications. A reference computer adds to the Talyrond graph a definite reference line from which to measure the undulations of the component. Maximum peak to valley height (inward and outward departure) shown in Figure 32, is used as a criterion for measuring waviness, and this can be easily spotted measured w.r.t. the reference circle. The maximum inward and

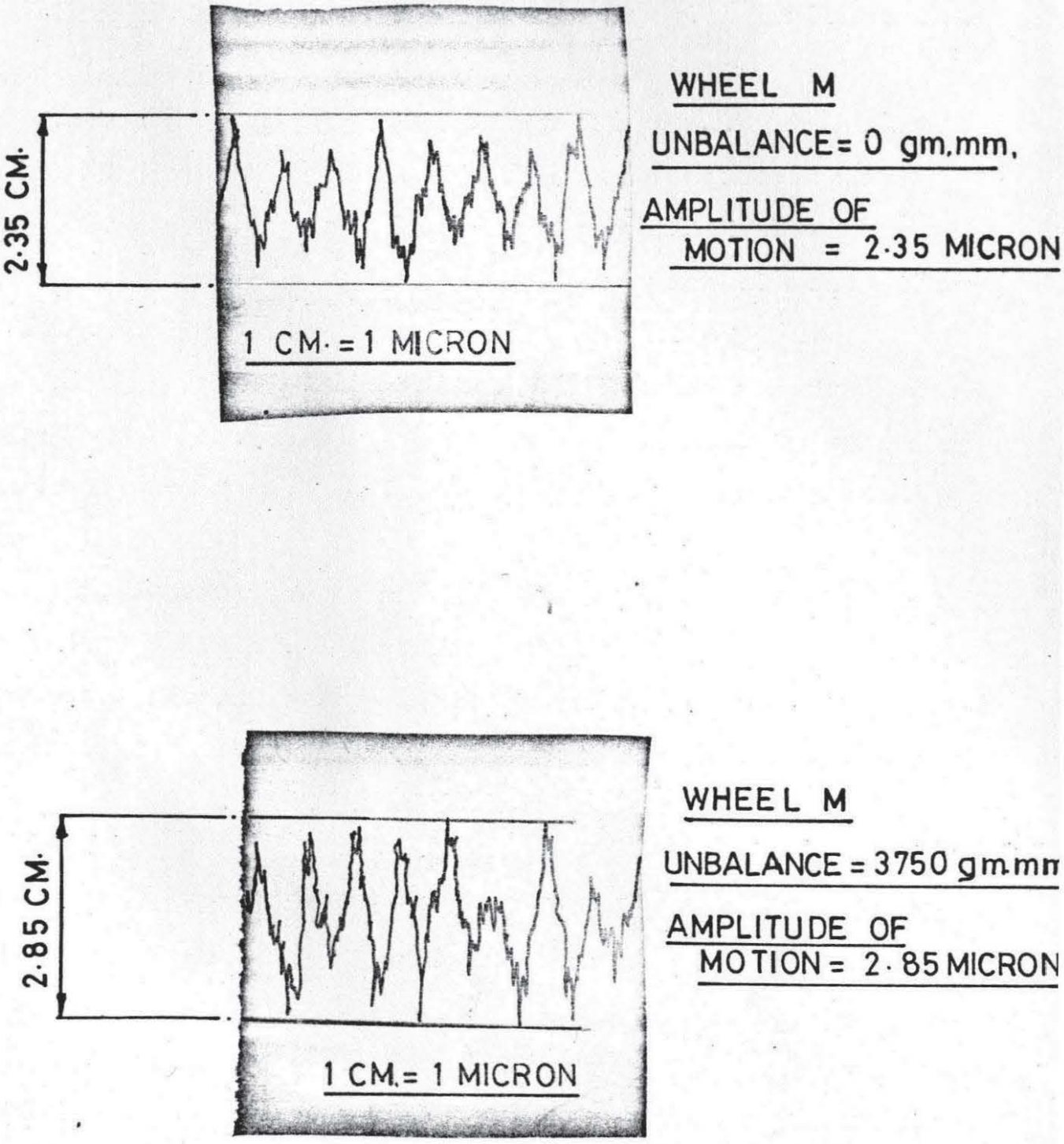

FIG 30. TRACE OF WHEELSPINDLE MOTION IN FRONT BEARING.

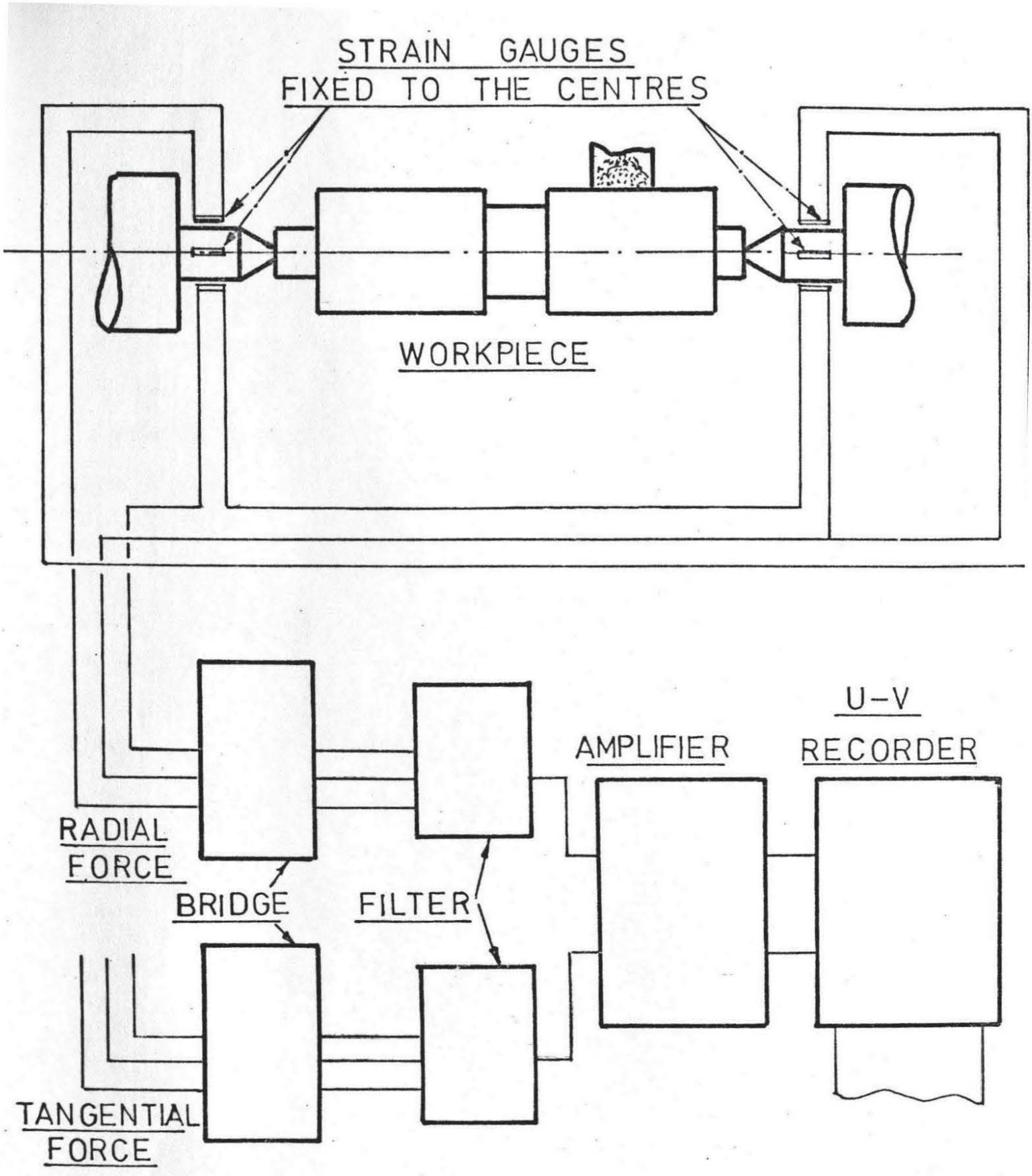

FIG 31. EQUIPMENT FOR MEASURING RADIAL AND TANGENTIAL FORCES

outward departure is also indicated by the computer on a meter.

The longitudinal waviness (or straightness error) along the length of the ground sample was measured by a Talylin. The instrument provides a graphic record of departures from a straight line of component surface over a maximum length of 4 inches (100 mm). It incorporates an electric displacement pick up which is guided over the sample. Movement of the stylus is measured relative to a straight datum surface contained within the instrument and mounted immediately above the pick up. A magnification of 10000 was used throughout for measuring the longitudinal waviness. The stylus traverse is set parallel to the workpiece surace so that the two points at the ends of the specimen are at the same height. The measurement of straightness error is the maximum upward and downward departure from the straight line joining the end points (Figure 32).

The remaining surface parameters i.e. CLA, peak to valley height, bearing area, etc., were obtained from computer results by digitising the surface. A photograph of the equipment for digitising the surfaces, involving A.D. converter and punch tape is shown in Figure 25. The value of the CLA was also read from the CLA meter.

The grinding ratio was calculated by finding the ratio of the volume of metal removed to the volume of wheel wear during grinding. Volume of the metal removed is found from the diameters of samples measured before and after the experiment. For measuring the wheel wear, an inductive pick up PR-9210 is used in conjunction with a Phillips bridge PR-9300/1. An amplifier and a U-V recorder were used for recording the wheel wear signal. A step 12 mm wide x 0.1 mm deep was made on the periphery of the wheel. This is shown in the diagram of the equipment, Figure 33. The step serves as a datum for measuring the wheel wear before and after grinding. The reading of the wheel wear is taken before and after grinding. The difference in the two

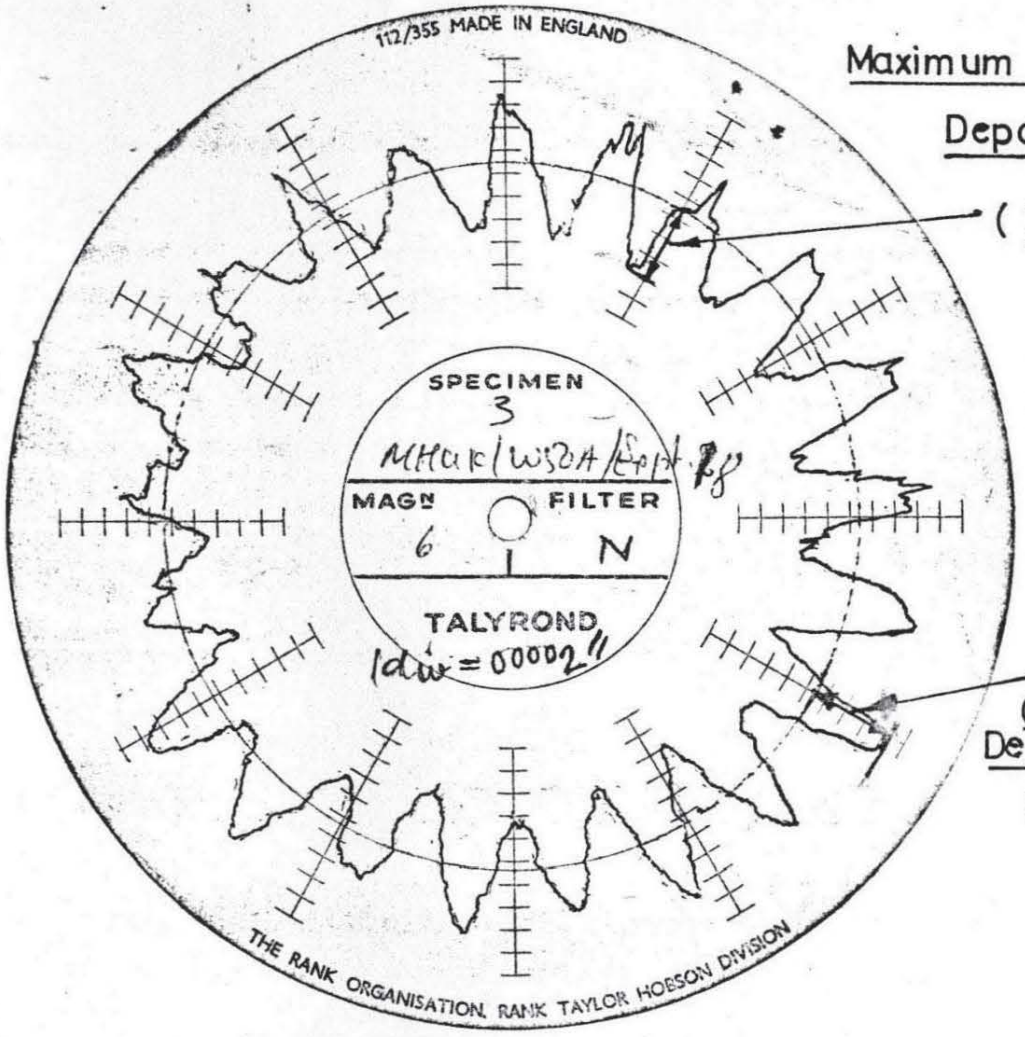

Maximum Inward Departure = ·00007"
(1·75 Micron)

Maximum Outward Departure = ·00008"
(2 Micron)

PERIPHERAL WAVINESS = 1·75 + 2·0 = 3·75 MICRON

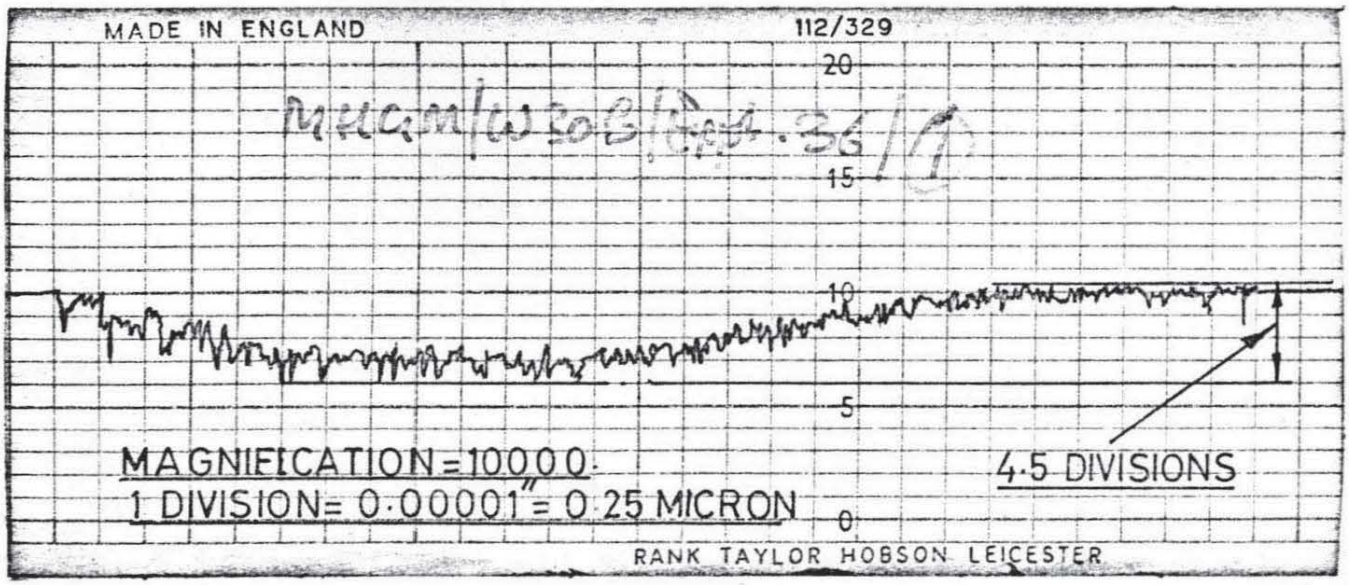

LONGITUDINAL WAVINESS = 4·5 (0·25) = 1·12 MICRON

FIG 32. TRACE OF PERIPHERAL WAVINESS AND LONGITUDINAL WAVINESS.

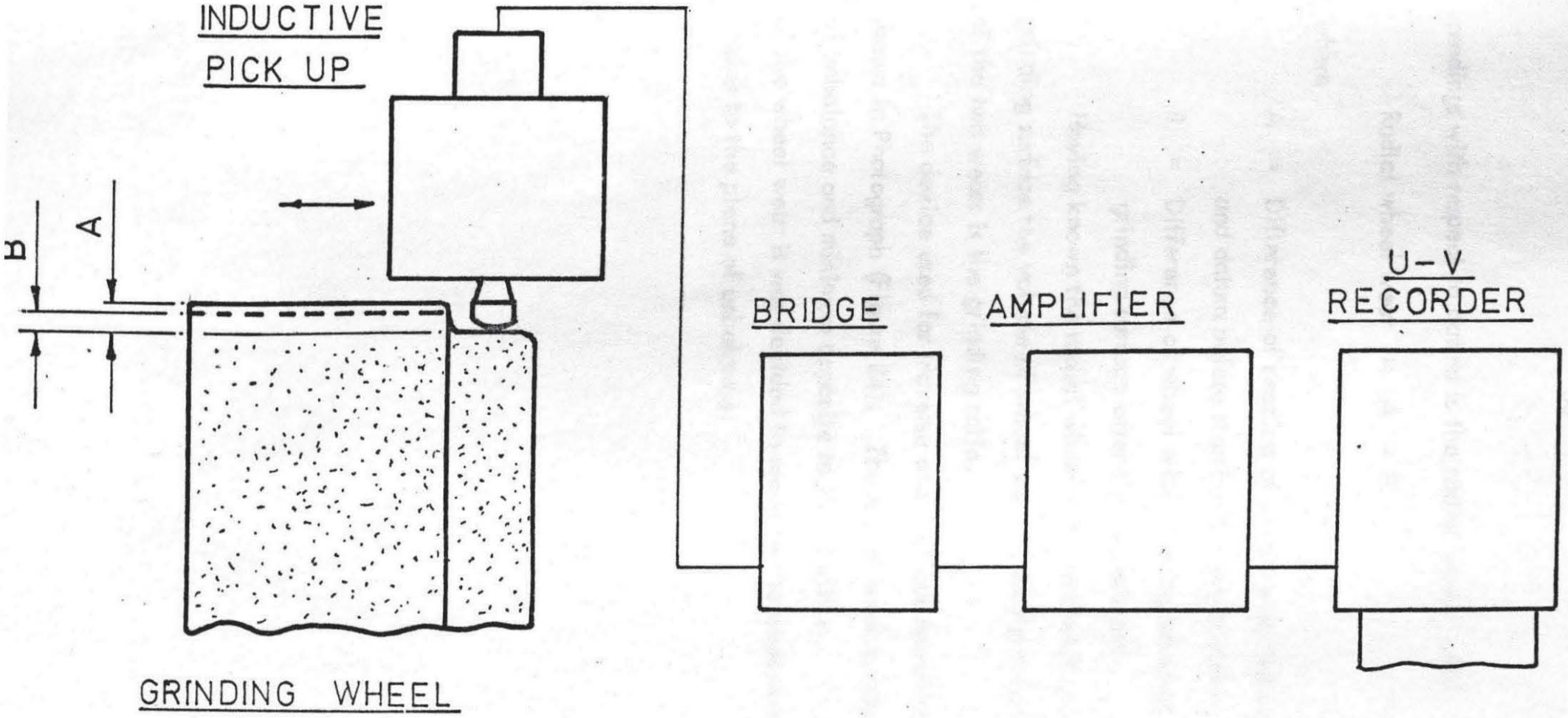

FIG 33. DIAGRAM OF APPRATUS FOR MEASURING WHEEL WEAR.

readings with respect to datum is the radial wheel wear. From Figure 33

Radial wheel wear = A - B

where

A = Difference of reading of wheel wear between grinding surface and datum before starting the experiment.

B = Difference of wheel wear reading between the datum and grinding surface after the experiment.

Having known the radial wheel wear and width of the effective grinding surface the volume of wheel wear is easily calculated. The ratio of the two wears is the grinding ratio.

The device used for traverse and vertical movement of the pick up is shown in Photograph (Figure 34). The wheel wear is maximum at the position of unbalance and minimum opposite to this position. To get the average value of the wheel wear it was decided to measure the wear at a position at right angles to the plane of unbalance.

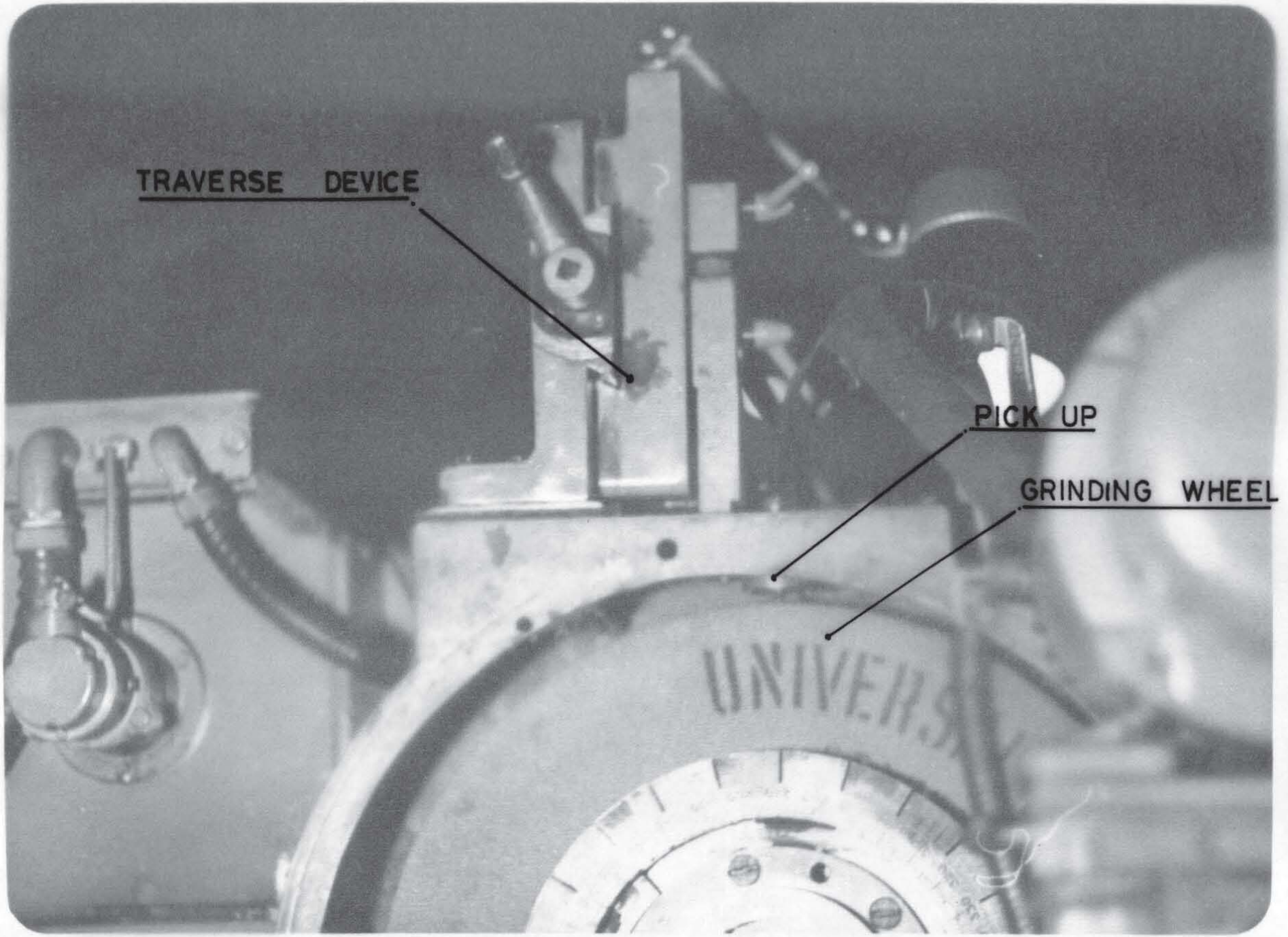

FIG. 34. PHOTOGRAPH OF PICKUP AND TRAVERSE DEVICE FOR MEASURING WHEEL WEAR.

CHAPTER 5

GRINDING RESULTS

5.1 Vibration of the Machine

As mentioned before in Chapter 2, the vibration behaviour of the machine requires the knowledge of the radial (horizontal) vibration of the wheelhead, wheelspindle and relative wheel work motion during grinding.

The effect of wheel unbalance on wheelhead vibration depends upon the rigidity of the wheelhead. The radial vibration of the wheelhead due to different amounts of wheel unbalance are shown in Figure 35. As can be seen from the graphs for the three wheels used, there exists a liner relationship between the amplitude of vibration of the wheelhead and wheel unbalance, which shows that at constant wheel speed the amplitude of vibration is directly proportional to the unbalance present during grinding. Although the amplitude of vibration is reduced when the unbalance is present before dressing as compared with the unbalance added after dressing, the effect of unbalance still persists. (The analysis of the above condition is given in Chapter 3). As can be seen from Figure 35, the amplitude of wheelhead vibration during grinding decreases with the increase in the wheel hardness. This is explained later in terms of wheel contact stiffness.

The horizontal vibration of wheelspindle measured inside the bearings as a function of unbalance are shown in Figure 36. As can be seen the amplitude of the spindle motion increases inside the front bearing with the increase of unbalance. The motion inside the rear bearing is not significantly affected by the unbalance. This behaviour is explained in Chapter 2. Further, the spindle motion in the front and rear bearings, using wheels of three greades, is shown in Figures 38 and 37 respectively. As would be expected the motion of the wheelspindle in the rear bearing is not affected by the hardness of the wheel

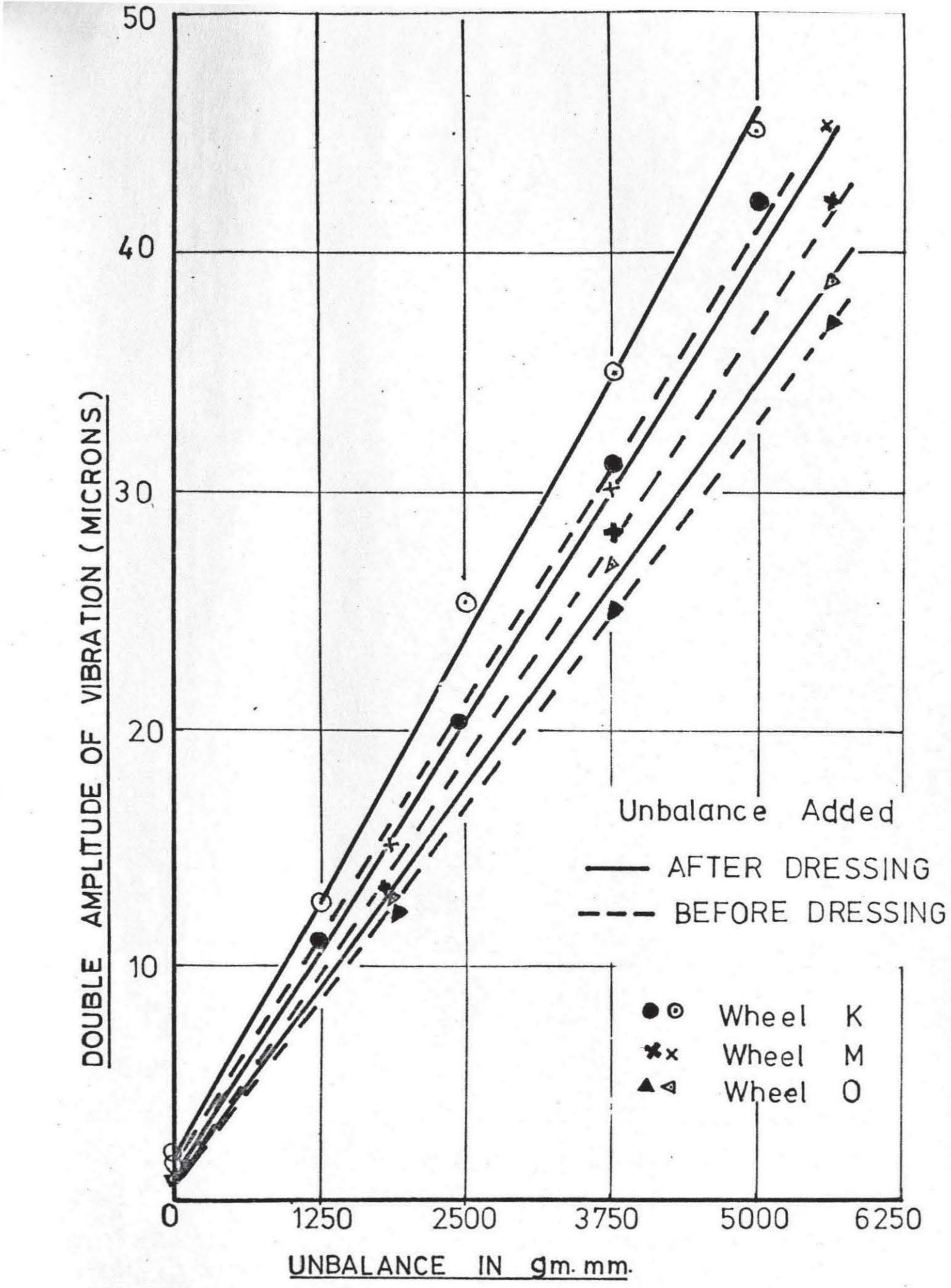

FIG 35. EFFECT OF UNBALANCE AND WHEEL GRADE ON WHEELHEAD VIBRATION.

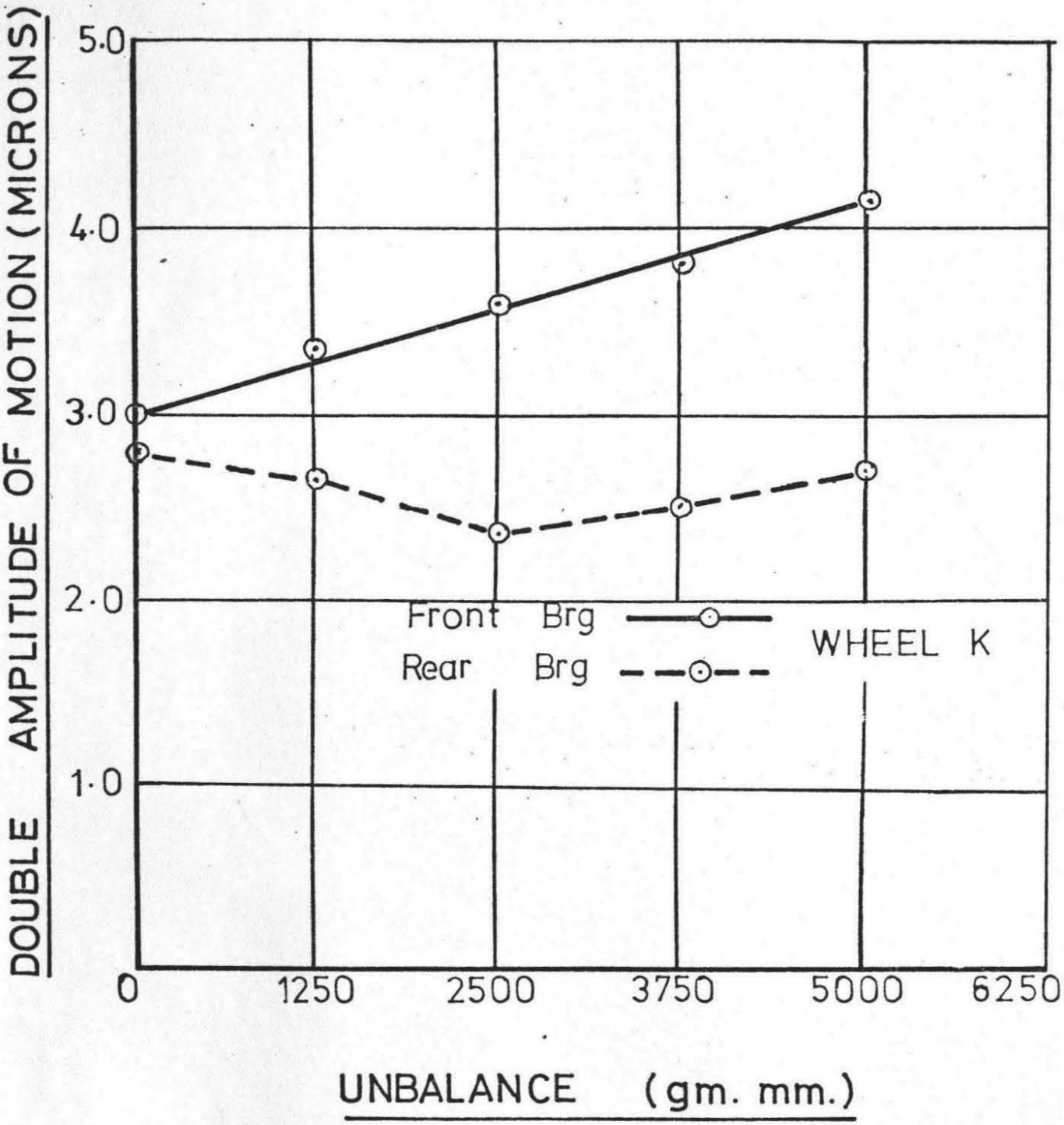

FIG 36. EFFECT OF UNBALANCE ON WHEEL SPINDLE MOTION IN BEARINGS.

(Figure 37), but again, as in the case of the wheelhead, the wheel spindle motion in the front bearing decreases as the hardness of the wheel is increased (Figure 38). The hardness has a certain influence on the wheel contact stiffness. As has been stated in Chapter 2, when the grinding is not taking place the grind-system consists of two sub-systems, i.e. the wheelhead - wheelspindle system and the workpiece holding system. During grinding the two systems are coupled together by an elastic spring (k_3) due to the structure of the grinding wheel. The contact stiffness between the wheel and the workpiece is represented by the spring k_3. The value of this stiffness depends upon the rigidity of the grinding wheel and particularly the bond strength of the grains. The bond rigidity is proportional to the elasticity of the wheel[24]. Tests for determining the modulus of elasticity "E" for different wheels were conducted by Singhal and Kaliszer [24]. The values for the three types of wheels used in this investigation are as follows:

$$K = 7.36 \times 10^6 \text{ Lbs/in}^2$$

$$M = 8.81 \times 10^6 \text{ Lbs/in}^2$$

$$O = 10.85 \times 10^6 \text{ Lbs/in}^2$$

which shows that wheel work contact stiffness increases for wheels of harder grades. It has been shown [24] that an increase in the wheel contact stiffness has a decreasing effect upon the forced vibration. It follows, therefore, that the amplidue of wheel-head vibration and spindle motion in front bearing decreases with wheels of harder grades.

The effect of using hard and soft workpiece materials during grinding is shown in Figure 39 and Figure 40. Figure 39 shows the behaviour of the wheel-head vibration. It can be seen that the amplitude of vibration increases for a harder material. This is because the wheel contact stiffness decreases in the case of a harder material as follows from previous investigations Kaliszer[1] and Grisbrook[26]. According to [26], the radial force decreases when grinding with harder material and since contact stiffness is directly affected by the radial force[1] therefore the wheel contact stiffness decreases in the case of harder material. The same follows in the case of the wheelspindle motion in the front bearing, Figure 40. The difference, however, is less

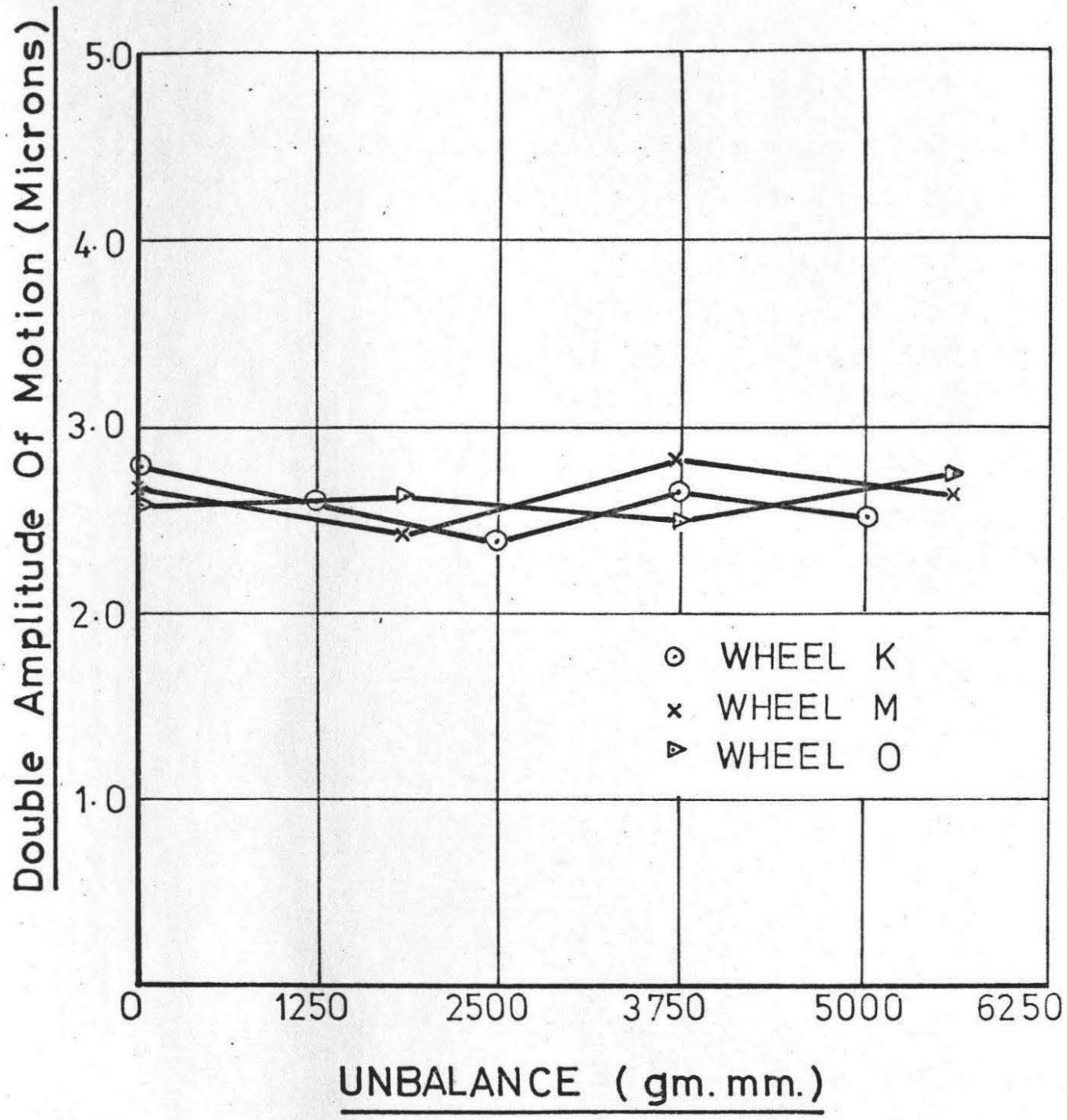

FIG 37. EFFECT OF UNBALANCE AND WHEEL ON SPINDLE MOTION IN REAR BEARING.

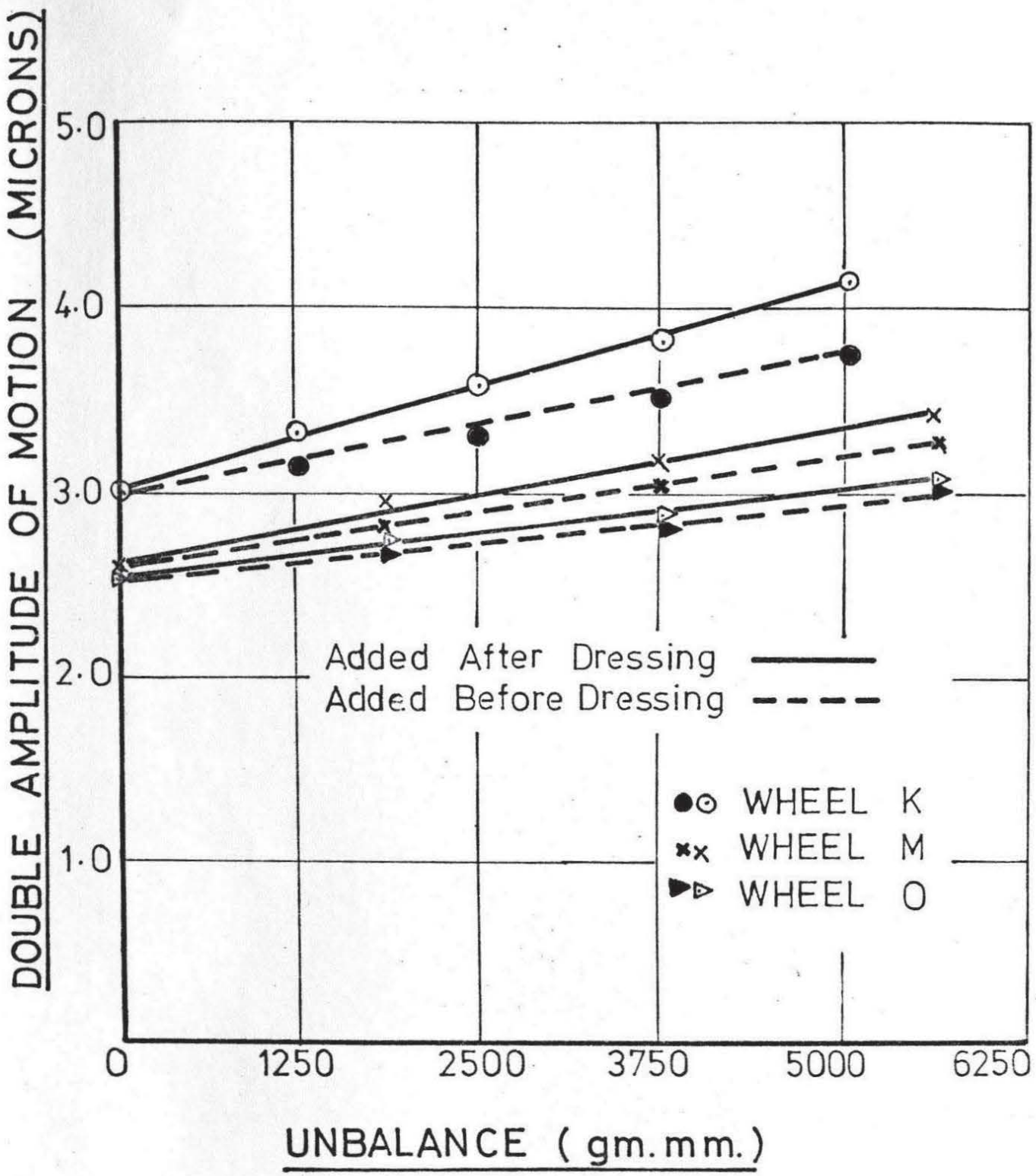

FIG 38. EFFECT OF UNBALANCE AND WHEEL GRADE ON SPINDLE MOTION IN FRONT BEARING.

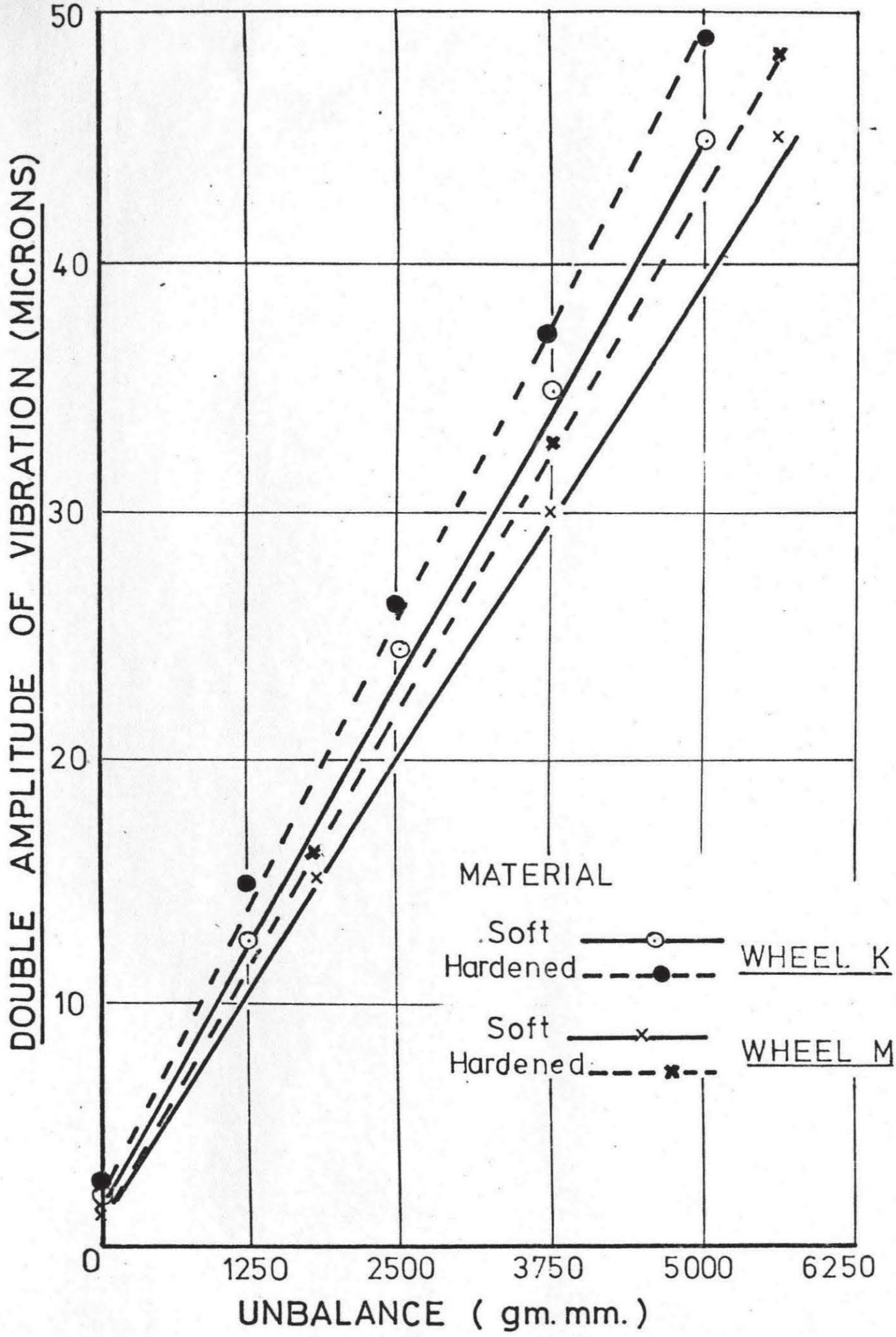

FIG 39 EFFECT OF WORKPIECE HARDNESS ON WHEELHEAD VIBRATION.

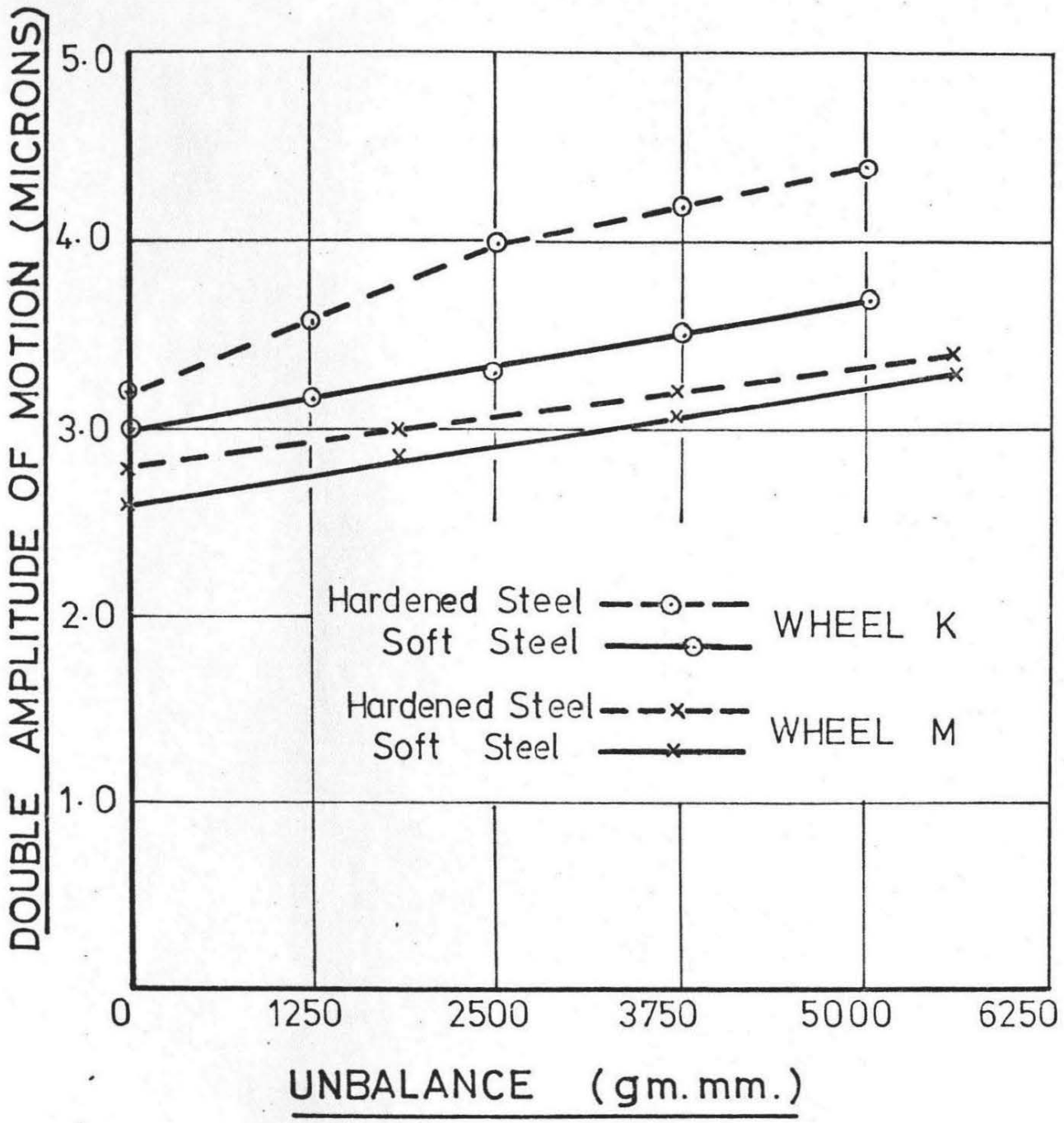

FIG 40. EFFECT OF WORKPIECE HARDNESS ON SPINDLE MOTION IN FRONT BEARING.

pronounced in the case of wheels with higher hardness.

The relative motion between the wheel and the workpiece plotted as a function of unbalance is shown in Figure 41. The relative motion increases with the increase of unbalance. As in the case of wheelhead and wheelspindle, the relative motion of the wheel-work also decreases in the case of harder wheels. The same explanation of wheel contact stiffness can be applied in this case. The relative motion resulting from the use of hard and soft workpiece materials is shown in Figure 42. The motion decreases with a soft material and increases with a hard material, as explained earlier.

In order to obtain a full picture of the spindle motion it would be desirable to measure the vibration at the wheel end. The equipment required for this was available, (Figure 29). This motion was, however, not measured after a few initial observations because, as explained earlier, the pick up mounted on the wheelguard was under the influence of wheelguard vibration.

The temperature inside the bearings does not seem to be affected by the wheel unbalance. This can be seen from the graph of Figure 43, where no definite relationship exists between the temperature and the unbalance. The temperature rises for half an hour of grinding and then tends to remain constant.

5.2 Forces During Grinding

The average radial and tangential forces for different amounts of wheel unbalance are shown in Figure 44. As can be seen from the graphs the average forces remain practically unchanged with unbalance. For the three wheels used in the experiments, the average forces have higher values in the case of harder wheels. This can be explained by the number of cutting edges taking part in the grinding. The number of cutting edges produced during dressing of various grades of wheels were studied by Peklenik [25]. As can be seen from Figure 45, the crushing effect is more predominant during dressing for softer wheels. For

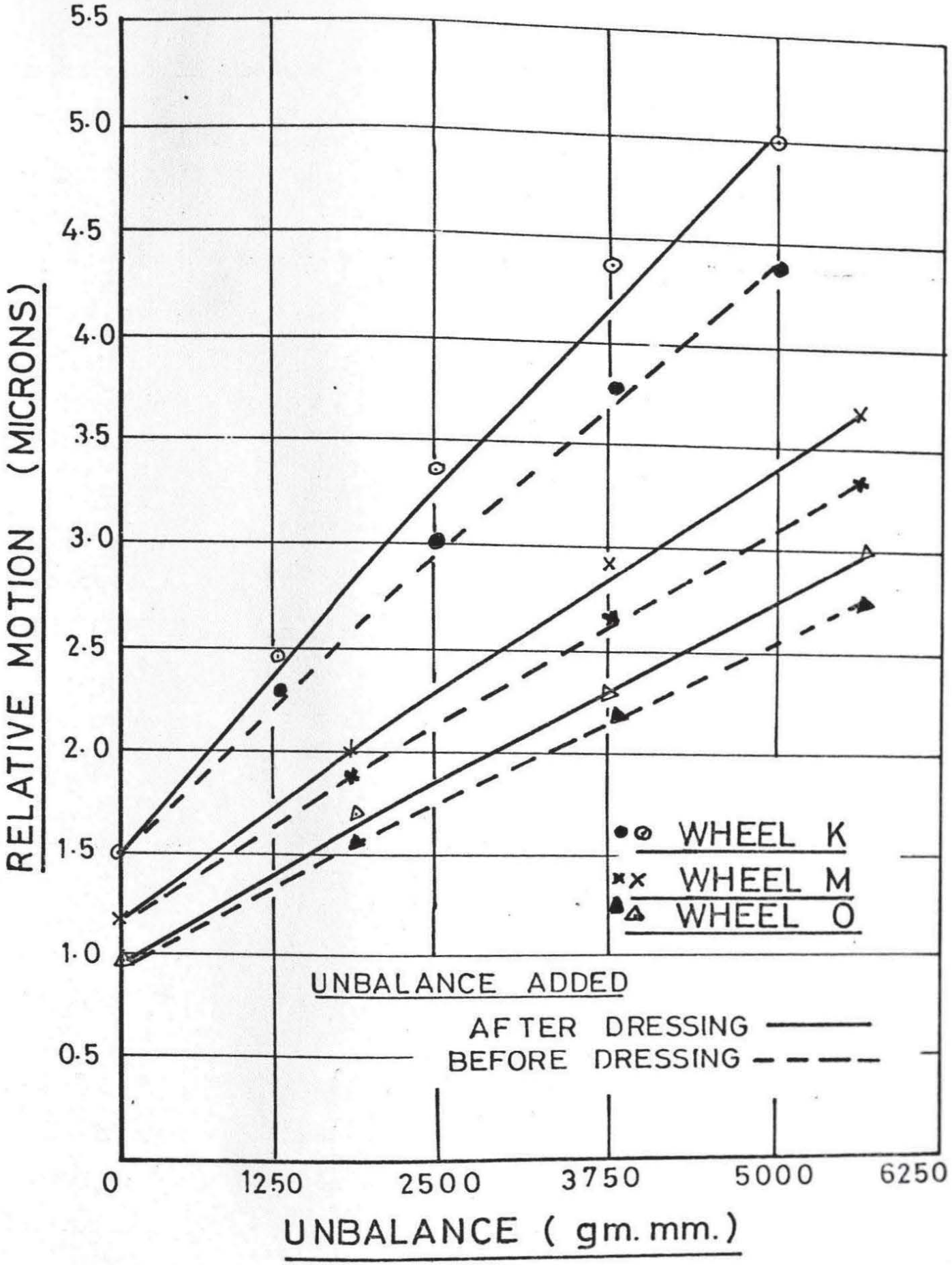

FIG 41. EFFECT OF UNBALANCE AND WHEEL GRADE ON RELATIVE WHEEL WORK MOTION

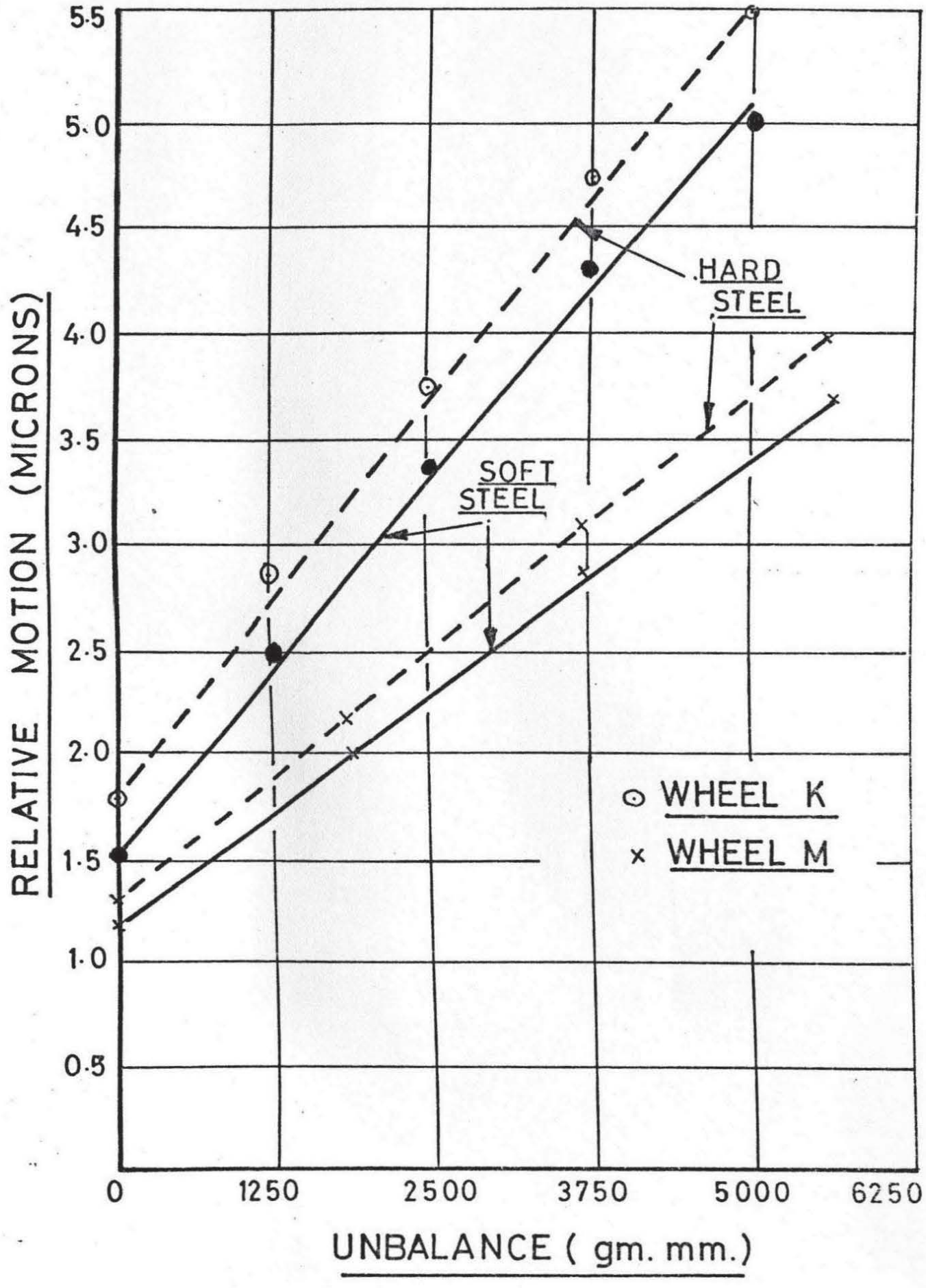

FIG 42. EFFECT OF WORKPIECE HARDNESS ON RELATIVE WHEEL WORK MOTION.

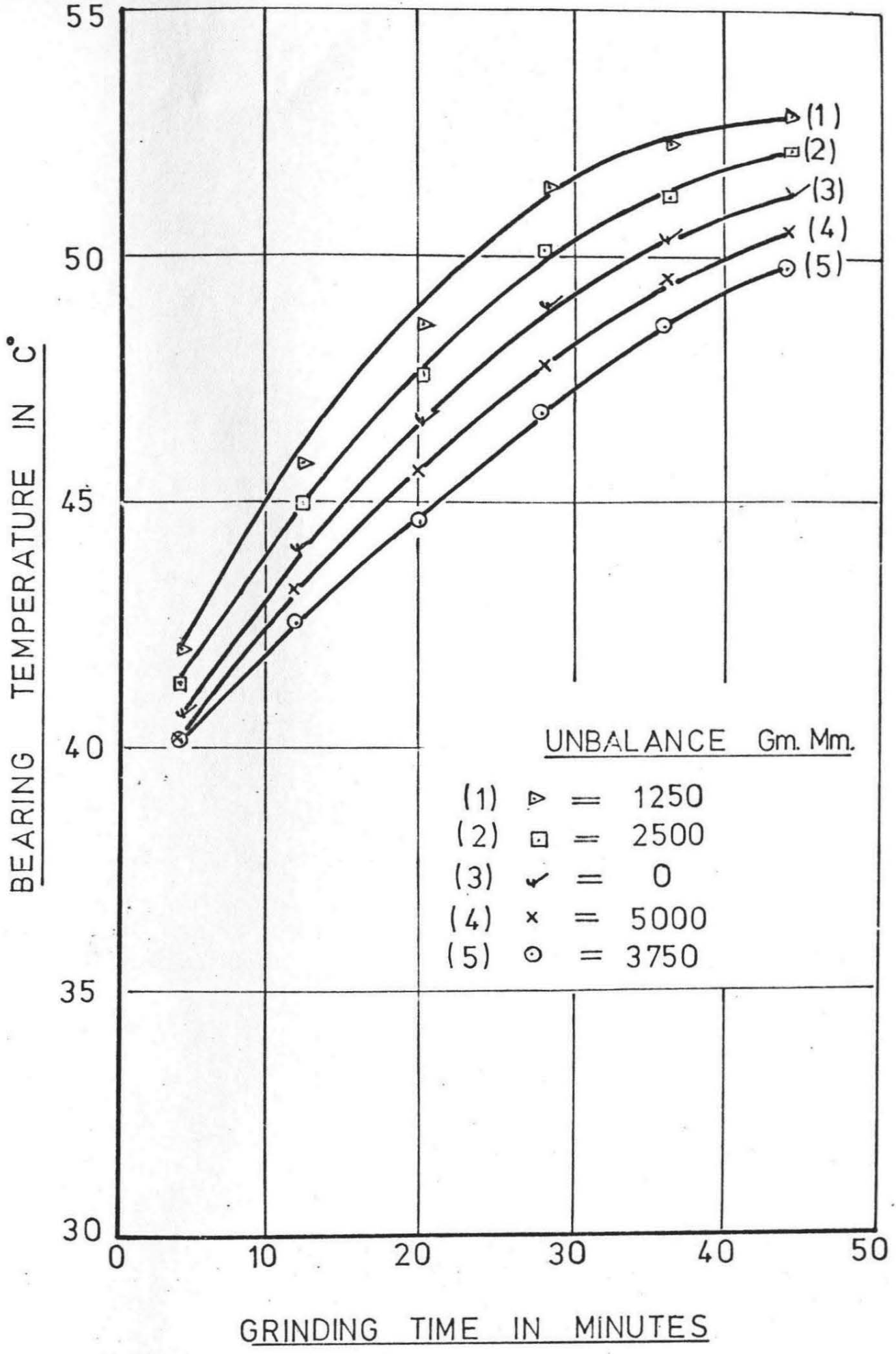

FIG 43. BEARING TEMPERATURE AS A FUNCTION OF UNBALANCE.

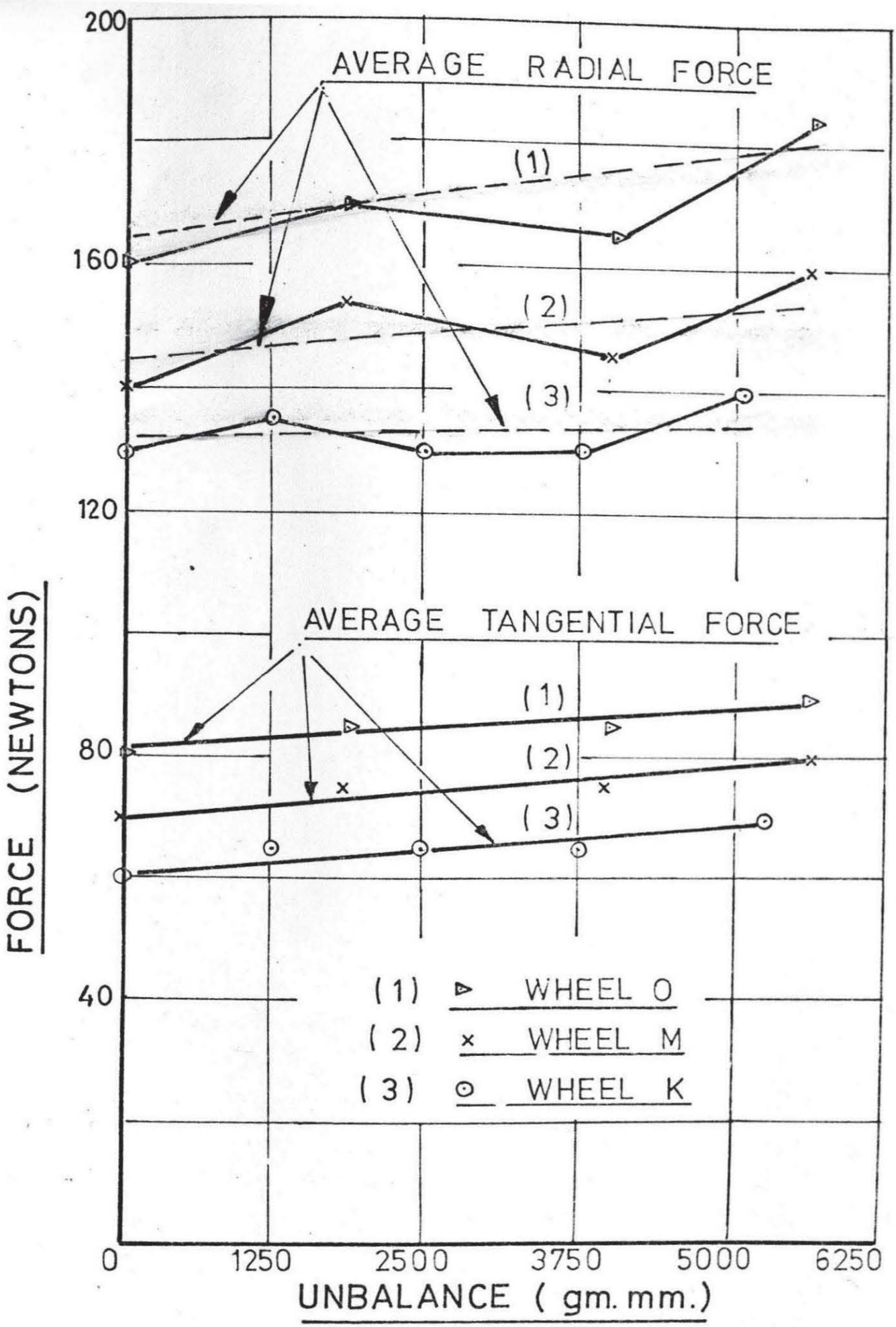

FIG 44. GRINDING FORCES AS A FUNCTION OF UNBALANCE AND WHEEL GRADE.

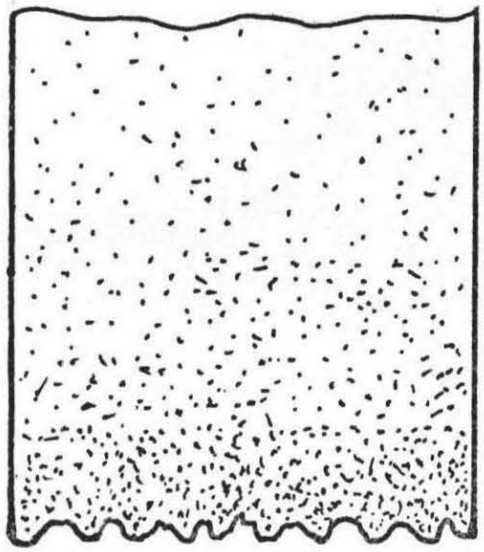

GRAIN SPACING IN A SOFT WHEEL

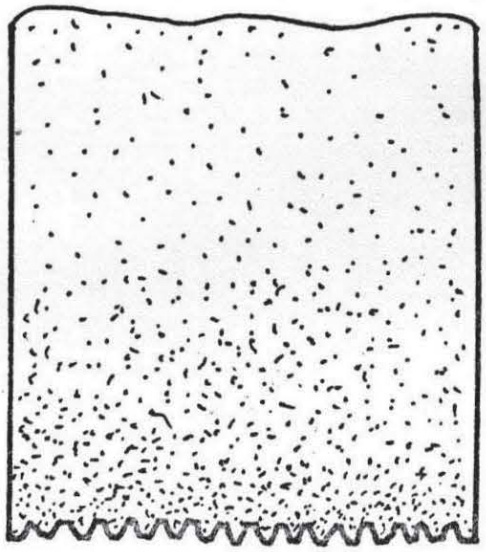

GRAIN SPACING IN A HARD WHEEL

(PEKLENIK[25])

FIG 45. DRESSING OF SOFT AND HARD WHEEL.

such wheels the spacing between the edges is also increased. In the case of a harder wheel, the cutting edge spacing is comparatively smaller resulting in a greater number of effective cutting edges. Therefore, in the case of harder wheels the average forces will also increase. It can also be seen from Figure 44 that the relationship between the normal and tangential forces is fairly constant irrespective of any unbalance. This ratio is nearly 2:1.

In addition to the average forces the cyclic variation in the grinding forces corresponding to the frequency of unbalance force were also investigated. This is shown in Figure 46 where the cyclic variation in the radial force is plotted against the unbalance. As can be seen from the graphs for various wheels the cyclic variation in radial force increases as the unbalance increases. This cyclic variation in force corresponds to the relative motion created between the wheel and the workpiece due to the wheel unbalance. Further, as in the case of relative wheel-work motion, this variation is found to be more in the case of softer wheels. Also, the unbalance added after dressing has more effect than the unbalance present before dressing. The average radial grinding force for soft and hardened workpiece materials is shown in Figure 47. The values are higher for softer workpiece materials, as was also observed by Grisbrook [26].

5.3 Surface Quality of the Workpiece

5.3.1 Peripheral Waviness

The amplitude of the peripheral waviness of the workpiece for different amounts of unbalance is shown in Figure 48. It can be seen that the amplitude of waviness increases with the increase of wheel unbalance. Here again the amplitude of waviness is greater for softer wheels. This generation of waviness can be explained by the wheel contact stiffness as stated earlier in the same Chapter. Figure 49 shows the amplitude of workpiece waviness as a function of workpiece hardness. An increase in the amplitude of waviness is observed in

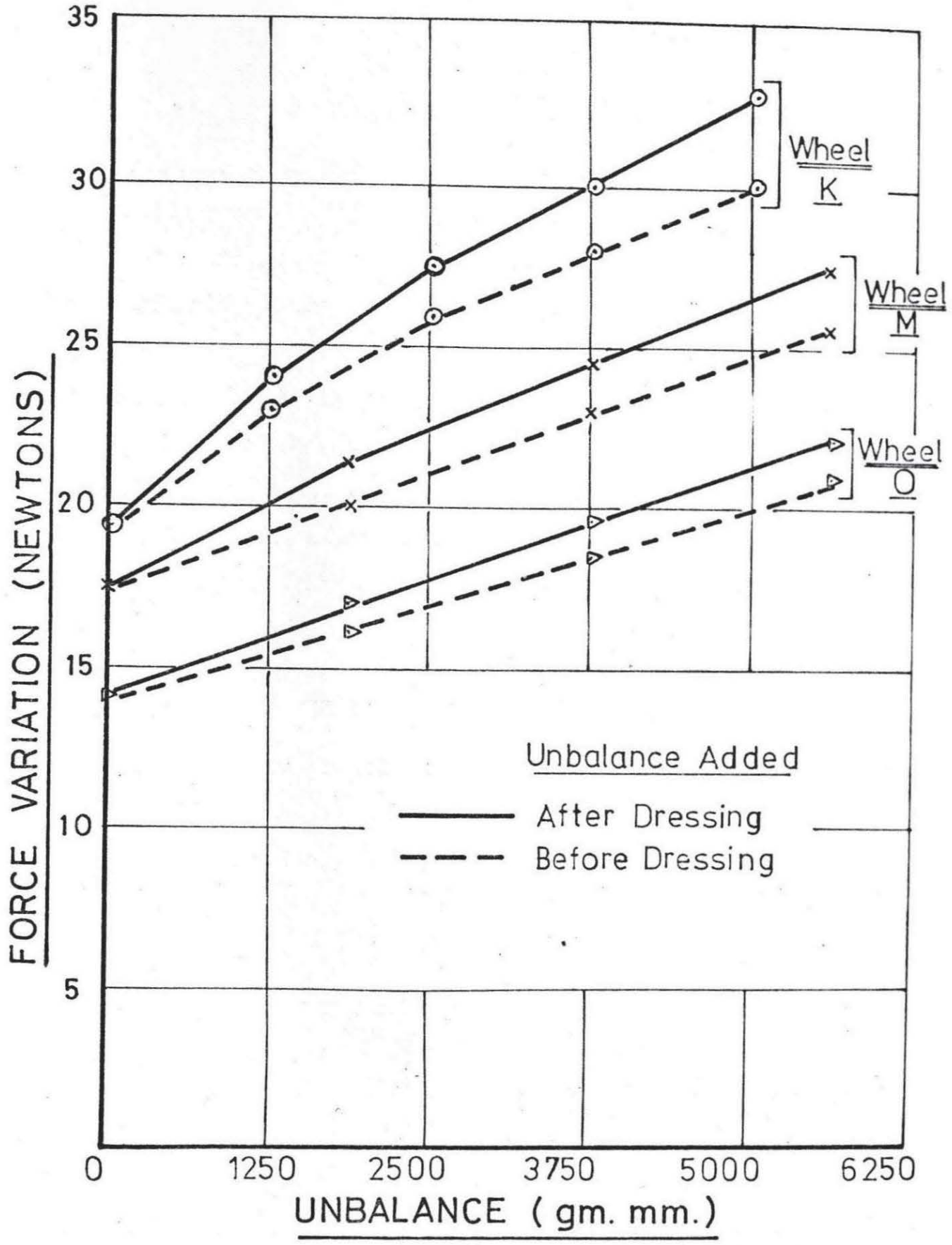

FIG 46. CYCLIC VARIATION IN RADIAL GRINDING FORCE AS A FUNCTION OF UNBALANCE AND WHEEL GRADE.

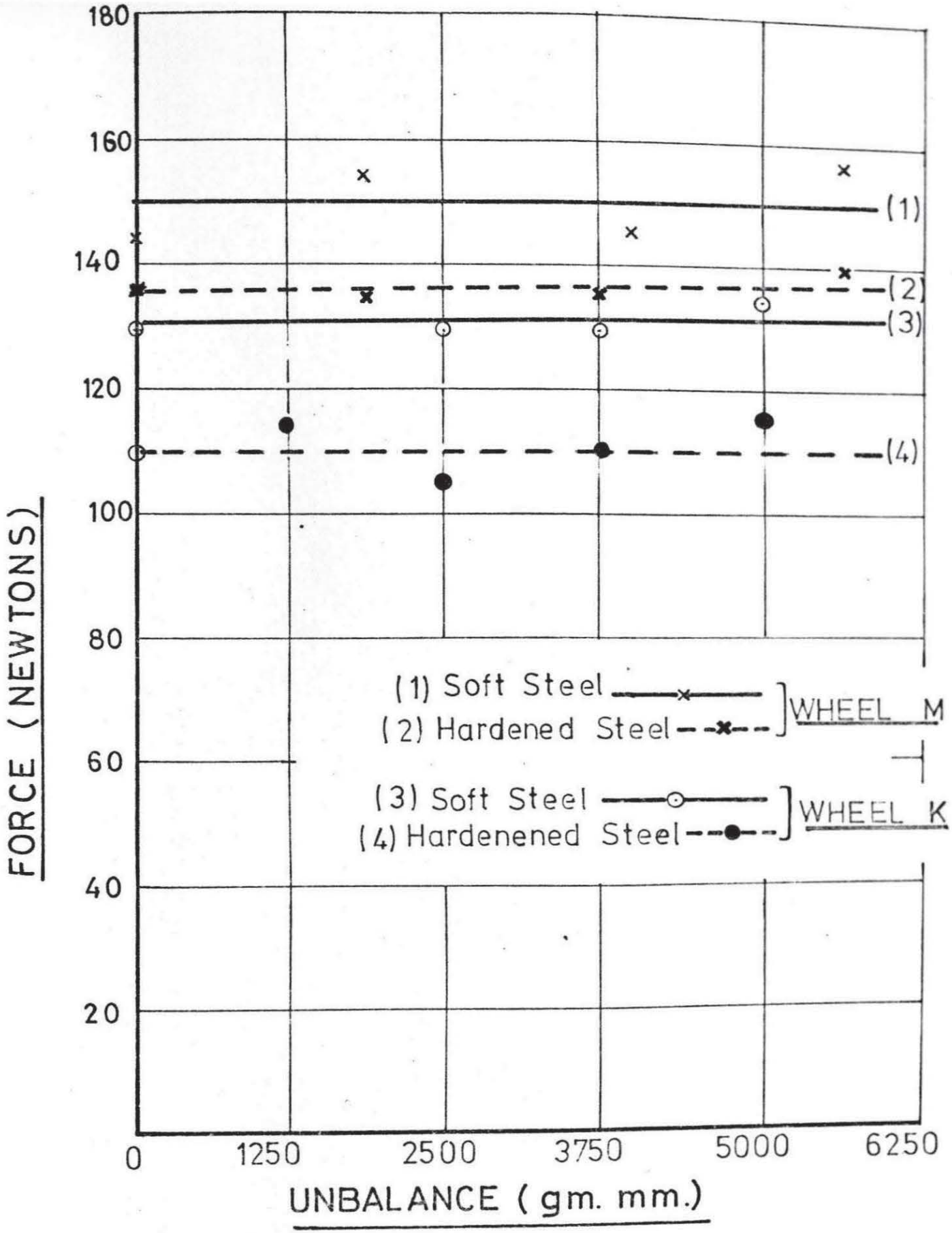

FIG 47. EFFECT OF WORKPIECE HARDNESS ON RADIAL GRINDING FORCE.

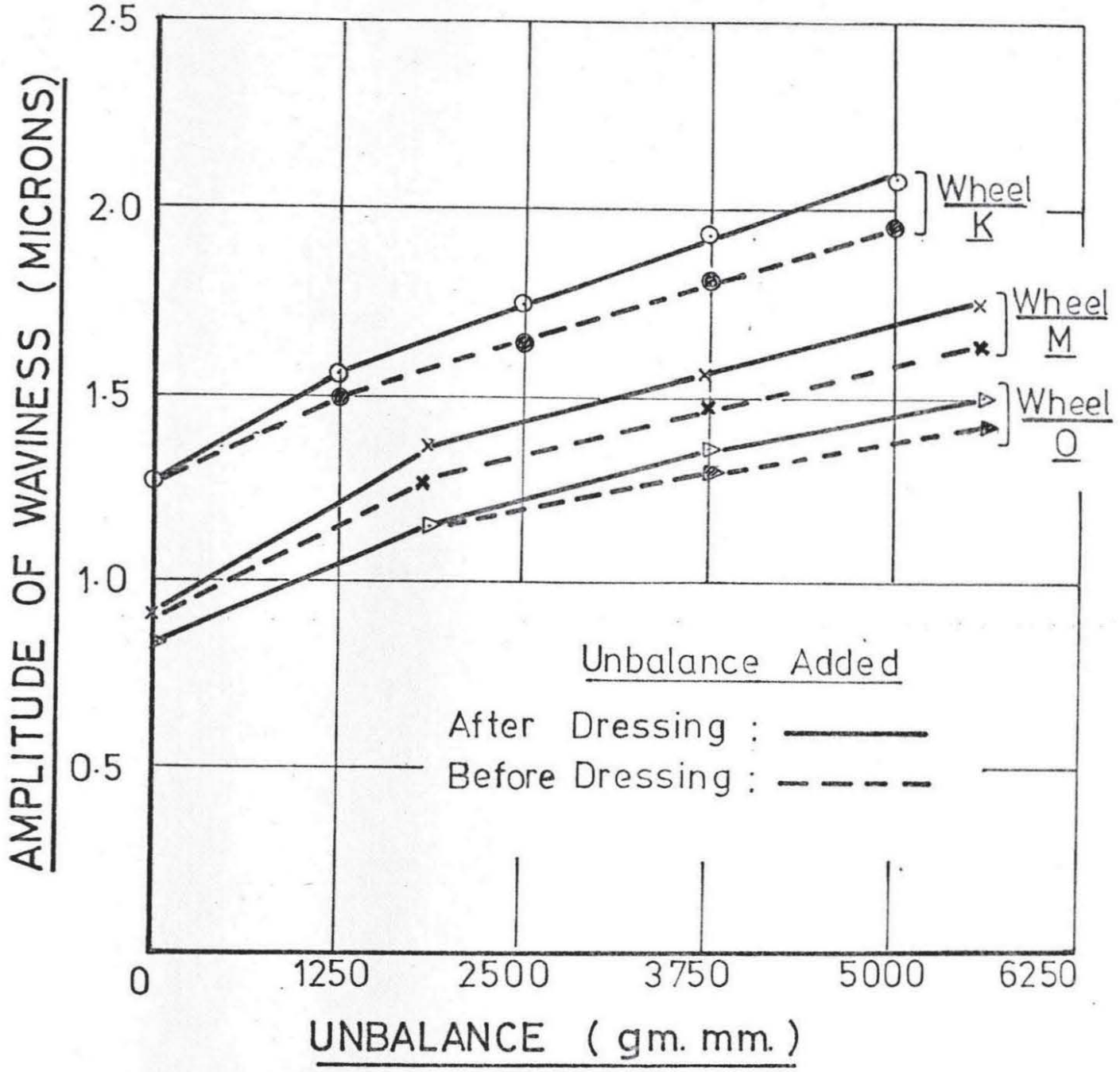

FIG 48. PERIPHERAL WAVINESS AS A FUNCTION OF UNBALANCE AND WHEEL GRADE.

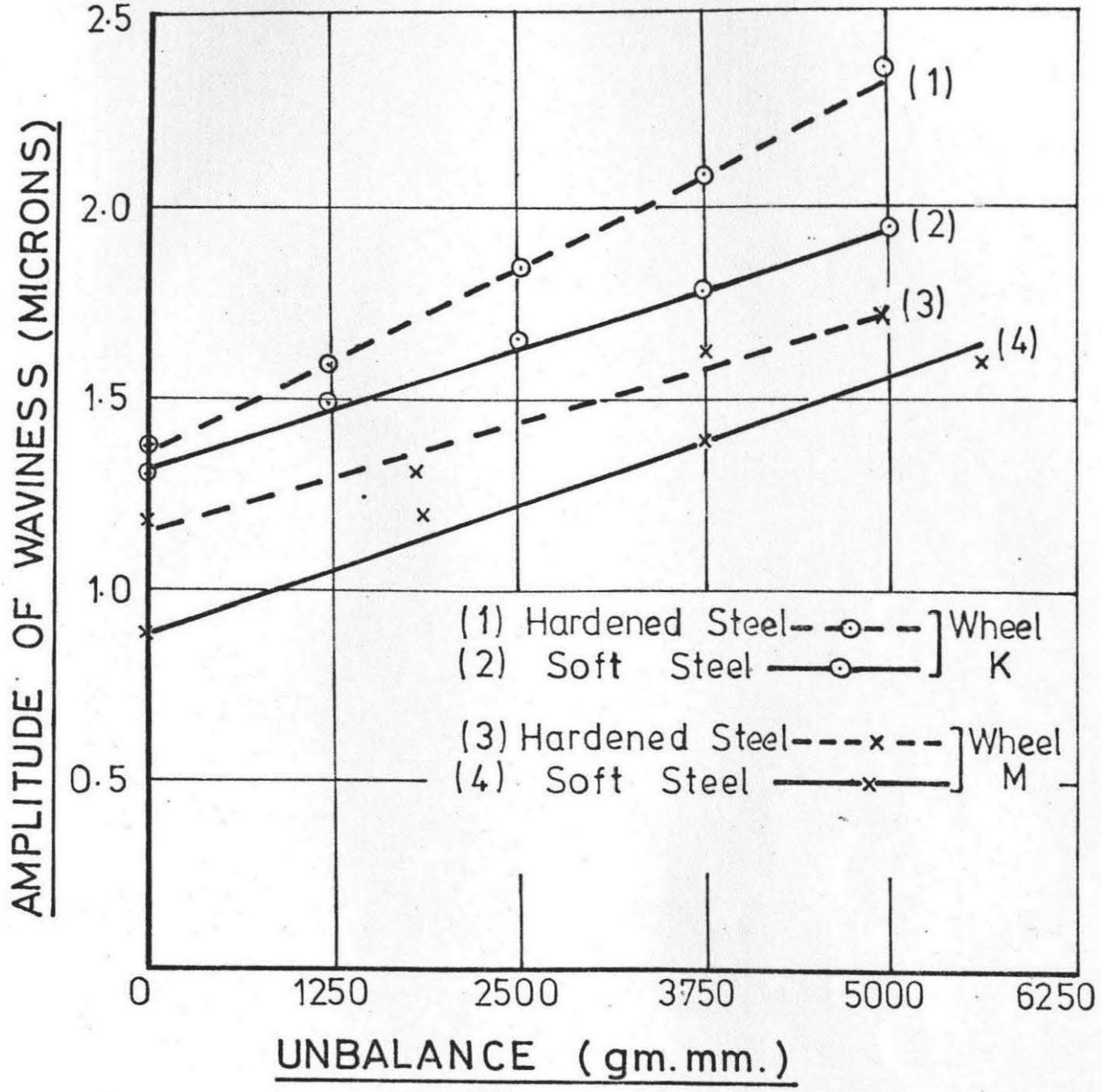

FIG 49. EFFECT OF WORKPIECE HARDNESS ON WORKPIECE WAVINESS.

the case of harder materials. This can be explained by the increase of the wheel contact stiffness, and an increase in contact stiffness results in higher amplitude of waviness.

5.3.2 C.L.A

The values of CLA obtained for different amounts of wheel unbalance are shown in Figure 50 and Figure 51. As can be seen from the graphs the CLA does not alter appreciably as a result of unbalance. This can be explained by considering the experimental results obtained by Hahn and Lindsay [27]. They have found that the two most important factors which determine the surface roughness during precision grinding are: i) the interface force intensity between the wheel and the workpiece, and ii) the wheel surface produced after dressing. Because, in the present case, the dressing criterion remains unchanged for a particular wheel the only other factor which will affect the surface roughness is the force intensity during grinding. It has been shown earlier that the unbalance does not affect the average force, therefore the surface roughness is not significantly affected by the unbalance. A similar effect of unbalance on CLA has also been observed by other authors, Farnworth [13], Bennet and May [15] and Inazaki [17].

Further, it can be seen from Figures 49 and 50 that the values of CLA are higher for softer wheels. To explain this both the force intensity and dressing criterion are to be considered. The authors [27], while explaining the effect of force intensity on surface roughness have stressed the importance of C/L factor. This factor is shown in Figure 52, where,

C = Depth of dress in mm

L = Dressing lead in mm/rev

In our case this value of C/L is about .07. Now, as can be seen from Figure 52, for this small value of C/L the effect of force intensity on CLA is not very significant. On the other hand the dressing criterion is a more pronounced effect for a harder wheel. As has been said earlier the spacing of grains as a

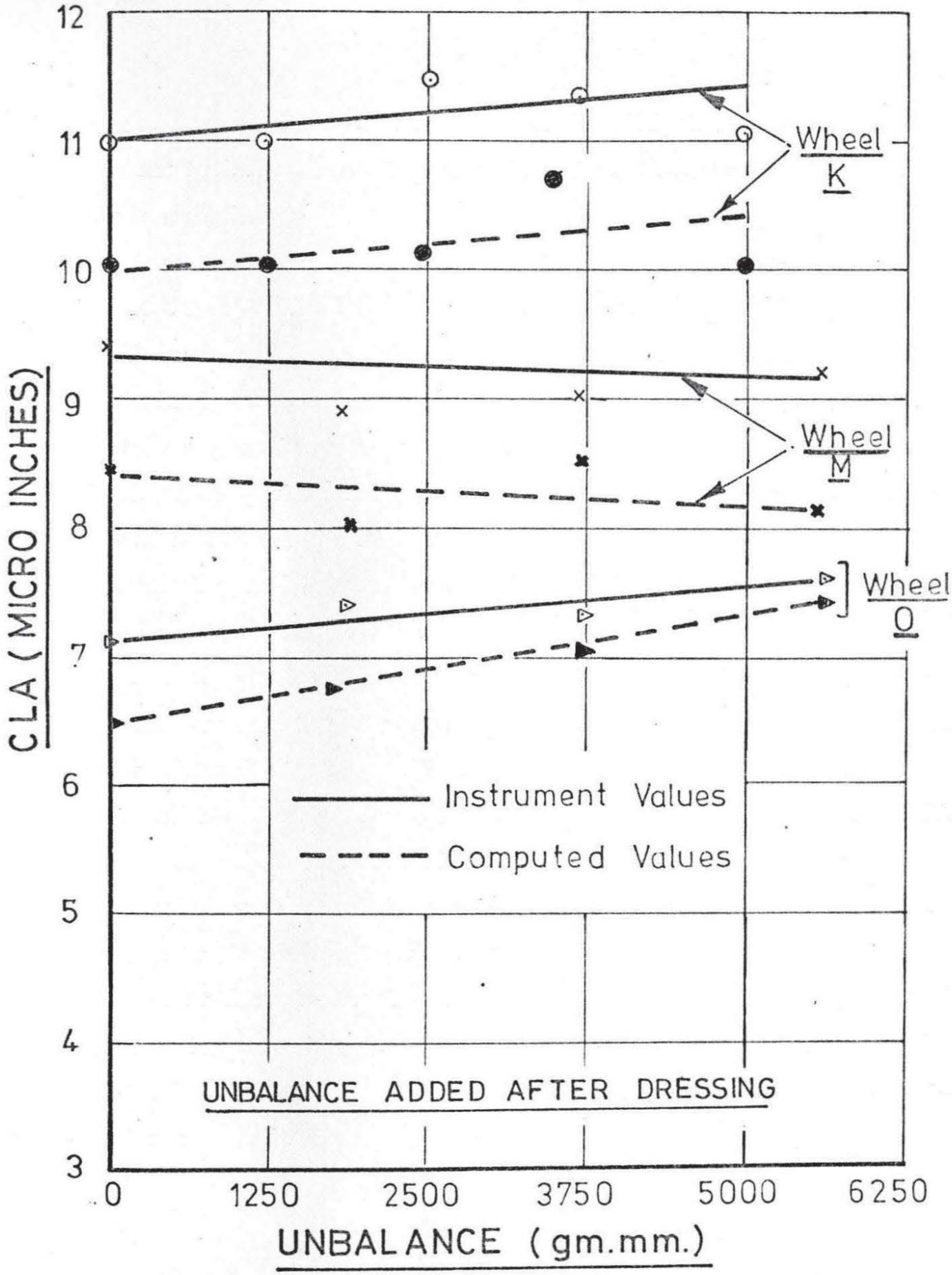

FIG 50. SURFACE ROUGHNESS AS A FUNCTION OF UNBALANCE AND WHEEL GRADE.

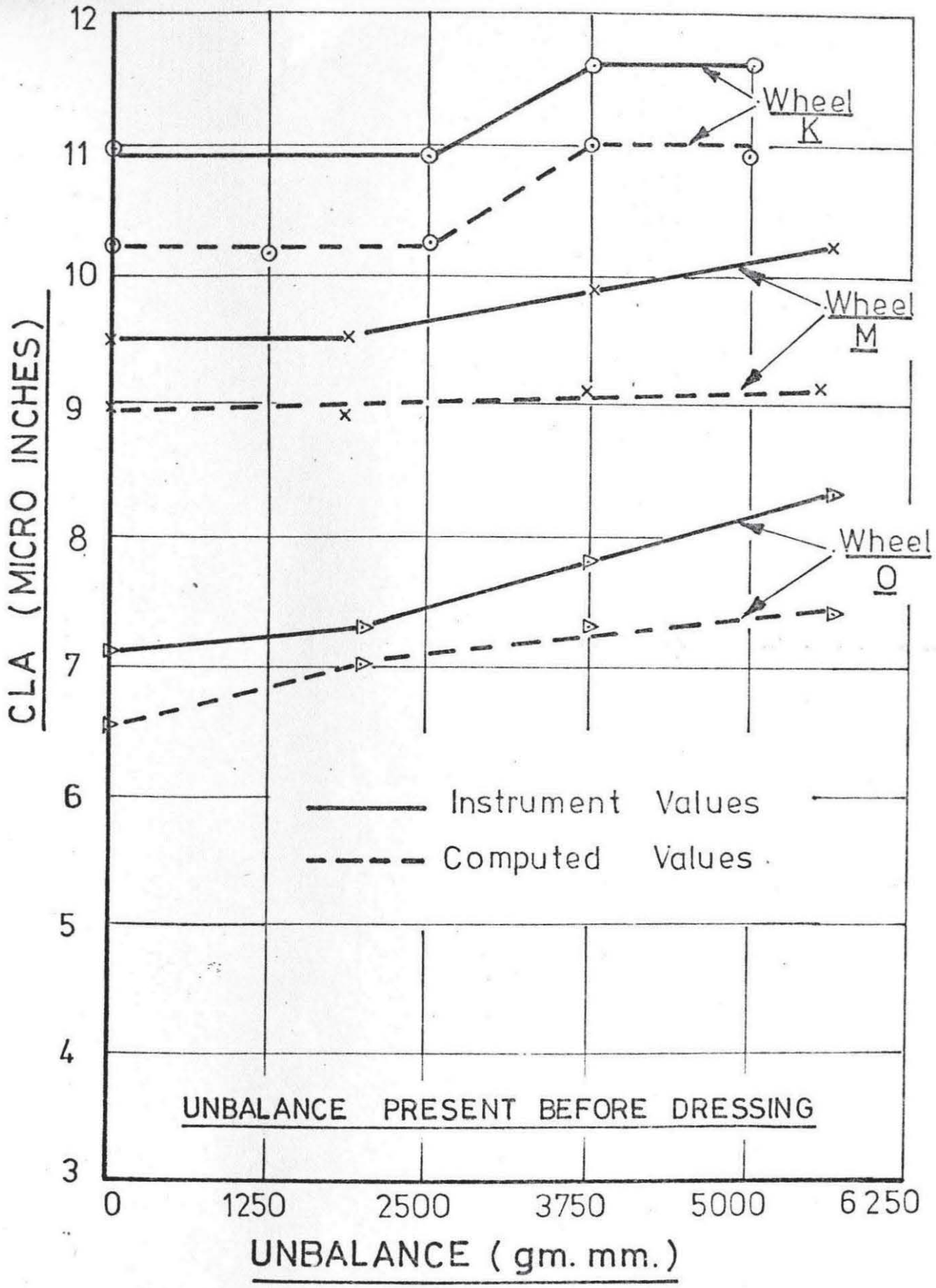

FIG 51. SURFACE ROUGHNESS AS A FUNCTION OF UNBALANCE AND WHEEL GRADE.

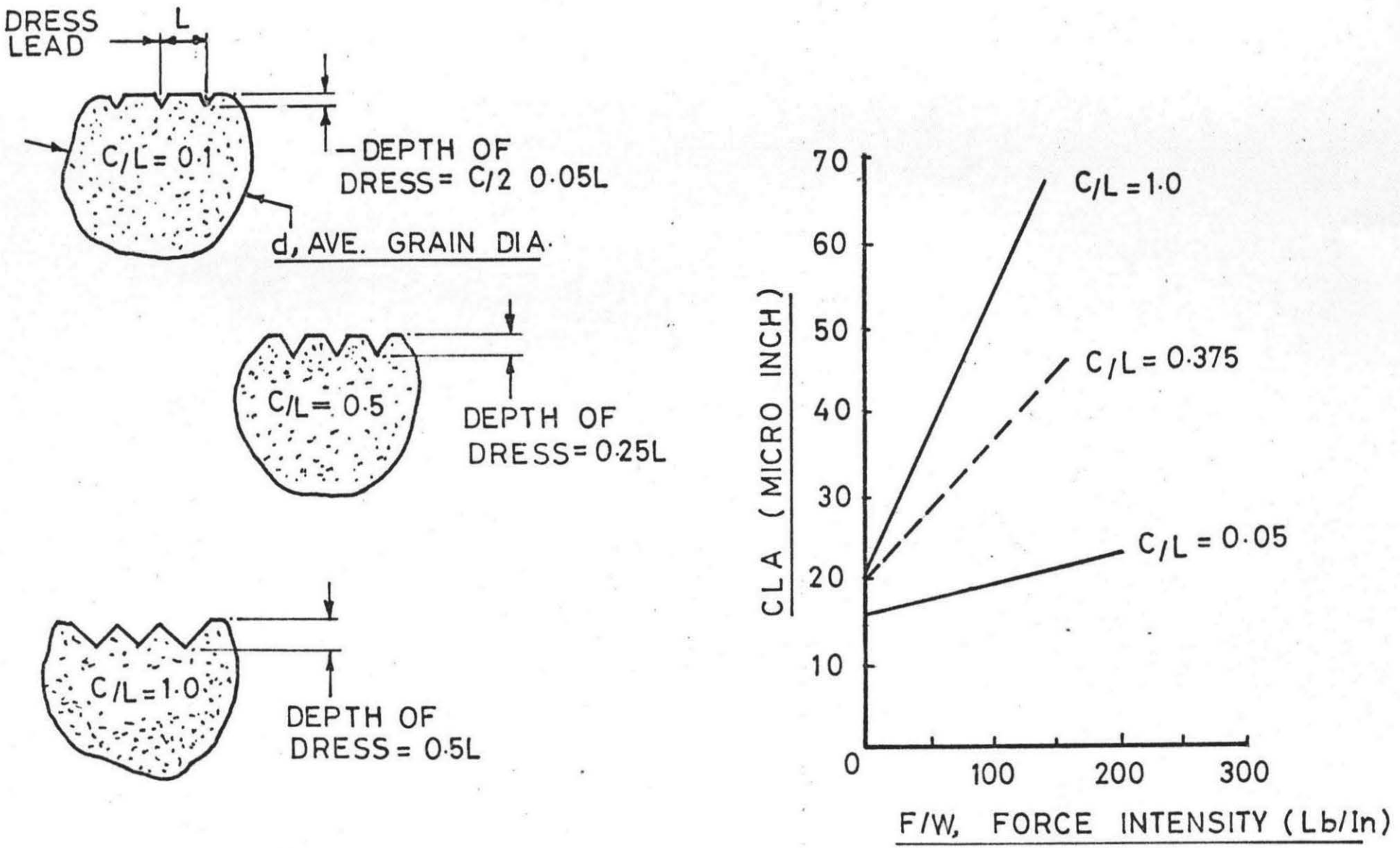

FIG 52· EFFECT OF NORMAL FORCE INTENSITY AND DRESSING RATIO ON SURFACE ROUGHNESS·

(HAHN AND LINDSAY [27])

result of dressing is closer for harder wheels. This leads to a more uniform wheel surface and consequently improved surface roughness. Both Figures 50 and 51 show the same tendency with wheel unbalance present before dressing (Figure 51)or added after dressing (Figure 50).

Lower surface roughness values are obtained in the case of harder materials as shown in Figure 53. This is due to the relatively lower values of radial forces present when grinding is done with harder materials. Besides, a softer material involves a tearing action of the metal because of the increased wheel contact stiffness. This results in higher roughness values.

5.3.3 5.3.3L Longitudinal Waviness

The results obtained for longitudinal waviness due to different amounts of unbalance are shown in Figure 54. The longitudinal waviness shows a slight increase due to the initial unbalance, but the waviness is fairly constant with further increase of unbalance. The trend is similar to the one obtained in the case of surface roughness. As in the case of CLA the longitudinal waviness also has higher values in the case of softer wheels. The longitudinal waviness using hard and soft workpiece materials is shown in Figure 55. Grinding with a harder material produces smaller amplitude of longitudinal waviness. It can be noticed from the results of longitudinal waviness that they reveal the same tendency as the results for surface roughness.

5.3.4 Peak to Valley Height

Figure 56 shows the computed peak to valley height as a function of unbalance. As can be seen, the value of peak to valley height does not change with the increase of unbalance. However, as in the case of surface roughness and longitudinal waviness, the peak to valley height is also decreased when grinding is done with harder wheels. No effect of workpiece hardness was noticed, as can be seen from the graphs of peak to valley height in Figure 57.

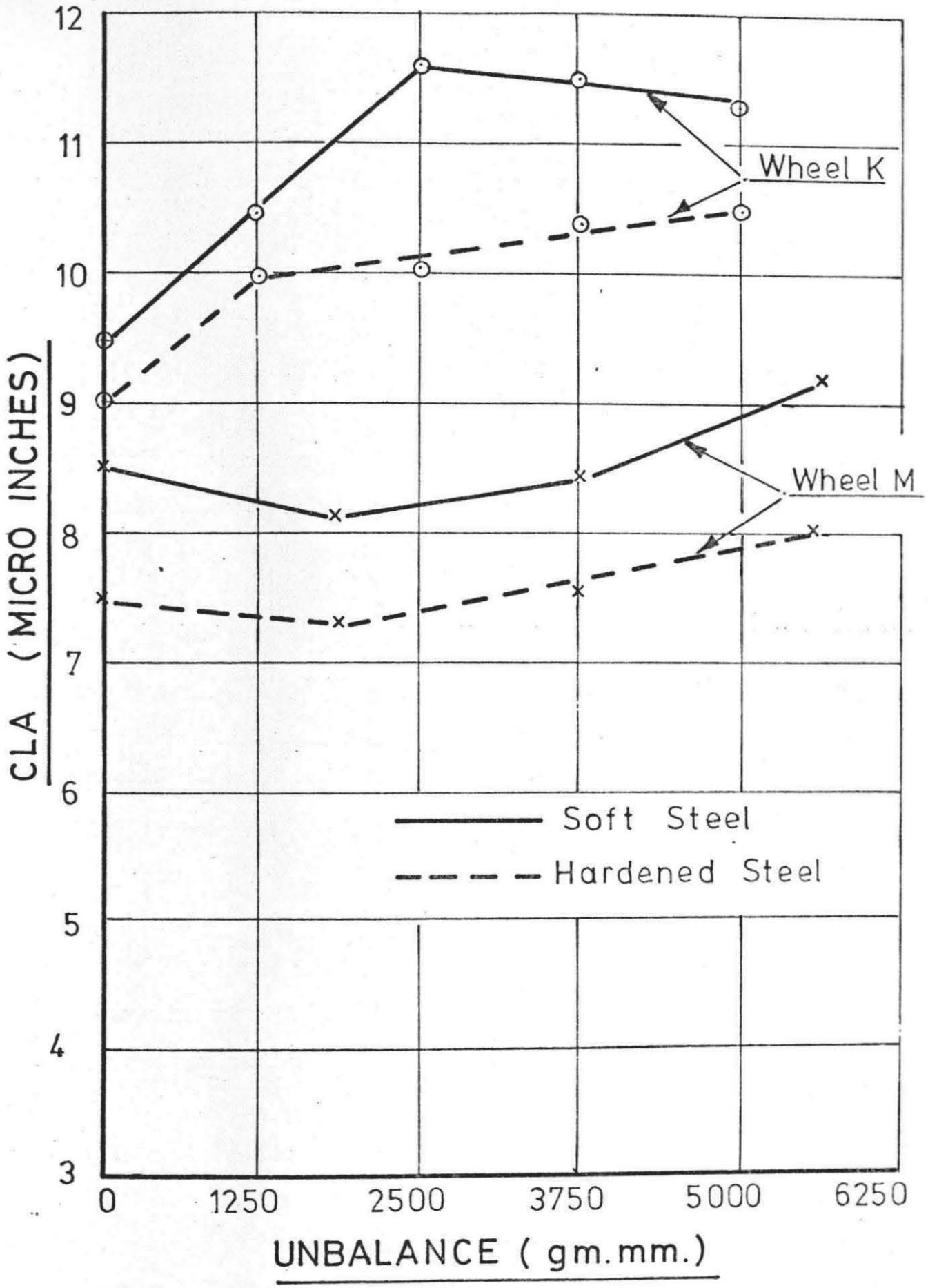

FIG 53. EFFECT OF WORKPIECE HARDNESS ON SURFACE ROUGHNESS.

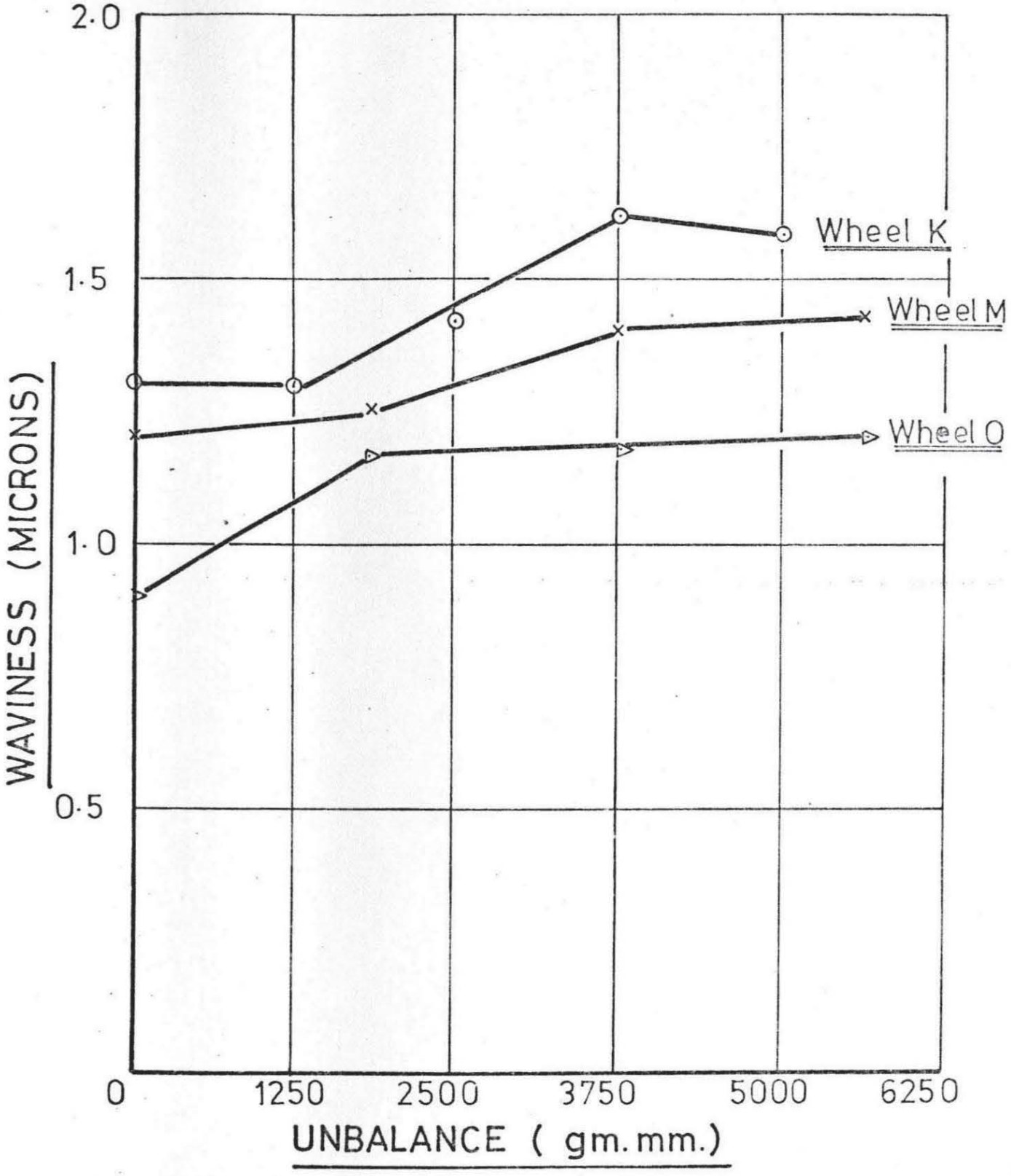

FIG 54. LONGITUDINAL WAVINESS AS A FUNCTION OF UNBALANCE AND WHEEL GRADE.

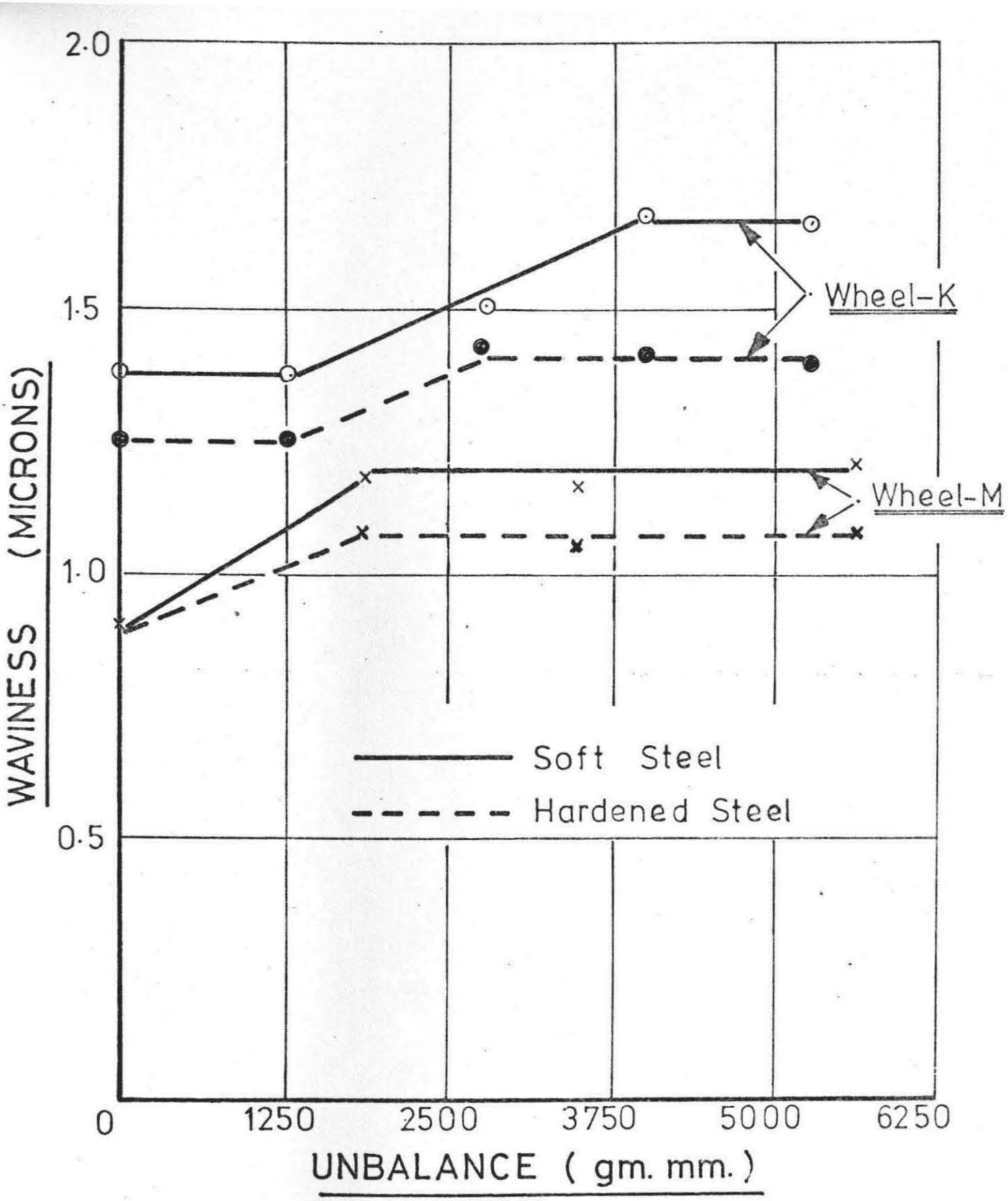

FIG 55. EFFECT OF WORKPIECE HARDNESS ON LONGITUDINAL WAVINESS.

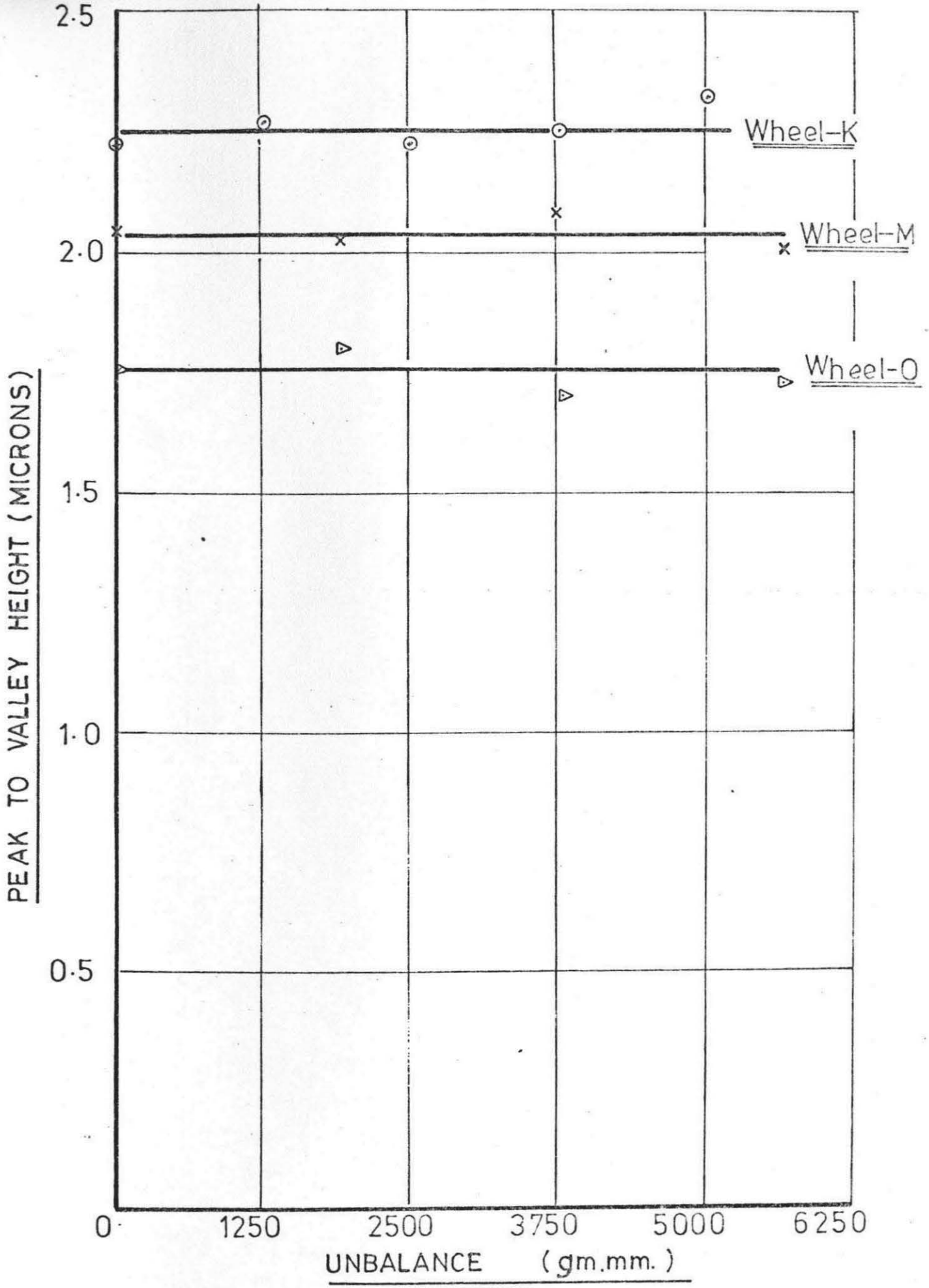

FIG 56. PEAK TO VALLEY HEIGHT AS A FUNCTION OF UNBALANCE AND WHEEL GRADE.

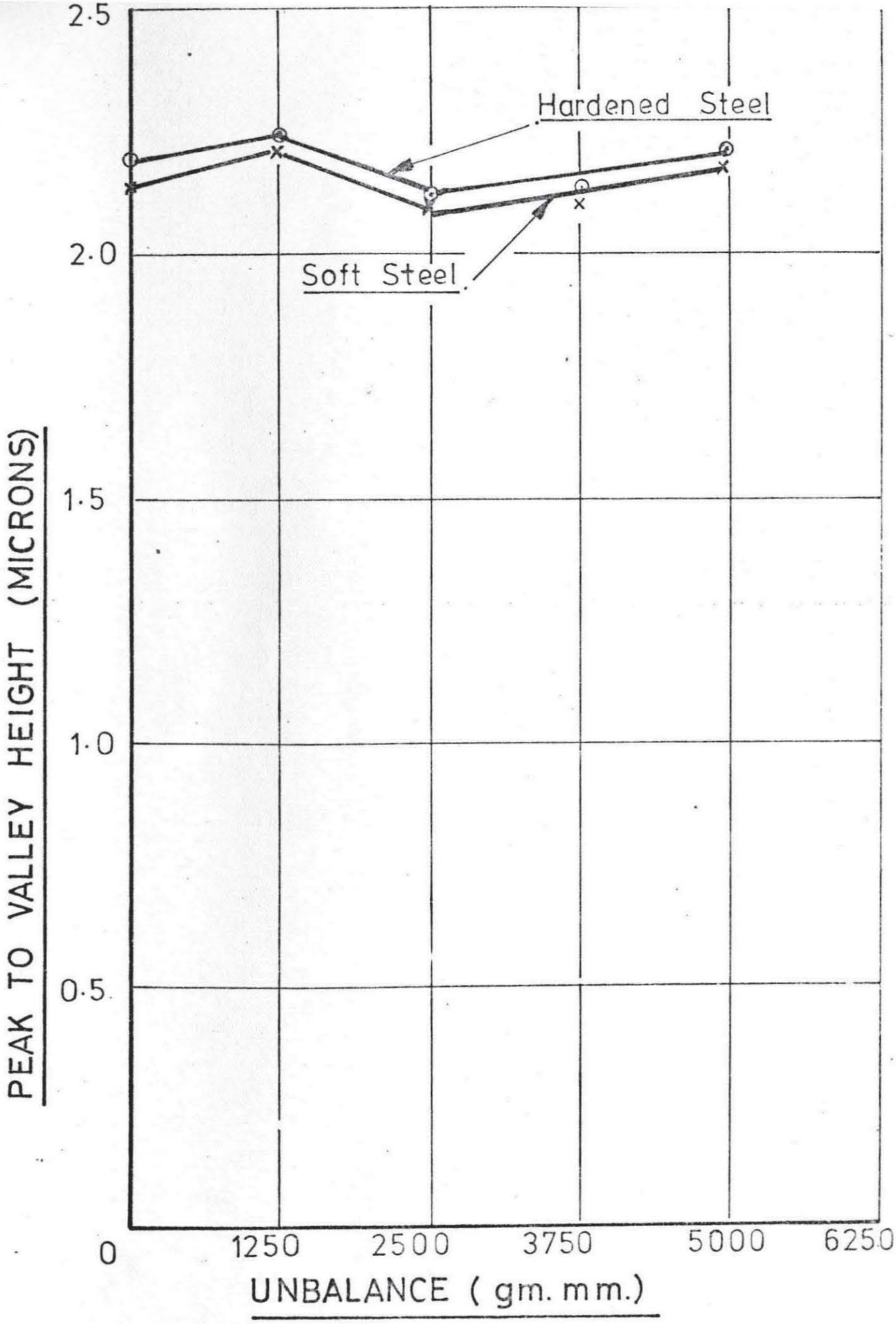

FIG 57. EFFECT OF WORKPIECE HARDNESS ON PEAK TO VALLEY HEIGHT.

5.3.5 Bearing Area

The bearing area or cumulative height distribution as it is sometimes called represents the relationship of the surface ordinates at or above a specified level expressed as a percentage of the total ordinates of the surface length considered. According to Greenwood and Williamson [33], the peak height distribution of the surface has a Gaussian distribution. Therefore, when bearing area is plotted on a normal probability paper it will appear as a straight line. Any deviation upwards from the straight line indicates the sharpening of the peaks and vice versa. The % bearing area plotted at different CLA height levels for various amounts of unbalance is shown in Figure 58. It can be seen from the graphs of different values of unbalance that with the increase of unbalance the deviation in the slope of the line increases downwards towards the top of the surface. This indicates the flattening of peaks with the increase of unbalance. In other words, the bearing area shows an improvement of the surface due to increased unbalance. This may presumably be due to the fact that the vibration caused by unbalance tends to break the sharp edges. Figure 59 shows the bearing area as a function of unbalance for three grades of wheels. It can be seen from the graphs that with the increase of wheel hardness the bearing area curve deviates upwards, which shows that the softer wheels are better so far as improvement in bearing area is concerned. This is because the relative wheel work motion increases in the case of softer wheels and so the influence of vibration in flattening the peaks increases. The effect is further illustrated when the grinding was done using a harder workpiece material (Figure 60). On comparing Figure 58 and Figure 60 it can be noticed that the effect of unbalance in flattening the peaks increases in the case of the harder material. As explained earlier, the relative wheel-work vibration increases in the case of harder material and therefore bearing area improves with a harder workpiece material.

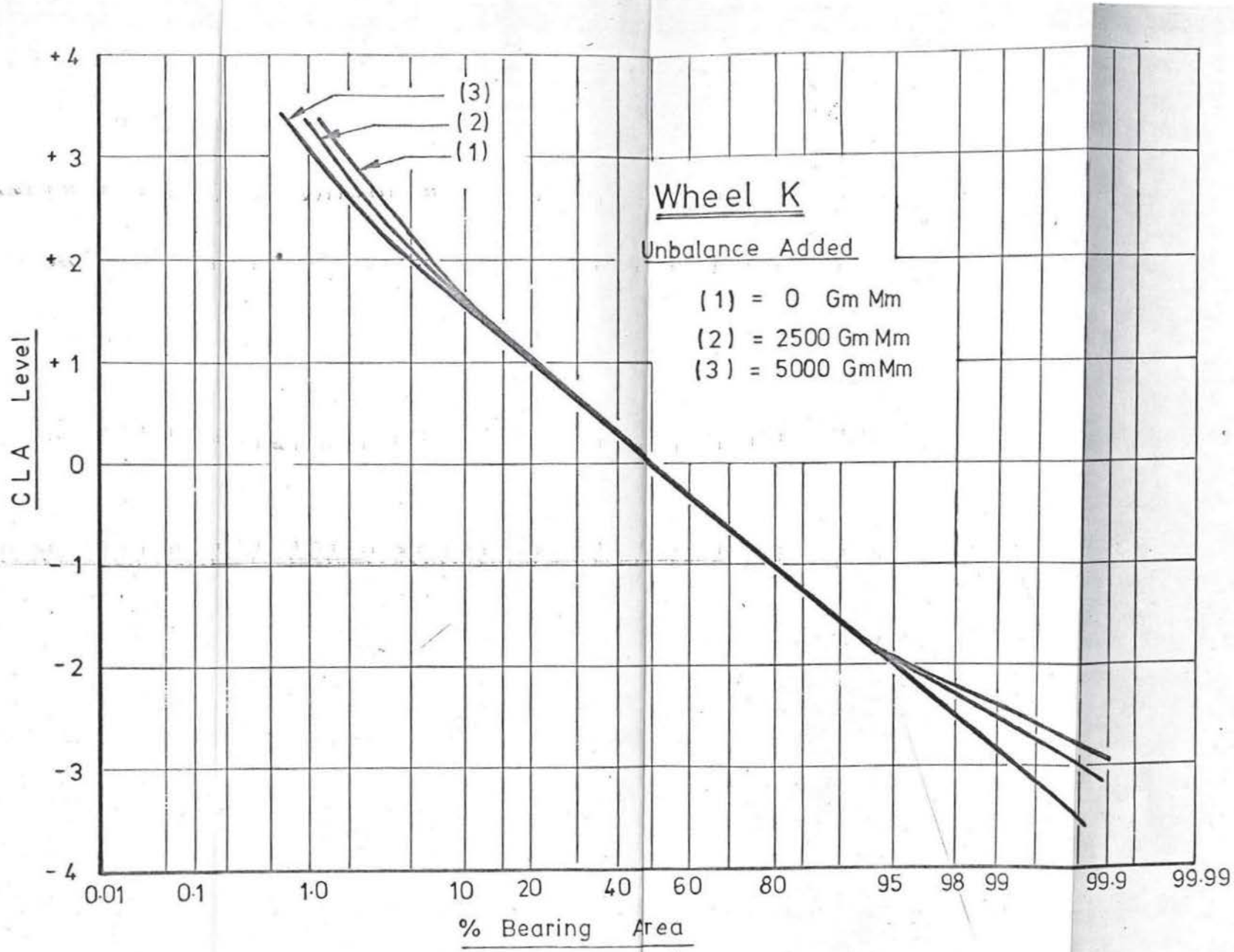

FIG 58. BEARING AREA AS A FUNCTION OF UNBALANCE.

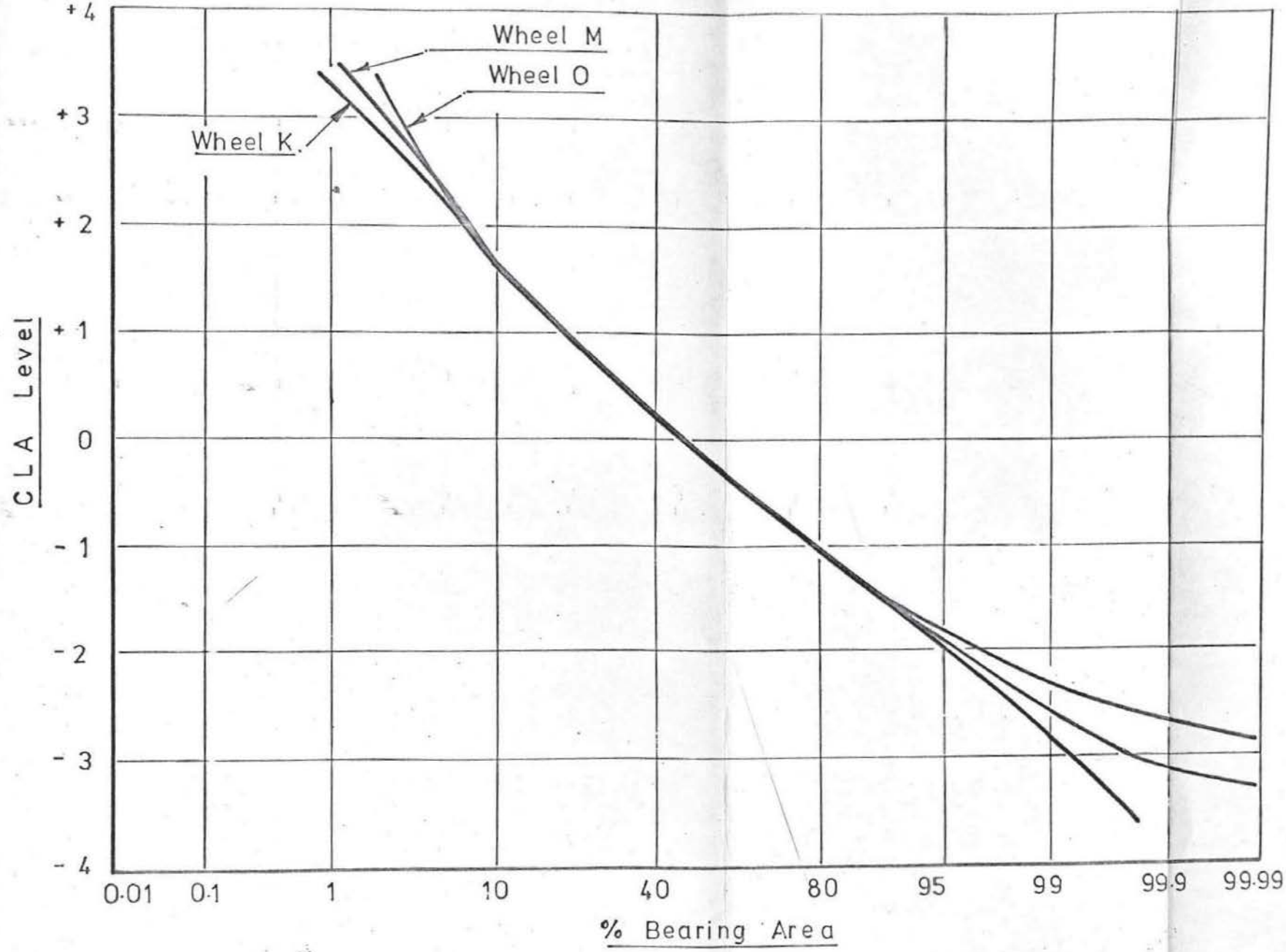

FIG 59. BEARING AREA AS A FUNCTION OF WHEEL GRADE.

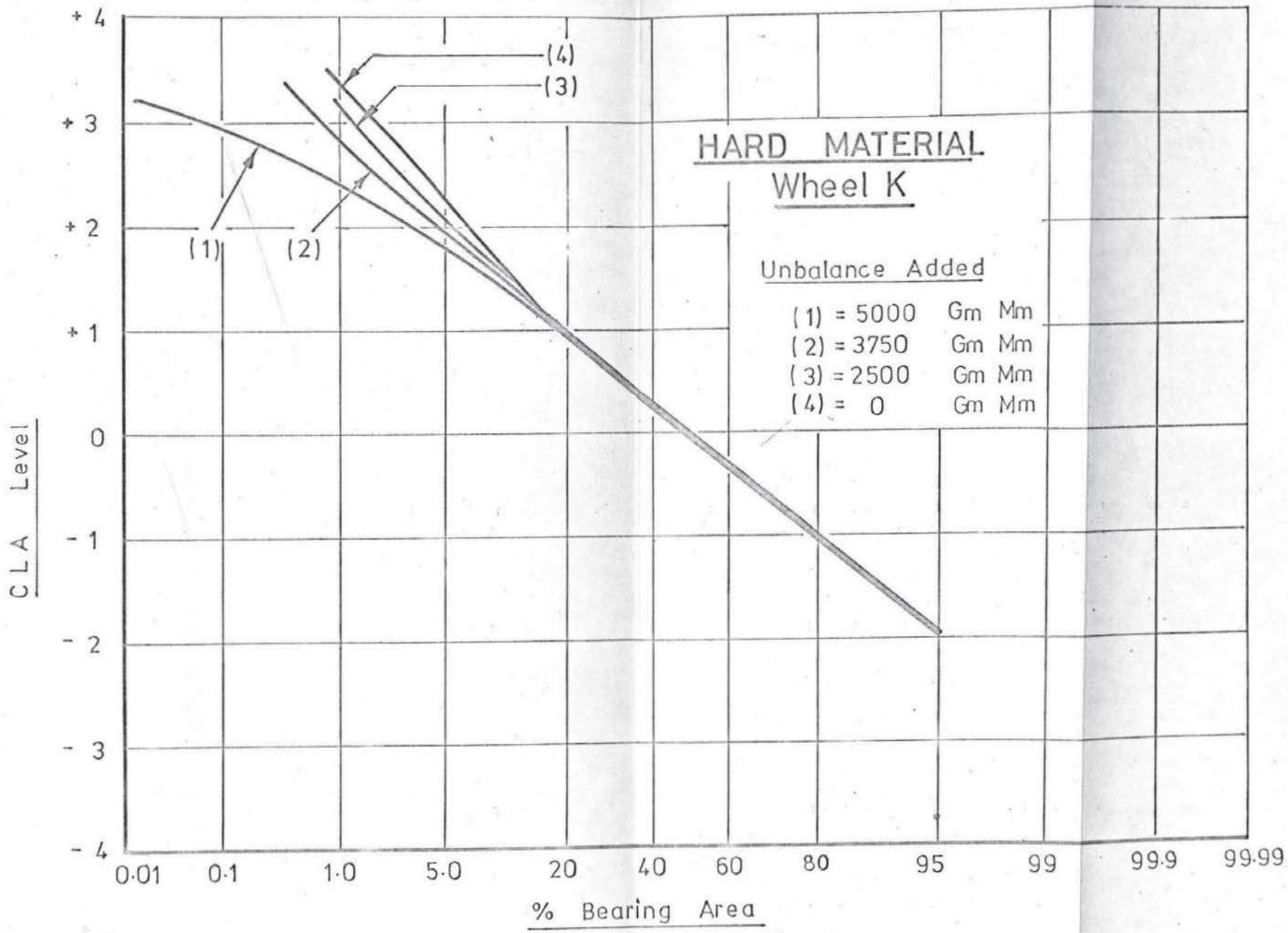

FIG 60. EFFECT OF MATERIAL HARDNESS ON BEARING AREA.

5.4 Grinding Ratio

The effect of unbalance on grinding ratio for three different wheels is shown in Figure 61. There seems to be a change in the grinding ratio with the increase of unbalance. However, this change is not very significant as has been shown in the previous investigations by Backer and Merchant [28]. During the experiments the authors [28] obtained a set of 15 values for grinding ratio ranging from 88 to 162 for the same material. Keeping this in view it can be said that the grinding ratio is not appreciably affected due to unbalance. It is also seen from Figure 61 that no special trend can be established for the hardness grade of the wheel so far as the grinding ratio is concerned. This is due to the fact that not enough metal was removed during the experiments, as follows from the previous investigation by Kaliszer and Limb [29] that although for a metal removal of 4 cubic inches the harder wheel 'O' has more grinding ratio (more metal removal) as compared with wheel K, but no definite trend can be noticed up to a metal removal of 2 cubic inches. This explains the indefinite trend in the present case.

From the graphs of grinding ratio using hardened and soft steel in Figure 62, it can be seen that the grinding ratio is increased in the case of hardened steel. In fact, this is possible. It has been shown by Grisbrook [26] that a harder material requires less specific energy than a softer material. Consequently, less heat is generated at the wheel work interface resulting in less wheel wear.

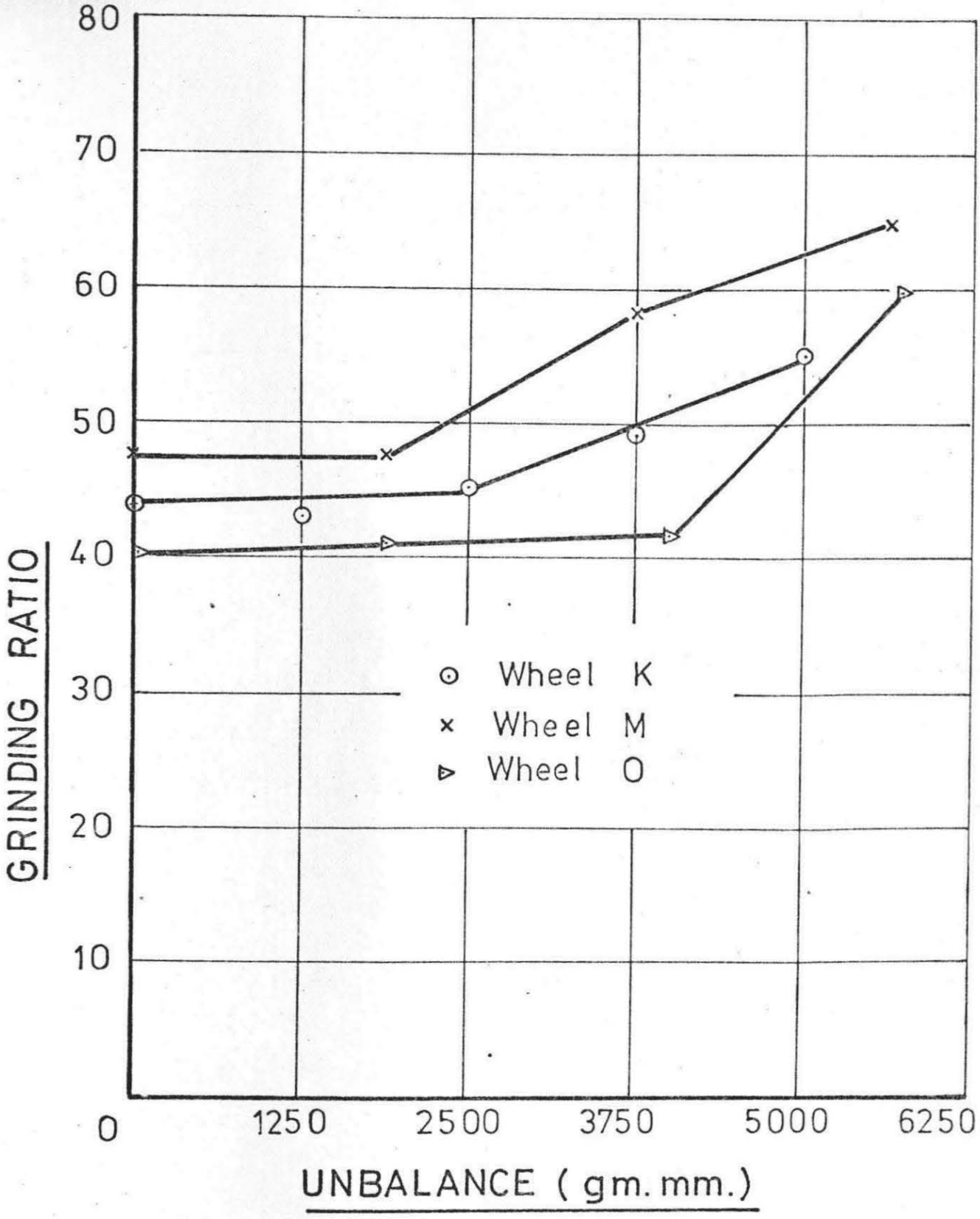

FIG 61. GRINDING RATIO AS A FUNCTION OF UNBALANCE AND WHEEL GRADE.

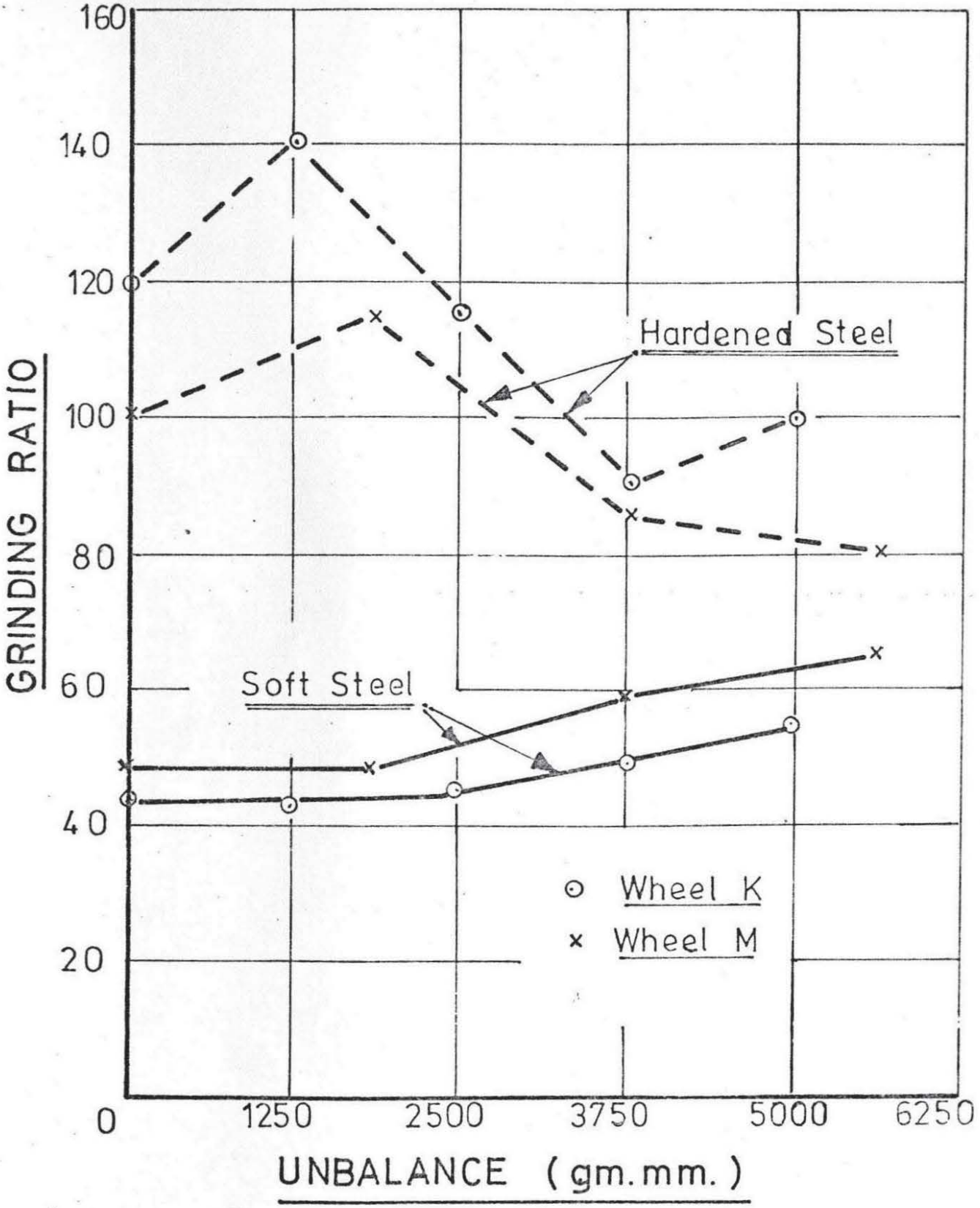

FIG 62. EFFECT OF WORKPIECE HARDNESS ON GRINDING RATIO.

CHAPTER 6

DISCUSSION AND CONCLUSIONS

6.1 Discussion of Results

The free running tests indicate that the wheelspeed affects the vibration behaviour of the various masses of the machine system. At a particular speed, the whole machine will be in the rocking mode. Therefore, the effect of a given unbalance will also depend upon the grinding speed of the machine. The grinding speed used in our investigation (1175 r.p.m.) happens to be in the vicinity of the rocking mode speed (1140 r.p.m.). Since the wheelhead and the workpiece move in the same phase and with the same amplitude of motion in the rocking speed range, the generation of surface irregularities will be determined by the wheelspindle motion only. The radial motion of the wheelspindle at the wheel plane was of the order of 4 microns as compared with the radial motion of the wheelhead equal to 25 microns at the rocking speed. This clearly points to the rigidity of the plain bearings incorporated in the grinding machine. Similar observations were also made by Doi [20], who states that the plain bearing offers better damping than the antifriction bearing (ball or roller). The damping characteristics of the two bearings are shown in Figure 63. In order to reduce the effects of vibration on spindle motion, a plain bearing should be used, as is apparent from Figure 63. This does not, however, imply that the antifriction bearing is unsuitable for grinding spindles. It is well known [20] that this type of bearing has excellent performance, in particular, where high speeds are involved.

The grinding results show that the level of wheel unbalance directly influences the vibration of the machine system. The peripheral waviness of the workpiece and the cyclic fluctuation of the radial force increases with the increase of the relative wheel work motion generated by the wheel unbalance.

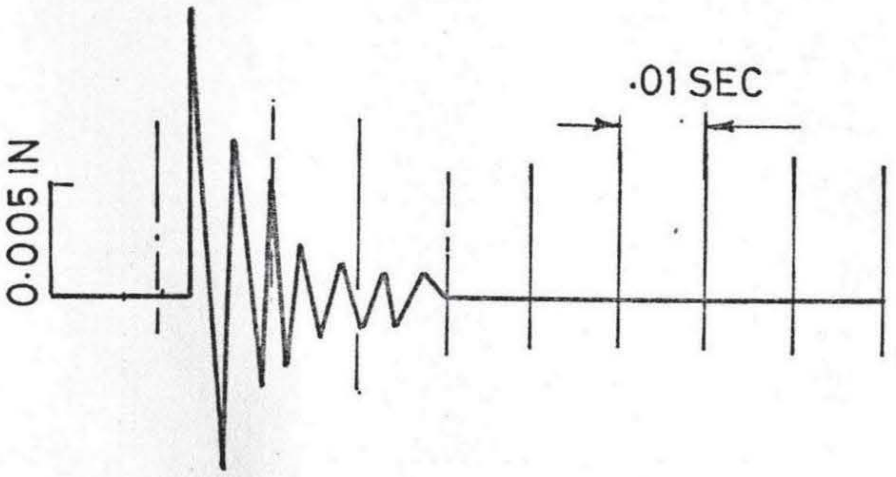

PLAIN BEARING

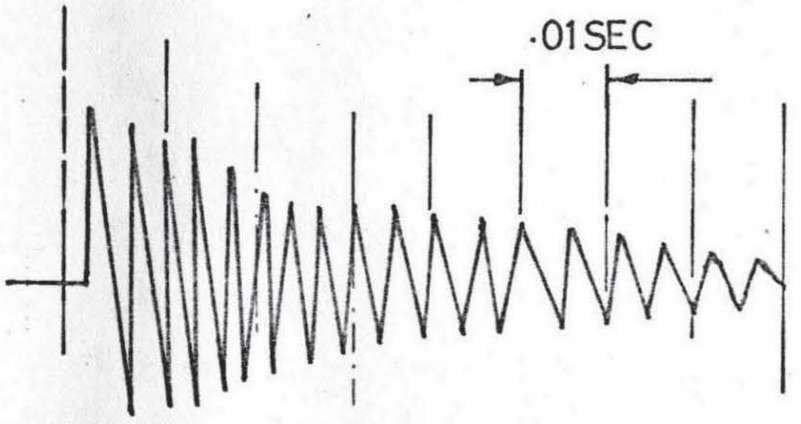

BALL BEARING

FIG 63. FREE DAMPING VIBRATION OF WHEELHEAD WITH PLAIN AND BALL BEARING.

It is also noticed that the effect of unbalance persists during grinding even if the unbalance is present before the dressing operation. The above statements follow from the expression for unbalance and waviness (Chapter 3).

For the same amount of unbalance, the peripheral waviness of the workpiece is also affected by the grade of the wheel and the workpiece material. This effect can be explained by considering the wheel contact stiffness. A harder wheel and a softer material will increase the wheel contact stiffness and an increase in this stiffness tends to reduce the effect of forced vibrations. The effects are clearly seen from the grinding results where the harder wheels and softer workpiece material tend to reduce the vibration of the machine system, the cyclic variation in radial force and peripheral waviness of the workpiece. The wheel unbalance does not have any significant influence on surface parameters in the longitudinal direction (CLA, waviness and peak to valley height). However, grinding with harder wheels improves these parameters. This has been explained by considering the radial force intensity and dressing criterion.

One may conclude from the above discussion that normally harder wheels should be used for achieving a better surface quality. This, however, has some limitations in practice. It has been shown by Muller [30] that a harder wheel needs more power than a softer one to remove metal at the same rate. Also grinding with very hard wheels results in quick wheel loading and therefore the tool life between dressings is reduced. On the other hand, too soft a wheel produces a poor surface quality and wears quickly. Therefore, a compromise is necessary in practice and the hardest wheel compatible with the material being ground should be used.

On the basis of the experimental results, it can be concluded that the bearing area improves with unbalance. However, the influence of unbalance is reduced in this respect when the grinding is done with harder wheels. Since the harder wheels are suggested in practice, therefore, this improvement in

bearing area will not be of any appreciable significance.

6.2 Conclusions

The study of unbalance in a grinding machine provides an insight into the problems of rigidity, vibration and resulting surface quality. The following conclusions are drawn: -

1. The grinding speed used in the investigation is close to the frequency of the rocking mode of the machine at which the wheelhead and workpiece experience the same type of motion. The relative wheel-work motion is therefore affected primarily by the spindle motion.

2. The forced vibration during grinding is influenced by the rigidity of the machine, the grinding speed of the machine, the amount of unbalance, and wheel contact stiffness.

3. The following factors increase with the increase of grinding wheel unbalance:

   (a) Vibration of wheelhead and workpiece.

   (b) The radial motion of the wheelspindle from front bearing towards the wheel end.

   (c) The relative wheel work motion.

   (d) The cyclic fluctuation in radial force.

   (e) Peripheral waviness of the workpiece.

4. The factors under 3 are influenced by the hardness grade of the wheel and workpiece material, which affect the wheel contact stiffness. A softer wheel and a harder material tend to increase the effect of unbalance during grinding.

5. Workpiece waviness increases with the relative wheel-work motion created by the wheel unbalance which may be added before or after dressing.

6. The unbalance does not affect the longitudinal parameters (ie, CLA, waviness, and peak to valley height). The harder wheels, however, improve these parameters.

7. The bearing area shows a slight improvement with unbalance particularly with the softer wheel and harder work material.

8. The average radial force, the temperature during grinding, and grinding ratio, is not affected by the unbalance. However, the grinding ratio improves with hard materials.

APPENDIX 1

DATA INPUT TAPE FOR PROGRAM

Data Title		
Surface	MSGK/WOA/ Expt. 1.U	
1200	N = Total number of ordinates	Control Variables
0.000000253	X = Vertical scaling factor	
0.0002	G = Ordinate spacing	
600	N' = Half number of ordinates	
695		
687	Input ordinates from profile	

589		
634		
20000	End of Data	Characters put at the end of data
+ -	causes computation to be restarted on next data tape	
??	End of paper tape	

APPENDIX 2

EQUATION OF THE LEAST SQUARE CENTRE LINE

The method of least squares was used to fit a straight line (centre line in our case) to the recorded profile. If we consider the data consisting of n ordinates

$$(x_i, y_i), \quad i = 1, n$$

The equation of any straight line is given by

$$y = a + bx \tag{1}$$

Hoel [31] shows that it simplifies the mathematical solution if the variable x is measured from sample mean $\bar{x}$. So the equation reduces to

$$y' = a + b(x - \bar{x}) \tag{2}$$

According to [31] the least square estimates of a and b for the equation of the line expressed in (2) above are

$$a = \bar{y} \quad \text{and} \quad b = \frac{(x_i - \bar{x})\, y_i}{(x_i - \bar{x})^2}$$

where x_i and y_i denote the ith pair of ordinates and $\bar{x}$ and $\bar{y}$ are the means of the n values of x and y respectively. Therefore, substituting the values of a and b the equation of least square line becomes

$$y' = y + \frac{(x_i - \bar{x})y_i}{(x_i - \bar{x})^2} \left[x - \bar{x}\right]$$

This is the equation of the least square centre line of the digitised profile.

APPENDIX 3

LEAST SQUARE POLYNOMIAL FOR PEAK HEIGHTS

Peaks are defined [23] as a smoothed ordinate above the adjacent smoothed ordinate on either side of the ordinates examined. To achieve these smoothed ordinates, a least square method is used to fit a fourth degree polynomial to seven adjacent points $u-3$, $u-2$, $u-1$, u_o, u_1, u_2, u_3. The only value of the polynomial required is the value of the polynomial at '0' position. Since this new value u'_o will replace u_o, the entire polynomial is not required. Only the expression for u'_o is required. The solution given by Whittacker and Robinson [32] is,

$$u'_o = \frac{1}{231}\ 131\, u_o + 75\,(u_1 + u - 1) - 30\,(u_2 + u - 2) + 5\,(u_3 + u - 3)$$

where $u - 3$, $u-2$, $u-1$, u_o, u_1, u_2, u_3 are the ordinates (here CL ordinates) being smoothed and u_o being replaced by the single ordinate u'_o. To calculate the next smoothed ordinate, the ordinates are incremented by one. Therefore, $u-2$, $u-1$, u_o, u_1, u_2, u_3, u_4, are operated upon to give u'_1. The series of u_i ordinates are calculated where u_i is the ith smoothed ordinate.

APPENDIX 4

FORMULAE FOR CALCULATION OF PARAMETERS

1. CLA: Average of the sum of the ordinate heights below and above the least square line throughout the sample

or

$$R_a\,(CLA) = \frac{1}{N} \sum_{i=o}^{i=N} \left| y_i - A_i \right|$$

where,

N is the number of ordinates in the sample length considered.

Y_i and A_i are the ith ordinates of the least square centre line and surface profile respectively w.r.t. voltmeter digital datum. The difference $\left|Y_i - A_i\right|$ represents heights w.r.t. least square line (CL).

2. Peak Height: Maximum value of the smoothed least square ordinates "C" above the centre line

or $C(P) = \phi_{Max}\ (C\ 0,\ 3,\ N - 4)$ (Always positive)

3. Valley Depth: Minimum value of the smoothed least square ordinates "C" below the centre line

or $C(Q) = \phi_{Min}\ (C\ 0,\ 3,\ N - 4)$ (Always negative)

NOTE: While evaluating peak height and valley depth 3 ordinates are omitted on each side of the sample length as these are not available when the ordinates have been smoothed.

4. Peak to Valley Height: Distance between the highest peak and lowest valley

or $G = C(P) - C(Q)$

C(Q) is subtracted from C(P) because of minus sign with C(Q).

5. Fullness Coefficient: Ratio of valley depth to peak to valley height

$$H = - C(Q)/G$$

APPENDIX 5-1

PROGRAM TO CALCULATE SURFACE PARAMETERS

This program starts at the beginning of Chapter 'O' although this chapter is physically situated last on the program tape. At instruction 5) of Chapter 'O' control passes to statement 5) in chapter 1. When all the instructions in Chapter 1 have been obeyed control passes to statement 55) in Chapter O (see following pages). This is a characteristic of the English Electric KDF-9 'K' autocode language compiler.

The accompanying flow chart shows the sequence as executed.

APPENDIX 5-II

FLOW CHART

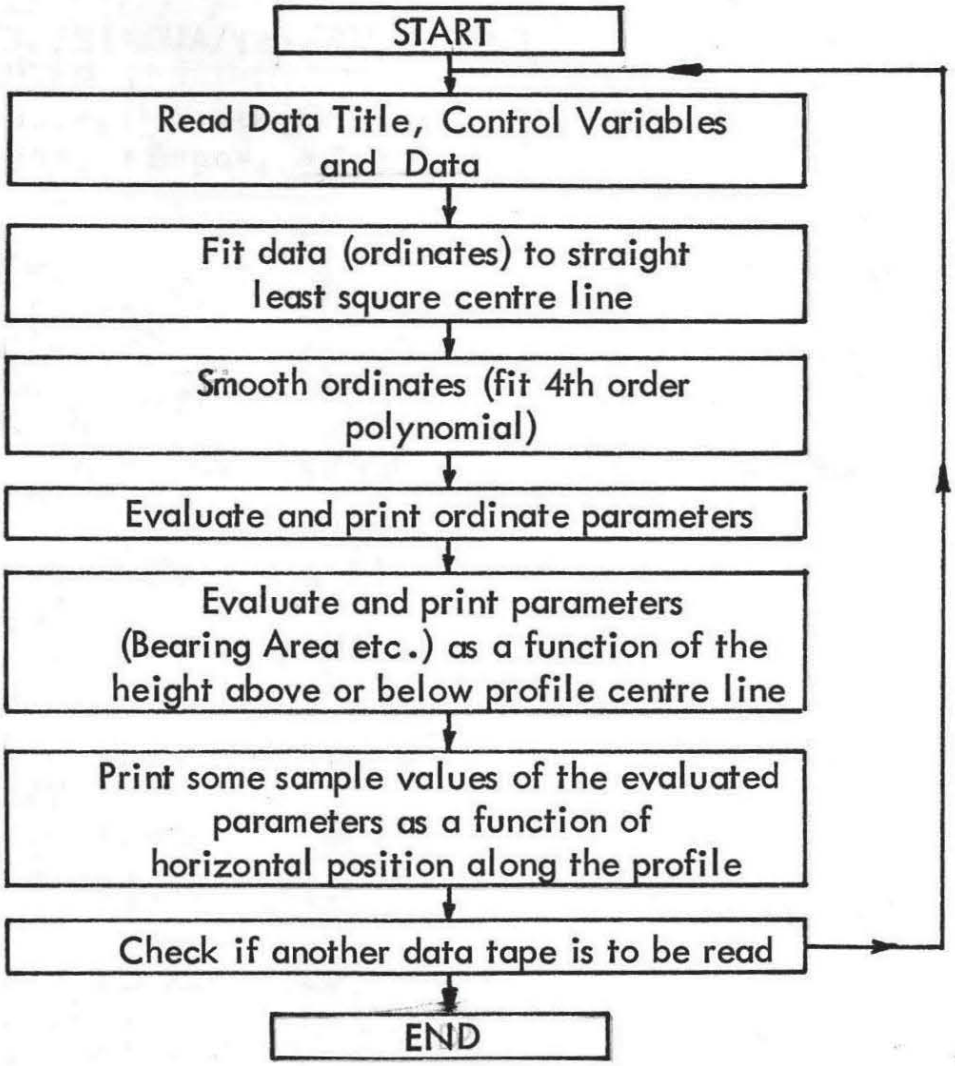

Appendix 5 - III

COMPUTER PROGRAM

```
AUTO JOB
JOB(S,P,3/20)
TITLE
AB/ME/SINDWA/101/ROUGHNESS
CHAPTER 1
A→2000*,B→2000*,C→2000
*A→90*, *B→90*, *C→90


5)C'=0
R=0,1,N-1
C'=C'+A(R)
REPEAT
D'=C'/N
(D' Y BAR THE AVERAGE INPUT ORDINATE VALUE)
*D'=0
R=0,1,N-1
*D'=*D'+*(R-N'*)A(R)
REPEAT
(*D' IS SUM XI-X BAR YI TERMS)
E'=0
R=0,1,N-1
E'=E'+*(R-N'*)*(R-N'*)
REPEAT
(E' IS XI-X BAR SQUARED SUM)
B'=*D'/E'
(B' IS FACTOR B IN LEAST SQUARES CL. EQN.)

(Y'-AR IS REQUIRED)
R=0,1,N-1
B(R)=D'+B'*(R-N'*)-A(R)
REPEAT
(BR ARE ORDINATES + OR - WRT LEAST SQUARES CL.)
(PRINT LEAST SQUARES CL. EQN.)
NEWLINES(2)
CAPTION
LEAST SQUARES CL. EQN.
NEWLINE
PRINTSYMBOL(121)
PRINTSYMBOL(80)
```

```
PRINTSYMBOL(85)
PRINT(D',2,10)
PRINTSYMBOL(29)
PRINT(B',3,12)
PRINTSYMBOL(88)
PRINTSYMBOL(120)
PRINTSYMBOL(30)
PRINT(N',5,1)
PRINTSYMBOL(89)
(FIT ORDINATES TO A 4TH ORDER POLYNOMIAL CONSIDER 7 POINTS)
R=3,1,N-4
C(R)=*(131B(R)+75*(B(R+1)+B(R-1)*)-30*(B(R+2)+B(R-2)*)
+5*(B(R+3)+B(R-3)*)*)/231
REPEAT


(FIND ORDINATE-PARAMETERS)
(CLA AND OTHERS)
Y'=0
R=3,1,N-4
Y'=Y'+ØMOD(B(R))
REPEAT
*Y'=Y'/*(N-6*)
(PRINT ORDINATE PARAMETERS)
NEW LINES(3)

CAPTION
ORDINATE PARAMETERS (IN INCHES WHERE APPROPRIATE)
NLCAPTION
ORDINATE CENTRE LINE AVERAGE,RA       =
PRINT(*Y',4,10)
P=ØMAX(Co,3,N-4)*,Q=ØMIN(Co,3,N-4)
*G=C(P)-C(Q)*,*H=-C(Q)/*G
NLCAPTION
PEAK HEIGHT                           =
PRINT(C(P),4,10)
NLCAPTION
VALLEY DEPTH                        =
PRINT(C(Q),4,10)
NLCAPTION
PEAK TO VALLEY HEIGHT RZ.             =
PRINT(*G,4,10)
NLCAPTION
```

```
FULLNESS COEFFICIENT                    =
PRINT(*H,4,6)

ACROSS(55,0)

PSA
CLOSE


CHAPTER 0
VARIABLES 1
2)READ DATA TITLE
READ(N,X,G,N')
NLCAPTION
NO OF TERMS  VERT SCALE  ORDINATE SPACEING  HALF NO ORDS.
NEWLINE
PRINT(N,5,2*,X,1,10*,G,5,7*,N',5,1)
(READ DATA)
R=0,1,N-1
READ(U)
JUMP(5)U=20000
A(R)=XU
REPEAT
(FIND LEAST SQUARES EQN.)

5)ACROSS(5,1)


(BEARING AREA AS A FUNCTION OF HEIGHT)
55) *A'=*Y'
*Bo=3.4*A'
NEWLINES(3)
CAPTION
:BEARING AREA  PARAMETERS
NEWLINE
R=0,1,35
Y'=0
T=4,1,N-5
JUMP(62)*B(R)>B(T)
Y'=Y'+1
62)REPEAT
*C(R)=100Y'/*(N-8*)
*B(R+1)=*B(R)-0.2*A'
REPEAT
```

```
NEWLINES(3)
CAPTION
  NO  HEIGHT ABOVE CL  BEARINGAREA
NEWLINE
R=0,1,35
PRINT(R,2,0*,*B(R),4,8*,*C(R),6,2)
NEWLINE
REPEAT
(PRINT SOME SAMPLE VALUES)
NEWLINES(3)
CAPTION
SAMPLE VALUES
NLCAPTION
  NO  IN ORDINATES CL ORDINATES AV ORDINATES

NEWLINE
R=20,1,60
PRINT(R,2,0*,A(R),1,8*,B(R),1,8*,C(R),1,8)
NEWLINE
REPEAT
70)JUMP(70)ØREADSYMBOL≠29
(SEARCHES FOR A PLUS SIGN ON DATA TAPE)
JUMP(2)ØREADSYMBOL=30
(GOES TO 2 IF NEXT SIGN IS MINUS)
PSA
END.
CLOSE
→
??
.*
```

Appendix - 6

PRINTER OUTPUT

```
START 16.06   DATE  17/04/70


AB/ME/SINDWA/101/ROUGHNESS

PSA   1 708 184 892
PSA   0 762 130 892


SURFACE                    MSGO/W30A/EXpT 40E


NO OF TERMS   VERT SCALE   ORDINATE SPACEING   HALF NO ORDS.
  1200.00   0.0000002530        0.0002000        600.0

LEAST SQUARES CL. EQN.
Y'=   0.0001307129   +  -0.000000017175  (X-   600.0  )


ORDINATE PARAMETERS (IN INCHES WHERE APPROPRIATE)
ORDINATE CENTRE LINE AVERAGE,RA        =     0.0000087920
PEAK HEIGHT                            =     0.0000532220
VALLEY DEPTH                           =    -0.0000256203
PEAK TO VALLEY HEIGHT RZ.              =     0.0000788423
FULLNESS COEFFICIENT                   =     0.324956
```

BEARING AREAPARAMETERS

NO	HEIGHT ABOVE CL	BEARINGAREA
0	0.00002989	1.34
1	0.00002813	1.85
2	0.00002638	2.27
3	0.00002462	2.85
4	0.00002286	3.69
5	0.00002110	4.78
6	0.00001934	5.79
7	0.00001758	7.21
8	0.00001583	9.23
9	0.00001407	10.74
10	0.00001231	12.75
11	0.00001055	15.94
12	0.00000879	19.04
13	0.00000703	23.41
14	0.00000528	28.02
15	0.00000352	33.64
16	0.00000176	39.68
17	0.00000000	46.22
18	-0.00000176	52.60
19	-0.00000352	59.06
20	-0.00000528	66.36
21	-0.00000703	71.56
22	-0.00000879	77.10
23	-0.00001055	83.31
24	-0.00001231	88.42
25	-0.00001407	91.36
26	-0.00001583	94.38
27	-0.00001758	96.39
28	-0.00001934	97.65
29	-0.00002110	98.74
30	-0.00002286	99.50
31	-0.00002462	99.75
32	-0.00002638	99.83
33	-0.00002813	99.92
34	-0.00002989	99.92
35	-0.00003165	100.00

SAMPLE VALUES

NO	IN ORDINATES	CL ORDINATES	AV ORDINATES
20	0.00014143	-0.00000075	-0.00000369
21	0.00014623	-0.00000558	-0.00000163
22	0.00013561	0.00000503	0.00000068
23	0.00013814	0.00000248	0.00000602
24	0.00012802	0.00001259	0.00001028
25	0.00012271	0.00001788	0.00002010
26	0.00011739	0.00002318	0.00001971
27	0.00012599	0.00001456	0.00001892
28	0.00011992	0.00002061	0.00001664
29	0.00012701	0.00001351	0.00001687
30	0.00012878	0.00001173	0.00000866
31	0.00014117	-0.00000069	0.00000053
32	0.00014016	0.00000031	0.00000345
33	0.00012878	0.00001167	0.00000495
34	0.00014801	-0.00000757	-0.00000152
35	0.00014244	-0.00000202	-0.00000491
36	0.00013637	0.00000403	0.00000488
37	0.00013030	0.00001009	0.00001028
38	0.00013105	0.00000931	0.00000865
39	0.00014295	-0.00000260	-0.00000368
40	0.00015003	-0.00000970	-0.00000703
41	0.00012903	0.00001128	0.00001117
42	0.00011208	0.00002822	0.00002512
43	0.00012625	0.00001403	0.00001639
44	0.00013839	0.00000187	0.00000133
45	0.00014320	-0.00000295	-0.00000191
46	0.00014219	-0.00000196	-0.00000466
47	0.00014750	-0.00000729	-0.00000385
48	0.00013763	0.00000256	0.00000026
49	0.00013789	0.00000229	0.00000271
50	0.00014219	-0.00000203	-0.00000231
51	0.00014143	-0.00000129	0.00000109
52	0.00013257	0.00000755	0.00000337
53	0.00014092	-0.00000081	0.00000179
54	0.00013257	0.00000752	0.00001077
55	0.00012018	0.00001990	0.00000987
56	0.00014826	-0.00000820	0.00000471
57	0.00012852	0.00001151	-0.00000030
58	0.00013839	0.00000163	0.00001212
59	0.00012296	0.00001705	0.00000719
60	0.00014269	-0.00000270	0.00000498

END

TIME 001 COST 005

REFERENCES

1. Kaliszer, H., and Singhal, P.D. — Contribution to the analysis of waviness generated during grinding, Annals of C.I.R.P. Vol. XV, pp. 245-251, 1967.

2. Landberg, — Experiments on Grinding, Microtecnic, Vol. II, No. I, p. 18, 1957.

3. Singhal, P.D., and Kaliszer, H. — The effect of workpiece dimensions and wheel parameters on surface waviness during grinding, 6th Int. M.T.D.R. Conf. Proc.1965.

4. G. Sweeney, — Dynamics of Grinding, University of Birmingham, Ph.D. Thesis, 1965.

5. G.B. Lurie, — Vibrations in Grinding, Machines & Tooling, Vol. XXX, No. 6, pp. 17, 1959.

6. Pahlitzsch, G., and Cuntze, E. — Reduction of Chatter Vibration during cylindrical and plunge grinding operations, Proc. 6th Int. M.T.D.R. Conf, 1965.

7. Polacek, M., and Ludvik, B. — Some problems connected with raising the output and precision of grinders, Czech. Heavy Industry, No. 12, p. 24.

8. Polacek, M., and Pluchar, L. — "Selbsterregte Schwingungsen beim Schleifen" Foko Ma, 1963.

9. Kalizer, H. — Uber den Einfluss der schleibenunwcht auf die schwingungen beim Schleifen, Industrie Anzeiger, No. 98, p. 22, 1960.

10. Kalizer, H. — Accuracy of balancing grinding wheels by using gravitational and centrifugal methods, Proc. 4th Int. M.T.D.R. Conf. 1963.

11. Kaliszer, H., and Singhal, P.D. — Analysis of the rigidity of the grinding wheel-workpiece-grinding machine system, The Inst. of Mech.Engr., Proc. 1966-67, Vol. 181, Part 1, Nr. 5.

12. Gelfeld, O.M. — Forced vibrations in a cylindrical grinding machine caused by wheel unbalance, Machines & Tooling, Vol. XXXII, Nr. 7, p. 19, 1961.

13. Farnworth, G.H. — The influence of vibrations on quality in grinding, Production Engineer, Vol. 42, p. 525, 1963.

14. Singhal, P.D. — Ph.D. Thesis, University of Birmingham, 1966.

15. Bennet, R.S. and May, C.F. — Performance studies on a typical centreless grinding machine with reference to truing and balancing of grinding wheel, Proc. 6th Int. M.T.D.R. Conf., Manchester, 1965.

16. Teratana, C., Nahao, R., and Hiura, M. — Study for improving the accuracy of internal grinder, Bulletin of J.S.P.E., Vol. 1, No. 2 March 1965, Tokyo, p. 89-90.

17. Inazaki, I., and Yonetsu, S. — Forced vibrations during surface grinding, Bulletin of J.S.M.E., 1969, Vol. 12, No. 50, pp. 385-391.

18. Colwell, L.V. — The effect of high frequency vibrations in grinding. Tans. A.S.M.E., Vol. 78, May No. 4, p. 837, 1956.

19. Peklenik, J. — Testing the grade of grinding wheels, Microtecnic, 14, Nos. 5,6, pp. 233, 1960.

20. Doi, S. — An experimental study on chatter vibrations in grinding operations, Discussion by R.S. Hahn, Trans. A.S.M.E., Vol. 80, p. 133, 1958.

21. Sharman, H.B. — Numerical assessment of surface texture based on R.M.S. and sample size, N.E.L. report 230, May 1966.

22. Reason, Hopkins, and Garron. — Report on the measurement of surface finish by stylus methods, Rank Taylor Hobson, Leicester, 1944.

23. Grieve, D.J. — Measurement in the examination of the normal wear process, M.Sc. Thesis, University of Birmingham, 1969.

24. Kaliszer, H., and Singhal, P.D. — Some problems connected with the grinding process, 7th Int. M.T.D.R. Conf., Proc. 1966.

25. Peklenik, J. — Industrie Enzeiger, 1961, pp. 929-938

26. Grisbrook, H. — Precision Grinding Research, The Production Engineer, 1960 (May and June).

27. Hahn, and Lindsay. — The influence of process variables on metal removal, surface integrity, surface finish and vibration in grinding, Proc. 10th Int. M.T.D.R. Conf., 1969.

28. Backer, and Merchant. — On the basic mechanics of grinding process, A.S.M.E., November 1966.

29. Kaliszer, H., and Limb, M. — Application of ultrasonic technique to grinding process, 7th Int. M.T.D.R. Conf., 1966.

30. Muller, J.A. — Factors influencing the performance in cylinderical grinding, Machinery, Jan. 1968, Vol. 93 (Abstract No. 47661).

31. Hoel, Paul G. — Elementry Statistics, John Willey & Sons, April, 1965, p. 145.

32. Whittaker, and Robinson. The calculation of observations, Blackie and Son, Limited, 1926, p. 295.

33. Greenwood and Williamson Proceedings of the Royal Society, A-295, 1966, p. 300.